Distribution Agreement

In presenting this thesis or dissertation as a partial fulfillment of the requirements for an advanced degree from Emory University, I hereby grant to Emory University and its agents the non-exclusive license to archive, make accessible, and display my thesis or dissertation in whole or in part in all forms of media, now or hereafter known, including display on the world wide web. I understand that I may select some access restrictions as part of the online submission of this thesis or dissertation. I retain all ownership rights to the copyright of the thesis or dissertation. I also retain the right to use in future works (such as articles or books) all or part of this thesis or dissertation.

Signature:

_____ _____

Jessica Eliason Date

Single Neuron Contributions to Sensory Behaviors in *Drosophila melanogaster*

By

Jessica Eliason
Doctor of Philosophy

Graduate Division of Biological and Biomedical Science
Genetics and Molecular Biology

_____
Ichiro Matsumura, PhD
Advisor

_____
Michael Reiser, PhD
Advisor

_____
Andrew Escayg, PhD
Committee Member

_____
Randy Hall, PhD
Committee Member

_____
Kenneth Moberg, PhD
Committee Member

Accepted:

_____
Lisa A. Tedesco, Ph.D.
Dean of the James T. Laney School of Graduate Studies

_____
Date

Single Neuron Contributions to Sensory Behaviors in *Drosophila melanogaster*

By

Jessica Eliason
B.S. Brigham Young University, 2008

Advisors:
Ichiro Matsumura, PhD
Michael Reiser, PhD

An abstract of
A dissertation submitted to the Faculty of the
James T. Laney School of Graduate Studies of Emory University
in partial fulfillment of the requirements for the degree of
Doctor of Philosophy in
Graduate Division of Biological and Biomedical Science,
Genetics and Molecular Biology
2017

Abstract

Single Neuron Contributions to Sensory Behaviors in *Drosophila melanogaster*
By Jessica Eliason

Sensory systems are key to understanding how neuron circuity translates environmental stimuli into behavioral output. Neurons transform information about our surroundings into electrical signals. By working in coordination, neurons relay information about our world and allow us to perceive and react appropriately to it. However, the rules by which sensory input is interpreted by neuronal circuitry is poorly understood.

My graduate work contributes to understanding sensory systems by mapping functions to sensory neurons. Mapping includes answering the following: Which sensory neurons contribute to a particular behavior? What features of the stimulus are extracted by a specific neuron? How does a single neuron incorporate with others in a circuit to produce a behavior?

I have used *Drosophila melanogaster*, the fruit fly, to better understand how single sensory neurons function and communicate. Fly brains have only around 100,000 neurons while human brains have around 100 billion neurons. Yet, fly sensory systems operate on the same basic principles as our own.[1] Flies are sufficiently complex to produce sophisticated behaviors but are sufficiently simple that an understanding of the causal neuronal mechanisms is within our reach. [2] *Drosophila* provides a simpler, more tractable, and more genetically malleable system to study the broadly-relevant principles by which sensory information is encoded by neurons.

Somehow through the structure of receptors and activity of neurons, *Drosophila* sensory systems carry out remarkably complex tasks. For example, flies use an olfactory system to discriminate among innumerable diverse chemicals. The olfactory system copes with the "noise" of irrelevant chemicals and distinguishes the relative quantity and quality of odorants. Ultimately, the animal produces a behavioral response to this information such as moving towards mates or avoiding predators. The visual system is likewise extraordinary. From the simple act of photons hitting a receptor, the intricate visual circuity encodes visual features such as contrast, speed, intensity, wavelength, complexity, direction, distance, texture, polarization etc. Flies use this information for myriad behaviors including navigation, breeding, feeding, and predator avoidance.

In the next three chapters, I will describe specific projects in the olfactory and visual sensory systems that aim to illuminate neuronal mechanisms of sensation and behavior.

Single Neuron Contributions to Sensory Behaviors in *Drosophila melanogaster*

By

Jessica Eliason
B.S. Brigham Young University, 2008

Advisors:
Ichiro Matsumura, PhD
Michael Reiser, PhD

A dissertation submitted to the Faculty of the
James T. Laney School of Graduate Studies of Emory University
in partial fulfillment of the requirements for the degree of
Doctor of Philosophy in
Graduate Division of Biological and Biomedical Science,
Genetics and Molecular Biology
2017

Acknowledgments

This thesis is dedicated to my late mother, Kimberly Ayers. She started law school when I was 7 years old, and, while running her own company and raising three children, graduated valedictorian. She was a model of the importance of education for women and was always proud and supportive of my dreams.

Thank you to my mentor Ichiro. Who always supported me wherever my interests led. And to my second mentor, Michael Reiser, who gave me unprecedented opportunities and trusted me with exciting projects. I'd also like to thank my committee: Randy Hall, Ken Moberg, and Andrew Escayg, who had the miraculous capability of actually making me feel better after each committee meeting.

Thank you for financial support from the Emory GMB training grant, National Science Foundation (MCB- 1413062), and the Janelia Graduate Fellowship.

The work in this thesis would not have been possible without my many collaborators: Austin Edwards, Matt Isaacson, Aljoscha Nern, Shiuan-Tze Wu, Jasmine Le, Allan Wong, Emily Nielson, Chuntao Dan, Heather Dionne, Yoshi Aso, Ali Afify, and Chris Potter. And to my lab members who served as my best cheerleaders and critics. Also thank you to the Women's Coding Circle (president Charlotte Weaver) for creating a comfortable and expert environment for learning how to code.

This journey would not have been possible without the support of loving family and friends who helped me to grow or to seek refuge as need be. Thank you my Eliason, Boyle, and Ayers families for your unwavering dedication. The friends I made are too many to list, but thank you for the love and the fun. I became who I am today because of you.

Contents

List of Figures

Chapter 1

Chapter 2

Chapter 3

Thesis Introduction

The perceived world is an illusion. The interpretation of electrical and chemical signals in the brain; the reaction of neurons internally processing environmental stimuli. In 1884, this query was posted in the April edition of Scientific American: "If a tree were to fall on an uninhabited island, would there be any sound?" No. Sound waves would be produced, yes. But not sound. Sound is the interpretation of those vibrations by the brain. Similarly, from the simple act of chemicals interacting with receptors, the brain creates smell and the body avoids aversive odors or seeks attractive odors. From the simple act of photons hitting a receptor, the brain creates vision and the body can dodge, navigate, chase etc. in response.

The fundamental goal of neuroscience is to understand how sensory perception is propagated and transformed into behavioral action. Much is known about neuronal anatomy, but the function of neurons and how they coordinate and communicate within a circuit remains elusive. Which sensory neurons influence to a specific behavior? What stimulus features are encoded by a particular neuron? How does one neuron integrate in a circuit to produce a behavior?

Drosophila melanogaster, the fruit fly, is an excellent model for understanding neuronal function and organization. Flies can produce remarkably sophisticated behaviors. They can navigate towards a food source during flight, avoid the looming hand that attempts to squash them, and fight over receptive females. But flies produce all these behaviors using a brain that is only the size of a sesame seed, with one-millionth the number of neurons as our own. Yet, our neurons perform tasks using the same

fundamental principles as fly neurons. *Drosophila* are more genetically adaptable, anatomically simpler, and less neuronally variable.

The first chapter demonstrates useful tools for isolating neuron contributions in the olfactory system. Flies use an olfactory system to distinguish hundreds of biologically relevant odors and respond appropriately to them. For example, flies will to avoid CO_2 but move towards apple cider vinegar. However, the noise and redundancy of the olfactory architecture makes it difficult for researchers to pinpoint the effective contributions that a single neuron makes to perception and reaction. Currently, researchers hardly ever try to connect an odorant receptor's function to an ultimate behavioral outcome, because the associations are too complex. The genetic systems necessary to examine receptor/behavior correlations are complex and limited (if not prohibitive.) The reagents will allow researchers to efficiently isolate only one or a few functional neurons in an otherwise nonfunctional olfactory background. These tools will make it possible to better understand the connections from how odorant input results in a behavioral output by examining the effect of only one neuron or a few peripheral sensory neurons at a time.

The content of chapters two and three is specific to the visual system. The neuroanatomy of the visual system was characterized over 100 years ago, how the neurons function to create vision in still largely unknown. A large-scale screen was performed to identify neural correlates of motion and color vision. The first phase of the screen generated many "hits," i.e. potential hypotheses of neurons involved in the detection of moving objects and color. The second phase of the screen was smaller-scale and more hypothesis driven. In the second phase, hits from the first screen were

specifically targeted to further narrow down contributing neurons and to characterize the identified neurons. The results of the dual screen will be a valuable resource for investigators seeking to map function to individual neuronal types.

Chapter three characterizes a particularly interesting neuronal type that was discovered in the screens. This neuron was previously unidentified and was named Lobula Plate Columnar Neuron 1 (LPC1.) LPC1 has several interesting features: it detects only translational and not rotational motion, it responds only to back-to-front or up motion and not front-to-back or down motion, and it affects forward walking speed but not turning of the animal. A nearly complete neuronal circuit was reconstructed for LPC1 from photoreceptor neurons on the periphery to output neurons in the central brain that control behavior. The LPC1 story is an excellent example of how sensory perception and reaction can be mapped to the function, characteristics, and connectivity of a single neuron type.

Chapter 1: A GAL80 collection to nullify transgenes in *Drosophila* olfactory sensory neurons

Introduction

The olfactory system of *Drosophila melanogaster* is a favored model in studies of learning and memory, protein and species evolution, gene choice, development, and how sensory stimuli are translated into behavioral output. *Drosophila* olfaction is a powerful standard for researchers because of its extensive genetic toolkit, complex behaviors, and relatively stereotyped neuronal circuitry. Here, an additional set of transgenic lines is presented to complement the available *Drosophila* genetic tools and to demonstrate their effectiveness and potential utility for behavioral, physiological, and neuroanatomical research.

In *Drosophila*, each olfactory sensory neuron (OSN) typically selects a single odorant receptor (OR) to express from its repertoire of 60 genes.[3-7] Therefore, using the promoter of an OR gene is a reliable method for genetically labelling the specific subset of OSNs that express a particular receptor. The OR determines the firing kinetics and odor-response dynamics of each OSN. ORs vary in sensitivity and specificity to a wide range of different odorants.[8-16]

In addition to a single selected OR, all OSNs express Odorant Receptor Co-Receptor (Orco). The Orco promoter is therefore a convenient genetic target for all OSNs. Orco is a highly conserved member of the olfactory receptor family.[17,18] Though Orco usually does not contribute to the structure of the odorant binding site,[19-22] it is essential for odorant-invoked signaling in flies. Without Orco, the co-expressed OR

cannot localize to the dendritic membrane or relay an odor-evoked signal.[23,24] Orco null flies are largely anosmic, though some chemosensation remains due to the presence of ionotropic receptors and gustatory receptors, which do not require Orco to function.[25-28]

The olfactory organs, the antenna and maxillary palp, contain OSNs dendrites within structures called sensilla. ORs and Orco are embedded in the dendritic membrane. OSN axons project to the antennal lobes in the brain of the animal. Each antennal lobe consists of ~50 globular synaptic sites called glomeruli. All OSNs on the periphery that expresses the same OR converge onto their own unique glomerulus. For example, all OSNs expressing Or22a will send axons to the DM2 glomerulus in the antennal lobe while all OSNs expressing Or82a will send axons to the VA6 glomerulus (**Figure 1**). The stereotyped organization of OSNs and their projections is known as the olfactory sensory map.[5,10,11,29] The regularity of this map is a

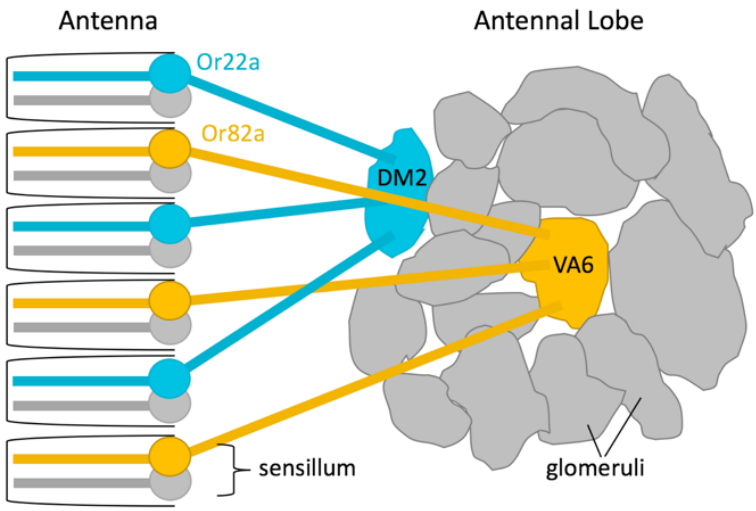

Figure 1: Olfactory Sensory Map. Each neuron in the olfactory system expresses one type of odorant receptor (OR). Or22a (teal) and Or82a (gold) are used here as examples. Neurons exist in pairs or groups in sensilla within the olfactory organs—antenna or maxillary palp. Neurons expressing the same OR are distributed throughout the periphery, but project their axons onto the same glomerulus in the antennal lobe of the brain. For example, all Or22a-expressing neurons synapse onto the DM2 glomerulus while all Or82a-expressing neurons synapse onto the VA6 glomerulus.

key feature that makes *Drosophila* olfaction such a useful model, as any aberration to the typical pattern will be apparent.

Studies using *Drosophila* olfaction have taken advantage of the GAL4/UAS system. GAL4 is a yeast transcription activator that binds to the Upstream Activating Sequence (UAS) and induces expression of downstream genes.[30] By driving GAL4 expression from an OR promoter, specific expression of a *UAS-transgene* can be obtained for any OSN subtype. An *OrX-GAL4* line exists for almost every receptor. This library of GAL4 lines is a powerful toolbox for researchers since different *UAS-transgene* lines can be substituted interchangeably. For example, human α-synuclein has been expressed in OSNs to model human Parkinson's disease.[31] Or protein expression levels can be knocked down using any specified *UAS-RNAi* transgene. And a variety of effectors exist that can be used study different aspects of neuronal communication. *UAS-Kir2.1* effector is used as an example in these experiments. This inward rectifier potassium channel electrically inactivates expressing neurons.[32-34] As additional effector examples: *shibire*^{ts} or tetanus toxin could be used to silence synaptic communications, [35-40] *reaper/grim/hid* genes could be used to physically kill neurons using their own apoptotic pathways,[41,42] ricin toxin can be expressed ectopically to kill neurons, or neurons can be selectively activated using *trp1a* or a variety of channelrhodopsin transgenes. [43,44]

If GAL4 is the on-switch for a desired transgene, then GAL80 is the off-switch. GAL80 is an antagonist of GAL4; it binds GAL4 proteins and inhibits their activity.[45] To accompany the existing GAL4 collection, an assortment of *OrX-GAL80* lines was created. Since an *OrX-GAL80* library to complement the *OrX-GAL4* library does not exist

yet, researchers commonly rely on strategies which involve genetic mutations or deletions. However, these strategies usually require homozygozity of the mutation/deletion. Achieving homozygozity of a mutation while also adding transgenes to the system may involve the time-consuming creation of recombinants and multiple generations of crossing. Using mutations limits the complex combinatorial genotypes one can achieve and therefore the experimental questions that can be answered.

An example of the advantage of a GAL80 strategy is given in **Figure 2**. In order to have a single functional OSN in an otherwise silent olfactory system, the traditional method uses an Orco null mutation.[23] In this genetic setup, Orco mutant flies are anosmic, but function is restored to one OSN subset with *Or-GAL4, UAS-Orco* transgenes[24,46-50] (**Figure 2a**). An *Orco-GAL4, UAS-effector, Or-GAL80* method can be used instead (**Figure 2b**). Kir2.1 is used as an example of an effector.[32-34] Though Figure 2a may look less complicated than 2b, it is actually more time-consuming and limited. The Orco mutation must be homozygous. Since most *Drosophila* transgenes are embedded into the same two chromosomes (Chromosome 2 or 3) recombinant creations may be required to achieve this homozygozity.

What if a researcher wants to expand upon the genetic scheme in Figure 2a to add function back to pairs or groups of neurons in a nonfunctional background? Neurons seldom operate autonomously, and investigating the effect of small circuits on development or behavior would require additional genes. If the genotypes were further expanded from what is shown in Figure 2, e.g. to restore pairs or groups of functional OSNs, the necessary recombinants and generations of crossing would become cumbersome if not prohibitive. A GAL80 strategy can shorten this process by achieving

similar results in only one or two generations with no necessary recombinant creation. Furthermore, a GAL80 strategy takes advantage of the interchangeable variety of existing *UAS-transgene* lines.

The GAL80 lines are effective, specific, and have potential utility to enhance current research using the *Drosophila* olfaction model.

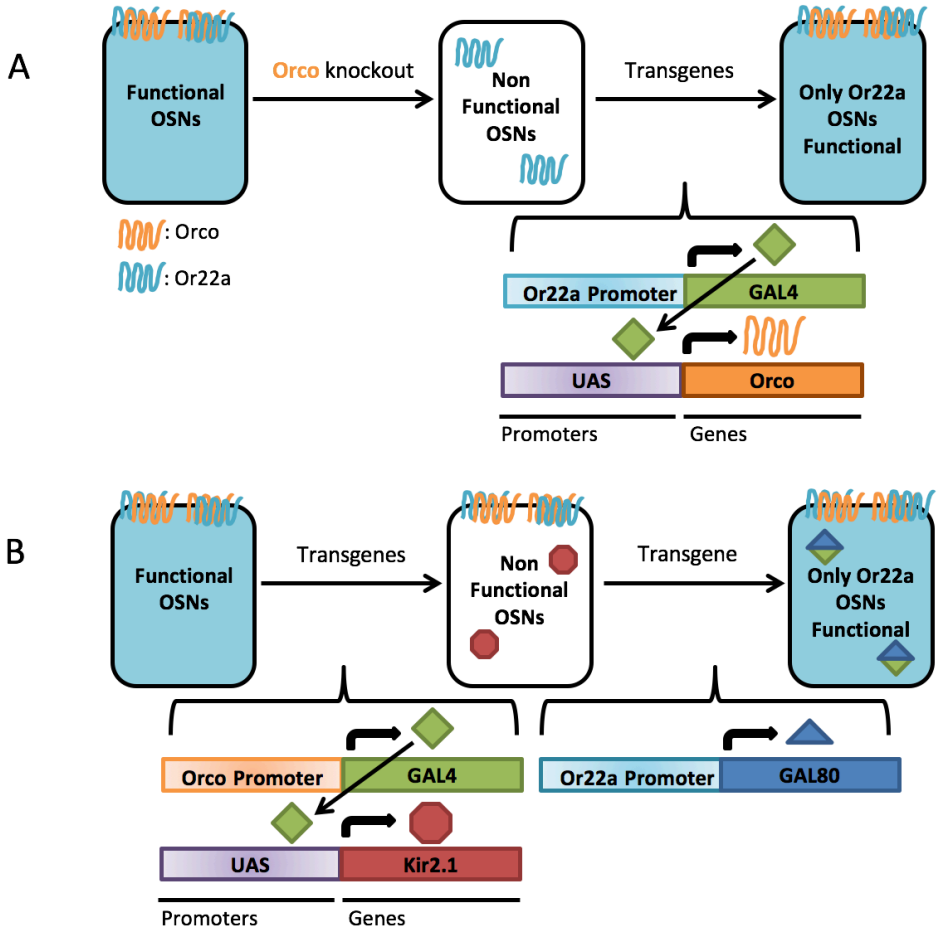

Figure 2: Advantages of using a GAL80 over a null mutation. a) **Current method with available reagents**. In order to examine a single type of Olfactory Sensory Neuron (OSN) without interference from other OSNs, one can use an Orco null mutant. Without Orco, ORs cannot reach the cell membrane or function properly. Orco mutants are mostly anosmic (unable to smell.) A single OR can then be restored using two transgenes, *OrX-GAL4* and *UAS-Orco*. *Or22a-GAL4* is shown here as an example. This fly often requires the making and validating of one or more recombinant, since the Orco mutation must be homozygous. In more complicated systems, e.g. restoring more than one OSN or using a foreign OR, multiple recombinants would need to be made and validated. This takes several months of crossing. *Figure caption continued, next page*.

Figure 2, continued b) **Using a GAL80**. GAL80 is a potent GAL4 inhibitor. All olfactory neurons could be silenced using any number of transgenes in an *Orco-GAL4, UAS-effector* genotype. *UAS-Kir2.1* is used in this figure as an example. A single OSN subtype can then be restored using an *OrX-GAL80*. *Or22a-GAL80* is used here as an example. This system requires no recombinant creation, and is amenable to using various effectors or adding additional transgenes without requiring recombinant construction. (Receptor appearance, orientation, and heterodimerization is based on previous designs.[24,51-53])

Results

Creating the GAL80 Constructs

OR promoters were chosen for the collection based on the following criteria: i) The ORs should be relevant to current research as shown by the number of studies which used that OR, ii) The ORs should represent a variety of expression patterns (larval or adult, antennae or maxillary palps, sensillary class etc.), and iii) The ORs should reflect a variety of different odorant response profiles. The promoter regions were defined based largely on the work of Couto *et al*, 2005.[10]

Equal parts GAL4 and GAL80 are not always sufficient to subtract GAL4 activity. In order to effectively eliminate GAL4 activity, the pBP-GAL80uW-6 vector was used. This vector contains a modified GAL80 sequence, designed to increase its stability and expression.[54] A few *OrX-GAL80*s were already made with this vector and used effectively.[55]

Testing GAL80 Efficacy and Specificity

To examine GAL4 subtraction *in vivo*, *OrX-GAL80* flies were crossed to flies with the genotype *OrX-GAL4, UAS-GFP*. As described in **Figure 1**, OSNs expressing the

same OR can be identified from their specific glomerulus in the antennal lobe. *OrX-GAL4, UAS-GFP* flies show robust expression of the GFP reporter gene in their respective glomeruli. However, when *OrX-GAL80* is added to the genotype, GFP expression is entirely absent, indicating a robust antagonism of GAL4 activity (**Figure 3**).

GAL80 lines were created for the following odorant receptor promoters: Or7a, Or9a, Or10a, Or13a, Or19a, Or22a, Or22b, Or33c, Or35a, Or42a, Or42b, Or43b, Or47a, Or56a, Or59b, Or 59c, Or67a, Or67d, Or71a, Or82a, Orco, Or85a, Or85b, Or85c, and Gr21a. Several of these lines also have expression in larvae. GAL4 subtraction was examined in larval brains using the *UAS-GFP* reporter gene. In larvae, GAL80 reduced but did not eliminate GAL4 activity (**Supplementary Figure 1**).

The *OrX-GAL80* lines were checked to ensure they would not have aberrant expression in untargeted OSN subtypes. The pBP-GAL80uW-6 vector contains a Drosophila Synthetic Core Promoter (DSCP). DSCP is an effective means of using enhancer elements to drive strong expression,[56] but it could also cause the GAL80s to have nonspecific or leaky expression. Therefore, a version of pBP-GAL80uW-6 was cloned with the DSCP removed. However, when the DSCP was absent, GAL80 expression was insufficient to subtract GAL4 activity (**Supplementary Figure 2**).

DSCP will not cause nonspecific GAL80 expression. I.e. an *OrY-GAL80* will not impede GAL4 activity of an *OrX-GAL4* neuron (**Supplementary Figure 3**). It can also be noted that the GAL80 subtraction does not interfere with reporter gene expression in a genetic system which does not use GAL4. When *Or22a-GAL80* is used in conjunction with *Or22a-GFP*, containing no GAL4/UAS intermediary, the GFP is still expressed

(**Supplementary Figure 3**). These images, showing subtraction of reporter gene expression, confirm that GAL4 activity is suppressed by the GAL80 lines.

To confirm GAL4 was suppressed physiologically by the GAL80s, Single Sensillum Recordings (SSRs) were used to assay electrical activity of OSNs. *Gr21a-GFP* was used to identify sensilla of interest without interfering with the GAL4/UAS/GAL80 system. Gr21a neurons are housed in ab1 sensilla. Carbon Dioxide exposure causes a robust response in Gr21a ab1C neurons [8,9,11,13,27,28]. When *Gr21a-GFP* flies were exposed to CO_2, their ab1C sensillar neurons showed robust responses (mean Δspikes/s=88, N=8 sensilla). Adding Kir2.1 to Gr21a neurons (genotype *Gr21a-GFP, Gr21a-GAL4, UAS-Kir2.1)* greatly reduced spiking responses to CO_2 (mean Δspikes/s=14, N=12 sensilla). When Gr21a-GAL80 was added (genotype *Gr21a-GFP, Gr21a-GAL4, UAS-Kir2.1, Gr21a-GAL80),* responses to CO_2 were restored (mean Δspikes/s=94, N=6 sensilla) (**Figure 4**). These results confirm that GAL80 is able to prevent GAL4-induced activity in a physiological experimental paradigm. (All physiology data collected and analyzed by collaborator Ali Afify.)

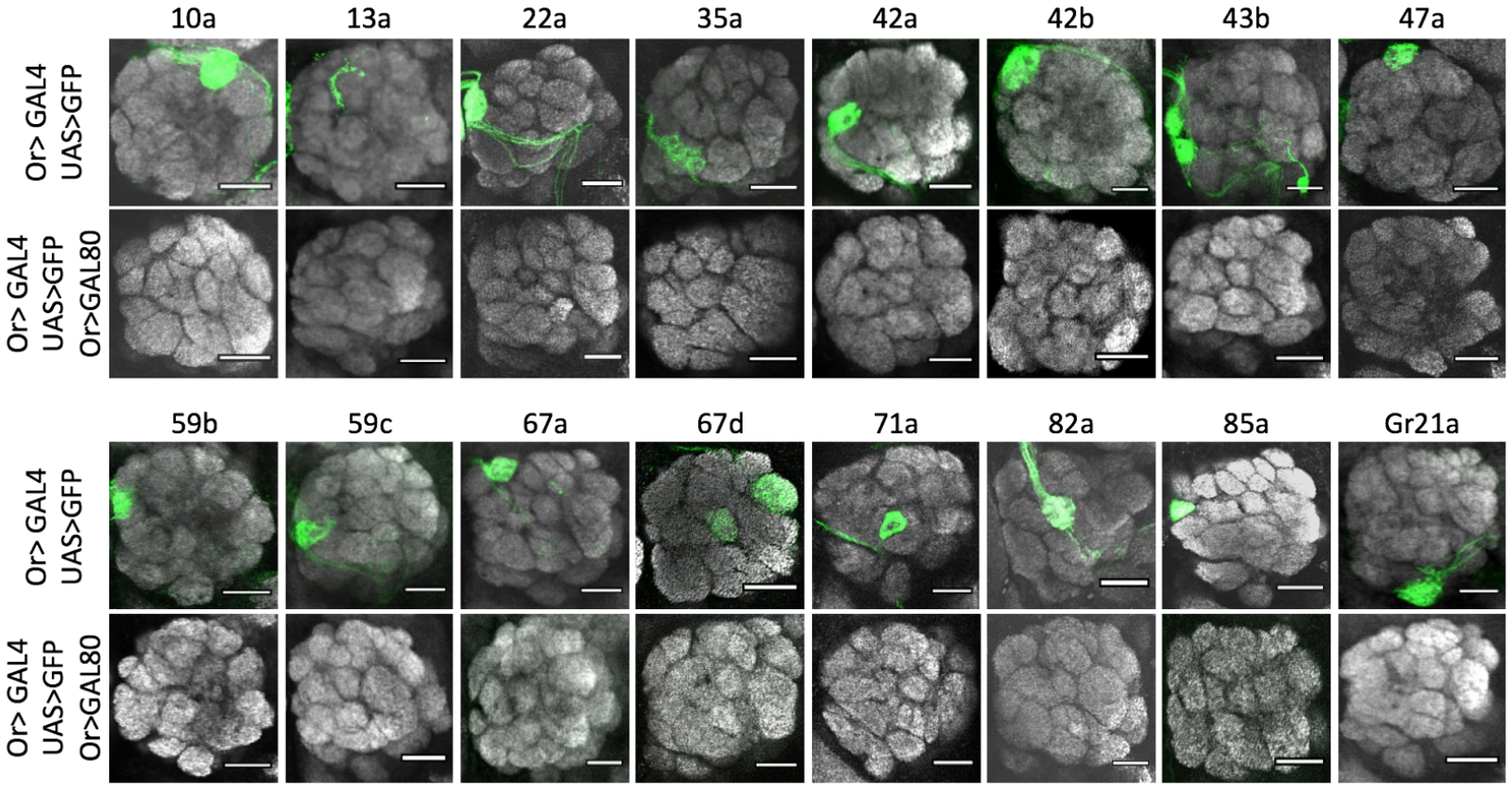

Figure 3: OR-GAL80 reagents eliminate GAL4 activity. All antennal lobes are stained with anti-nc82 (a general neuropil marker, grey) and anti-GFP (green). The orientation of each image is dorsal-up, ventral-down, lateral-right, medial-left. Scale bars indicate 20μm. Each of the brains shown has the genotype *OrX-GAL4, UAS-GFP*. The specific receptor promoter is given above each column. The top row in each set shows GFP expression in these lines without GAL80. Notice how each neuron's target in the antennal lobe glomeruli is expressing GFP. Each bottom row shows the brains containing an additional *Or-GAL80* gene. Note how GAL80 effectively inhibits GAL4, as seen by the elimination of GFP expression. The images are representative of the 5-20 brains examined per genotype. GAL4 inactivation was 100% penetrant in one day old female flies. Not shown to save space: Or 7a, Or9a, Or19a, Or22b, Or33c, Or56a, Or85b, Or85c, and Orco.

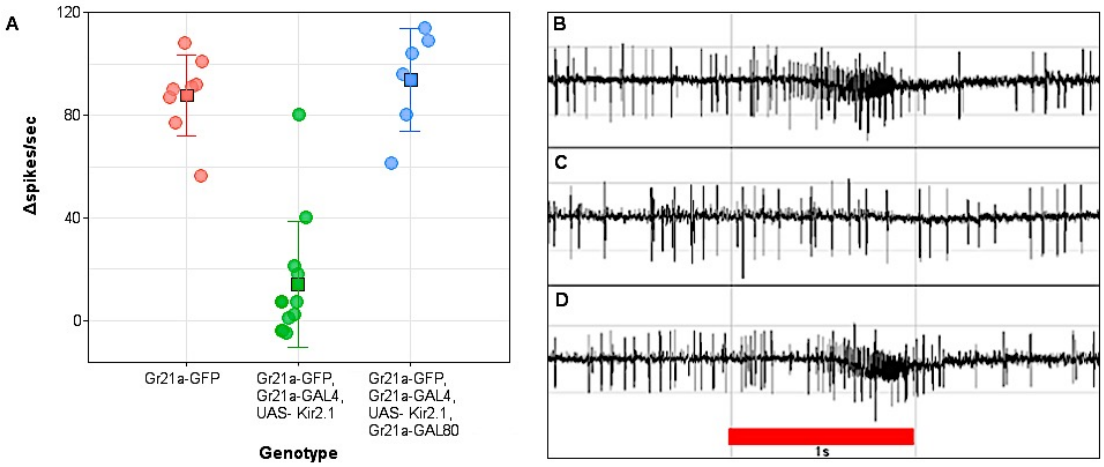

Figure 4: ORN responses to CO_2 in Single Sensillum Recordings (SSR). a) **Box plot of SSR responses.** Ab1C neurons in *Gr21a-GFP* flies respond strongly to CO_2, adding *Kir2.1* reduces response to CO_2, and response is restored when *Gr21a-GAL80* is added. Each circle shows response in an individual sensillum, and filled squares indicate the means. b-d) **Examples of SSR traces** for: b) *Gr21a-GFP*, c) *Gr21a-GFP, Gr21a-GAL4, UAS-Kir2.1*, and d) *Gr21a-GFP, Gr21a-GAL4, UAS-Kir2.1, Gr21a-GAL80*. Figure and caption credit: Ali Afify.

Behavior

To demonstrate how experiments can be simplified using GAL80 reagents, the GAL80s were used alongside a genetic strategy to create flies with a single functional OSN (**Figure 2**). The transgenic genotypes are easier to construct than those created by classical genetics, but the two systems are expected to be quite similar in behavior. Insect olfactory neurons do not require odor-evoked activity to develop with complete fidelity [14,23,57-59], and therefore both Orco null and *Orco-GAL4, UAS-Kir2.1* brains should have normal circuitry, despite their nonfunctional neurons. Orco null mutants also have greatly diminished spontaneous activity, and Kir2.1-containing neurons are expected to show little to no spontaneous firing [46,48].

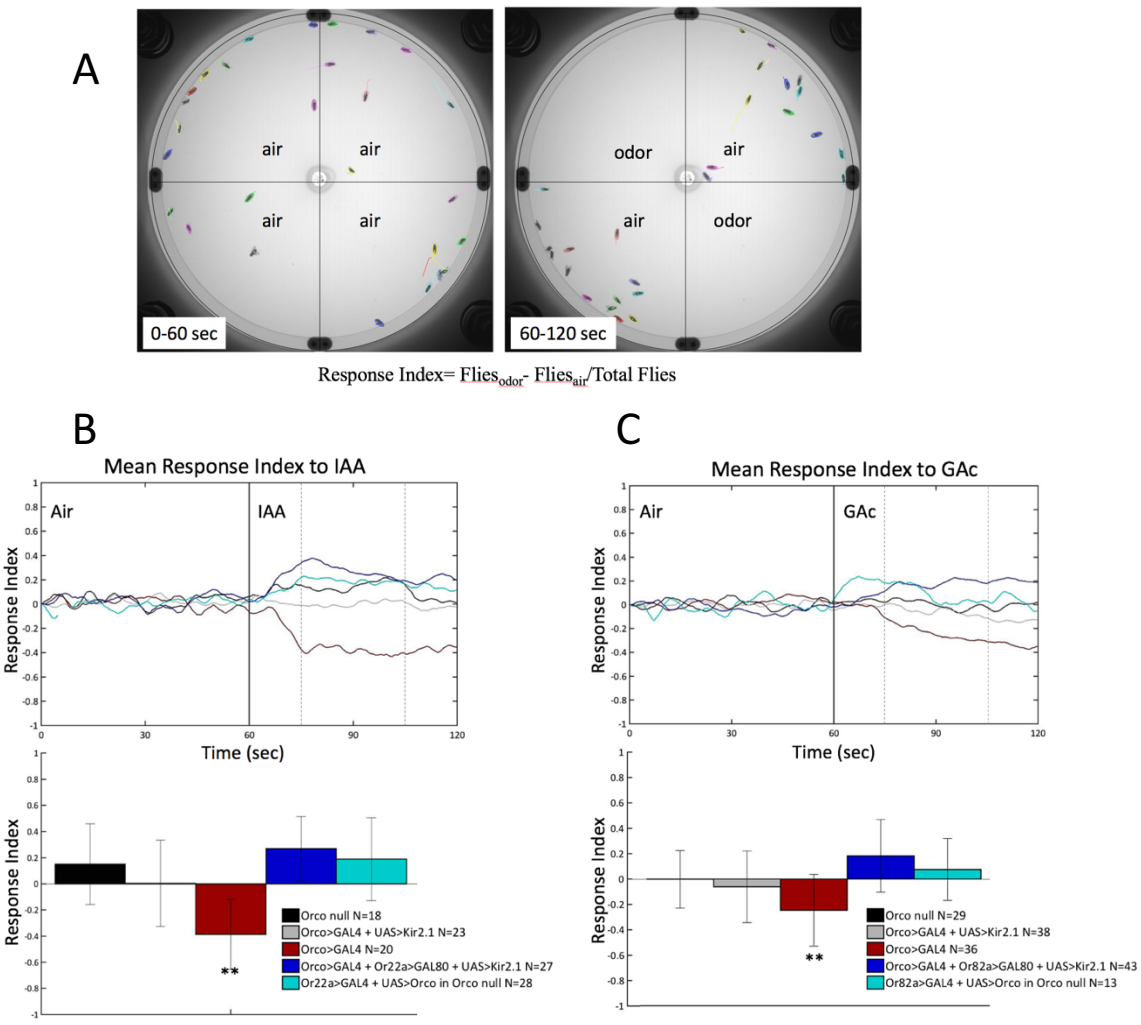

Figure 5: Use of OR-GAL80 reagents in a behavioral experiment a) **Olfactory Arena Setup.**[60] Flies are freely walking in a circular enclosure. The vertical and horizontal lines are added to indicate quadrant barriers, but no such physical barriers exist in the arena. All four quadrants receive air for one minute, and then two quadrants along a diagonal receive odorant for one minute. Diagonal quadrant pairing is randomized. In this example, flies find the odorant aversive and segregate into air quadrants. The colored outline around each fly was added during tracking using Ctrax software.[61] The response index in each frame is measured. Response Index= Flies$_{odor}$- Flies$_{air}$/Total Flies. Each N represents a trial of 20-30 flies. E.g. A response index of -0.5 indicates ~23 of 30 flies are in the air quadrants and the odorant is aversive. b) **Comparison of reagents in olfactory behavior using Isoamyl acetate (IAA)**. Flies are added to the arena as described in A. Odorant is 1:1000 Isoamyl acetate (IAA) in mineral oil. Neurons expressing Odorant Receptor 22a (Or22a) respond to IAA.[6,7,9,11] The top panel shows the mean response index of each genotype over the entire course of the trial. Dotted lines indicate the time interval of the analysis shown in the bottom panel, time= 75-105 seconds. The bottom panel shows the mean response index of flies over the middle part of the odorant exposure. *Figure caption continues, next page*

A simple odor preference test was used to assay both types of adult flies. Flies were allowed to walk freely in a circular arena. The arena is divided into four quadrants that are separated by air flow but not by physical barriers. After one minute of all four quadrants receiving air, odorant is delivered to two quadrants along the diagonal [60]. The diagonal quadrants receiving odorant were randomized. Flies were video recorded by a suspended camera and their motions tracked using Ctrax software [61] (**Figure 5a**). Response index was measured in each frame. Response Index= $Flies_{odor}$- $Flies_{air}$/Total Flies, so 0 indicates no response, +1 would be total attraction, and -1 would be total aversion. Each N represented an experiment involving 20-30 flies. Therefore, if an N had an RI of -0.5, about 23 of 30 flies were in the air quadrants.

Or22a and Or82a were tested since they represent opposite ends of the odorant tuning spectrum. Or22a is broadly tuned and its OSN responds to multiple odorants; Isoamyl acetate (IAA) is one odorant that evokes a strong response. Or82a is narrowly tuned, responding to only one known odorant, geranyl acetate (GAc) [8,9,11,13]. Or22a genotypes (**Figure 5b**) received 1:1000 IAA in mineral oil and Or82a genotypes (**Figure 5c**) received 1:100 GAc in mineral oil. The mean response index for the middle part of the odorant exposure (time = 75-105 seconds) was calculated. The positive control was *Orco-GAL4* with no effector added; this line and the OrX-GAL80 lines were made in a w^{1118} background. These flies find both odorants aversive, as shown by a negative and significantly lower response index to all other genotypes ($p \leq .0001$ for IAA and $p \leq .006$ for GAc). *Orco* null and *Orco-GAL4, UAS-Kir2.1* flies served as negative controls and had response indices around 0, showing they are anosmic as expected. *Or22a-GAL4, UAS-Kir2.1* flies did not find IAA aversive, and *Or82a-GAL4, UAS-Kir2.1* flies did not

find GAc aversive (**Figure 5b and c**), suggesting that Or22a and Or82a are each necessary for behavioral responses to their respective odorants.

As noted previously, two genotypes for each OR had only a single functional OSN subset in an otherwise nonfunctioning olfactory system (**Figure 2**). One group represents the classic strategy (*OrX-GAL4, UAS-Orco* in an Orco null background) and the other represents the GAL80 strategy (*Orco-GAL4, UAS-Kir2.1, OrX-GAL80*). When O22a or Or82a OSN function is restored, neither of the single-functional OSN genotypes is sufficient alone to restore normal aversive behavior. However, for both Or22a genotypes with IAA and Or82a genotypes with GAc, the behavioral variance for the classical method vs the GAL80 method is comparable (F-test for the 75-105sec window is p=.44 for the Or22a/IAA group and p=.45 for the Or82a/GAc group). Since both groups have similar variance, this result supports the idea that the GAL80 strategy can be adopted as a substitute for the more traditional and time-consuming breeding strategy.

Discussion

The lack of aversive behavior in flies with a single functional OSN subtype is not consistent with some previous studies that showed one functional OSN was sufficient to restore aversive behavior. Fishilevish et al (2005) used larvae in their study to restore aversion with a single functional OSN subtype, but the larval olfactory system may be fundamentally different in this respect. Gao et al (2015) gave convincing evidence of aversive restoration in adults, though they didn't use Or82a and they tested Or22a with a different odorant (E2-hexenal) of a higher concentration. It could be that the principle of single-OSN aversive behavior is highly dependent on the odorant and receptor used. [62]

also showed that single glomerular activity is sufficient to invoke a behavioral response, but that study was done using an intact and fully functional olfactory background, so some neuronal cooperation may still have occurred. [47] provided evidence that a single functional OSN subtype is sufficient to learn odor discrimination, but the experiments here do not extend to assess learning or memory.

Despite some specific circumstances, the lack of aversive rescue is generally consistent with the current models of odor coding by the olfactory system. I.e. a coordinated effort of many OSNs is usually required to produce a behavioral output. Paired neurons in sensilla can affect the firing dynamics of their neighbors in the periphery [14,63,64], and downstream neurons such as interneurons and projection neurons may rely on synchronized input from multiple OSN types [2,46,65-70]. The behavioral conditions here give no effect and are included as a demonstration of GAL80 possibilities. The hope is that additional researchers will use the reagents and validate them in their own assays and use them to study effects of interest.

The collection of GAL80 lines subtracts GAL4 activity efficiently and specifically in OSNs. In anatomical studies, reporter gene expression from the GAL4/UAS system is suppressed. Neurons silenced with Kir2.1 expression have normal firing capacity restored when GAL4 is antagonized using the GAL80 lines. In behavioral assays, the GAL80s have comparable variations to traditional methods that use mutant backgrounds. However, using a GAL80 transgene will be more flexible than mutant lines and less cumbersome than crafting the required recombinants as the complexity of the genotype increases.

Though in some special circumstances, olfactory sensory neurons can produce behaviors autonomously, this is not a widely applicable principle. Researchers encounter a significant technical obstacle to the understanding of olfactory function if they need to create genotypes with small groups of interacting neurons in isolation. The tools presented here facilitate the activation or deactivation of combinations of particular neurons, thereby overcoming this obstacle. The lines are available to order through Bloomington Stock Center.

Supplemental Figures

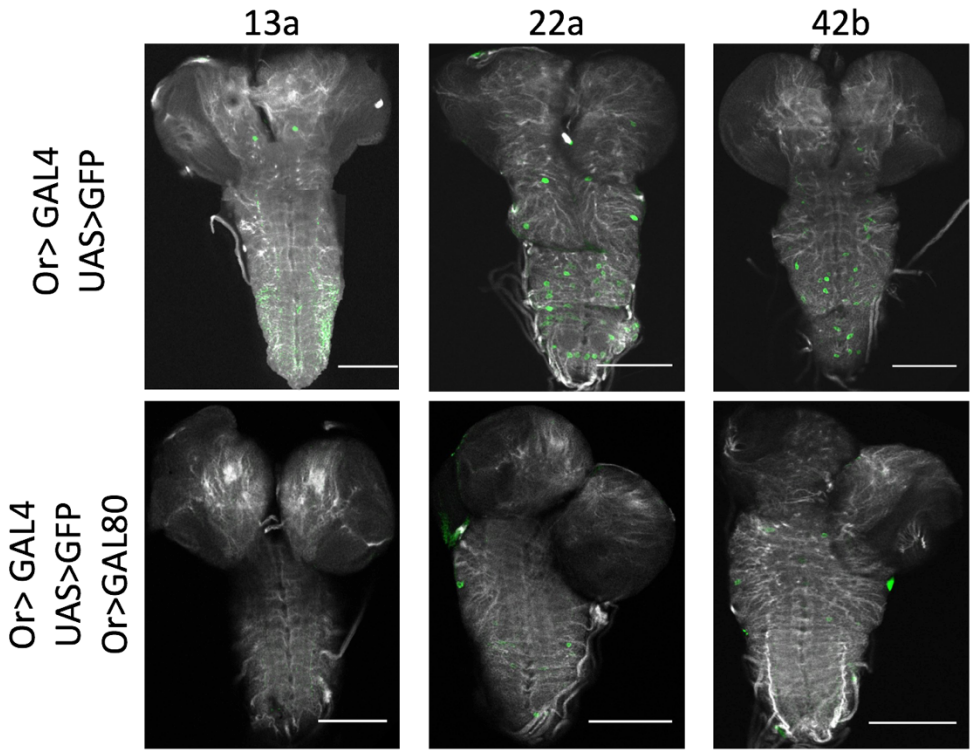

Figure S1: GAL80 reduces GAL4 expression in larvae. Brains are immunostained with anti-nc82 (grey) and anti-GFP (green). Scale bars indicate 100μm. Or13a, Or22a, and Or42b are examples of odorant receptors expressed in larvae. *OR-GAL4, UAS-GFP* genotypes give GFP expression patterns specific to the odorant receptor expression pattern. When the *Or-GAL80* is added, there is some reduction of GFP expression, but it is not entirely eliminated. For example, adding *Or13a-GAL80* subtracted GAL4 activity from cell bodies in the brain but did not entirely remove expression from the GFP-expressing axons in the ventral nerve cord.

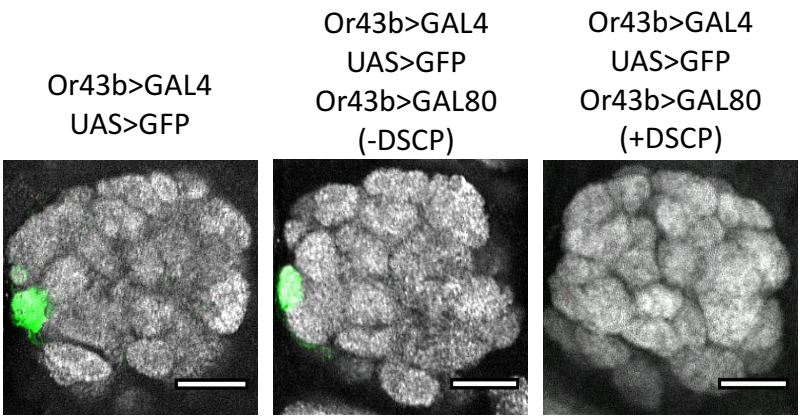

Figure S2: DSCP required in destination vector for effective GAL80 expression. Antennal lobes are oriented and stained as described in Figure 3. Scale bars indicate 20μm. OSNs expressing Odorant Receptor 43b (Or43b) are shown as an example of an *Or-GAL80* made with a vector that does not contain DSCP. DSCP is a powerful promoter, and it was removed from the pBP-GAL80uW-6 destination vector so that no aberrant expression of the GAL80 would be present. However, without the DSCP, the OR promoter itself was insufficient to eliminate GAL4 activity. I.e. GFP is still expressed specifically in the Or43b glomerulus of the antennal lobe. When flies were made using a vector with DSCP added back, the GAL80 expression was sufficient to eliminate the GAL4 activity.

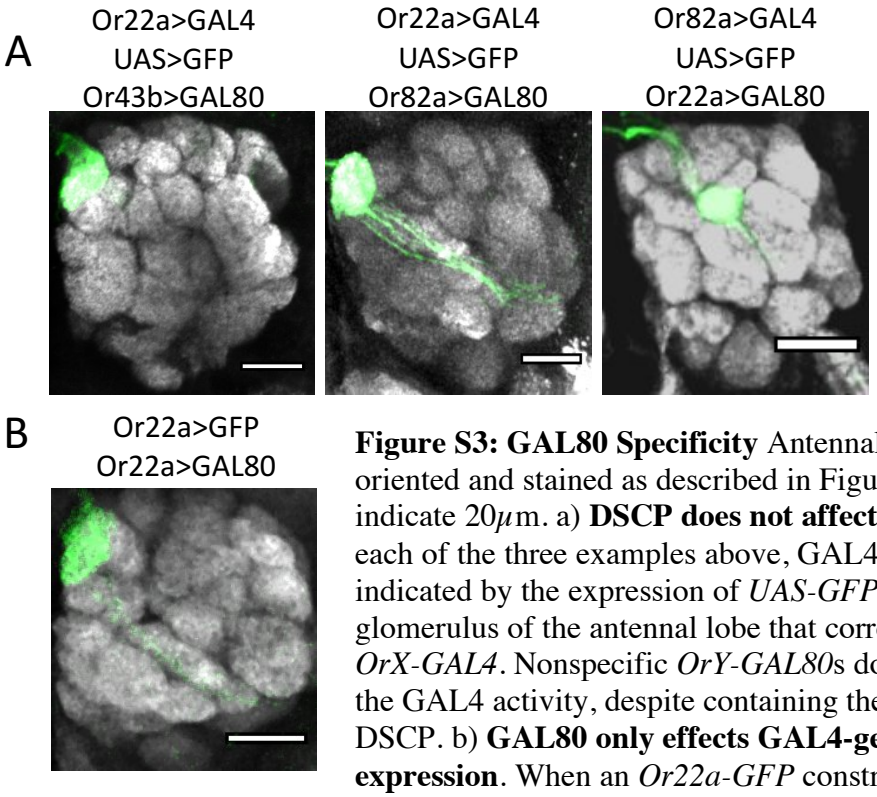

Figure S3: GAL80 Specificity Antennal lobes are oriented and stained as described in Figure 3. Scale bars indicate 20μm. a) **DSCP does not affect specificity**. In each of the three examples above, GAL4 is active as indicated by the expression of *UAS-GFP* in the specific glomerulus of the antennal lobe that corresponds to the *OrX-GAL4*. Nonspecific *OrY-GAL80*s do not eliminate the GAL4 activity, despite containing the promoter DSCP. b) **GAL80 only effects GAL4-generated expression**. When an *Or22a-GFP* construct is used to express GFP, instead of the GAL4/UAS system, *Or22a-GAL80* does not interfere with GFP expression.

Receptor	Gene location	PCR Size (bp)	Primer	Primer Sequence 5'-->3'	Tm (C)	Primer Length	Primer Location
Or7a	X: 8,164,266- 8,165,708 [-]	1291	JE_Or7aP_right	GCTGATGGACTTTTGACGCCTGGGAATATTCGAATGGC	65.2	38	X: 8,165,710- 8,165,747
			JE_Or7aP_left	CACCGGACACCGCATCCCGATCAAGACACACG	66.2	32	X: 8,167,000- 8,166,969
Or9a	X: 10,458,186- 10,459,676 [-]	1074	JE_Or9aP_right	GCGGACTGTACAGTCGTTGGGTTCTTATACTTTCCAC	65.3	37	X: 10,459,686- 10,459,722
			JE_Or9aP_left	CACCCGGTCTTCGATAACAGAAGGGTATGCCAGTCGTTGC	64.6	40	X: 10,460,759- 10,460,720
Or10a	X: 11,413,467- 11,417,422 [-]	5241	Or10aP_right	GATGGATATAACTATGTGAACGACATCCTGGCAAGGAATACTC	62.1	43	X: 11,417,404- 11,417,446
			Or10aP_left	CACCGCTGTTTGCTCGGCTCGTCAGGTCG	64.8	29	X: 11,422,644- 11,422,616
Or13a	X: 15,974,425- 15,976,706 [+]	1132	Or13aP_right	GACTATCTGATAAATGCCACAGCACTAGGTACATCTTAAGGC	62.6	42	X: 15,974,424- 15,974,383
			Or13aP_left	CACCCAATCCCGGCCATCCCATCCATACC	65.2	30	X: 15,973,293- 15,973,322
Or19a	X: 20,141,819- 20,143,188 [-]	4814	JE_Or19aP_right	GGTTGTTCGCCTCTTTGAAGCAGCTCTCCG	65.4	30	X: 20,143,189- 20,143,218
			JEOr19aP_left	CACCGAATTCCCCTCTACCCCGCATCCAC	65.7	29	X: 20,148,002- 20,147,974
Or22a	2L: 1520613-1522151 [+]	5293	Or22aP_right	CTTGTCCGTGGCTTTGTTTGAATATTTGCTTGAGCTGGG	65	39	2L: 1,520,612- 1,520,574
			JEOr22aP_left	CACCGCC AGC GGG GTT GAA GGA TGG AAT GTG G	58.4	32	2L: 1,515,324- 1,515,351
Or22b	2L: 1,522,697- 1,524,257 [+]	1304	JE_Or22bP_right	CGTCCGTGGCTCTTTTTGATTATTTGCTTGAGCTGG	64	36	2L: 1,522,700- 1,522,665
			JE_Or22bP_left	CACCGCTCACCGAGTGCATTCGGGATCATCGATTGC	65.2	36	2L: 1,521,397- 1,521,432
Or33c	2L: 11,937,969- 11,939,202 [+]	1895	JE_Or33cP_right	GTTCACCTAATGCACATTTCCCAGCAAGGCTGGAG	64.8	35	2L: 11,937,967- 11,937,933
			JE_Or33cP_left	CACCCGCAGTAAATTGATGGGCGTAACGATGTGGGAC	65.4	37	2L: 11,936,073- 11,936,109
Or35a	2L: 15,622,068- 15,623,558 [-]	2522	Or35aP_right	GGAGTGAAGACTGTTGAATAATGGCTGCTCTCCTCCG	65	37	2L: 15,623,562- 15,623,598
			Or35aP_left	CACCGACGGCCCAACCAAGGAAAAGAAGAAGCGAC	63.1	34	2L: 15,626,083- 15,626,050
Or42a	2R: 5,791,441- 5,792,967 [-]	1276	Or42aP_right	GCACTCTAATTTCAACAATTGAACTAAAGCACCGTCTGCAATG	62.7	43	2R: 5,792,971- 5,793,013
			Or42aP_left	CACCGGACTTTTAGCTCTTGGTACCCCGGTAC	66	32	2R: 5,794,246- 5,794,215
Or42b	2R: 5,797,195- 5,798,512 [-]	5340	Or42bP_right	CGGCGTTATTGTGCGCACTGCTCTGG	65.4	26	2R: 5,798,515- 5,798,540
			Or42bP_left	CACCGCCAGAGGATGCGTGTGTGTCTGTCTGAGTC	62.4	33	2R: 5,803,854- 5,803,822
Or43b	2R: 7,920,835- 7,922,604 [-]	486	Or43bP_right	CGAATGTTTAAGGCTATAATAATACTGGCGATAGGAGGAGCTCGG	64.6	45	2R: 7,922,553- 7,922,597
			Or43bP_left	CACCGCTGTAGCTGTAGGGCAGACTGAATTTGTCCGTTCAC	65.4	41	2R: 7,923,038- 7,922,998
Or47a	2R: 11,250,368- 11,251,913 [+]	5591	Or47aP_right	GTCGACAAGGGTTAATTCGGCCTCACACTAAGTCAAG	65.2	37	2R: 11,250,377- 11,250,341
			Or47aP_left	CACCGCCGTTGGTTCGGCATCAGGAGCAG	65	29	2R: 11,244,787- 11,244,815
Or56a	2R: 19,769,461-19,771,233 [-]	5289	JE_Or56a_right	GTTAAACTGTTTAGCGTTAACCATATTCAAGGGTC	59.6	35	2R: 19,771,234- 19,771,268
			JE_Or56a_left	CACCGGGCTGTTTTTCGACTGCTTCTGCTGGTGAC	65.2	35	2R: 19,776,522- 19,776,492
Or59b	2R: 23,470,165..23,471,775 [-]	650	Or59bP_right	CCCACTGACCGGTGTCGGTG	65.4	21	2R: 23,471,715- 23,471,735
			Or59bP_left	CACCGGCGAGAAGTTCTTCAGTGACAGGAGCAATGGC	64.6	37	2R: 23,472,364- 23,472,328
Or59c	2R: 23,472,300..23,473,753 [-]	2094	Or59cP_right	GCAGGCGCTTGAAGAAGAACTTGGTCATCTTTGCG	65.4	35	2R: 23,473,576- 23,473,610
			Or59cP_left	CACCGCCTGACGACGACTTTCAAGACAAGAACAGCCATCG	63.9	40	2R: 23,475,669- 23,475,630
Or67a	3L: 9,529,067..9,531,386 [+]	1564	Or67aP_right	CACTTTCAATATGGTTTGAATAAACACTGATTGATACAGGAAAG	58.8	44	3L: 9,529,900- 9,529,857
			Or67aP_left	CACCGCTCGCAAATTCAGTACCACACGCCACTTCC	65.8	35	3L: 9,528,337- 9,528,371
Or67d	3L: 10,273,204..10,274,624 [+]	5129	Or67dP_right	GTTTGTTAGCTATGCAACTTAAAGGAGAACTGTTTTTTAATTGTC	60.1	45	3L: 10,273,202- 10,273,158
			Or67dP_left	CACCGCGACAGGACAACCCGCAGCAGAAG	65	29	3L: 10,268,074- 10,268,102
Or71a	3L: 15,076,907..15,078,447 [-]	4059	Or71aP_right	GCACAAGTCCAAGCTCGGATTATTAAAGTCCGATTTTGGAGC	64.9	42	3L: 15,078,449- 15,078,490
			Or71aP_left	CACCGTGGAGATGTCACGGAGGGATGAGTTGATTGCC	63.6	37	3L: 15,082,507- 15,082,471
Or82a	3R: 82694-84166 [+]	1423	Or82aP_right	GACCCCACTTTCTAGAACATGAAAGGATTGCGCTGCTAACG	65.6	41	3R: 82,693- 82,653
			Or82aP_left	CACCGGATCGCACACGGGCAATGCATAC	65.8	28	3R: 81,271- 81,298
Orco	3R: 5,407,183..5,412,406 [-]	5058	JE_OrcoP_right	CCTGTTGAGCGGCGGAAATTGCACGAC	65.3	27	3R: 5,409,924- 5,409,950
			JE_OrcoP_left	CACCGCCTATGTCCTGGCTGCTCCTCATTCCC	63.1	32	3R: 5,414,981- 5,414,950
Or85a	3R: 8,321,747..8,323,054 [+]	2503	Or85aP_right	GAAAGTTTAGAGGTTTCGATTGACTTGAACTTTGTCACCTGAAG	62.8	44	3R: 8,321,742- 8,321,699
			Or85aP_left	CACCGACCACCCCGAACTCAAAACGCAAACAATCCG	66.2	36	3R: 8,319,240- 8,319,275
Or85b	3R: 8,510,077..8,511,358 [-]	2657	JE_Or85bP_right	CCTTTAGTTGGTCGGAACTGAGGTAGAGAAGTGTCCTTTCTG	66	42	3R: 8,511,359- 8,511,400
			JE_Or85bP_left	CACCGTTCGTTTTGCTTTTGACCCGCTTGGTTCGC	65.9	34	3R: 8,514,015- 8,513,982
Or85c	3R: 8,511,734..8,513,022 [-]	4822	JE_Or85cP_right	CCGACGTGAAAATAATCCAATAAGTGATGGTCGGAATTC	61.9	39	3R: 8,513,026- 8,513,064
			JE_Or85cP_left	CACCGCGGAGACCCATGGTTCCAGTGATGTAGC	64	33	3R: 8,517,847- 8,517,815
Gr21a	2L: 780,482..782,885 [+]	1756	Gr21aP_right	CGTGCGATCGAGGAAAGTCATACGGCTTCC	65.2	30	2L: 781,296- 781,267
			Gr21aP_left	CACCCGAGTCATCCCCTGCTTAAGGCGCAG	65.6	30	2L: 779,541- 779,570

Table S1 PCR Primers: The primer sets used to generate the PCR products for odorant receptor promoters. Promoter locations were chosen based on the work of Couto *et al* 2005.[10] Promoters were created so their orientation to the *GAL80* gene in the destination vector matched their orientation to the *OR* gene on the chromosome. "Right" primers always indicate those closest to the start codon of the gene. "Left" primers are on the far end of the promoter and have an added CACC to the 5' end for insertion into a pENTR/D-TOPO entry vector.

Sequencing Primers for OR Promoters	
Attr_Forward	5′-ggcgtatcacgaggccctttcgtcttcaag-3′
Attr_Reverse	5′-cggtgtgcctaggcatcagtggttgaacc-3′
Or10a_seq1	5′-cgtctggacgggcagacggtc-3′
Or10a_seq2	5′-cgctgcggtcatcaccccactcc-3′
Or10a_seq3	5′-cggtgggaaattagagtatacaccgacacgagtgc-3′
Or10a_seq4	5′-cgcattcgcattcggtttcagtttcagtttcaggcc-3′
Or10a_seq5	5′-cgtgttgcgtgttaagcagtgggtgtgc-3′
Or10a_seq6	5′-ggtcgcactcgaaaacgcaaactcgaactc-3′
Or19a_seq1	5′-gcaggtcgctagtactaggcggtacctg-3′
Or19a_seq2	5′-cgagaatcttgacttctgctggctgcgtgg-3′
Or19a_seq3	5′-cgtctagtcgaaggggtttggcaaaagcg-3′
Or19a_seq4	5′-ggcattcggtgtatggagttcagcggagac-3′
Or19a_seq5	5′-gctgaagccatgtcaacctgctcggattctcag-3′
Or22a_seq1	5′-ggacagcaaaccacacccgaaggacc-3′
Or22a_seq2	5′-ccttcgacttgaacgatttggccatgtcagtccag-3′
Or22a_seq3	5′-cgagggcaaaggacgctccagttgtg-3′
Or22a_seq4	5′-gcgtgcgtaccaatccatttgtcatcagatcgc-3′
Or22a_seq5	5′-cgcagcgggtccctcgatcaactc-3′
Or33c_seq1	5′-gcctggtttccatacgatgtgcaggccac-3′
Or35a_seq1	5′-ggcacagtttcgggccgtgctacag-3′
Or35a_seq2	5′-ggattgtcgggattttgcagagcggagtgg-3′
Or42b_seq1	5′-ggcgaccaaaggagcaagtgacaacaagaagtgc-3′
Or42b_seq2	5′-ccgtctcaatgtattgctcgggttctaccg-3′
Or42b_seq3	5′-gccgaacaactgcagctcattgacacaaccg-3′
Or42b_seq4	5′-ccggctgtacgcttgcttgtctgtgtg-3′
Or42b_seq5	5′-gcgcgctccgaaaatgtgtgtaagctactgc-3′
Or47a_seq1	5′-ggggtcagggccttagaacttctcttctgcaag-3′
Or47a_seq2	5′-ccgcagctttggttccaaaagttacagttgcac-3′
Or47a_seq3	5′-ccatacaaatcagtaggcgtgttatttcttgactcgcacg-3′
Or47a_seq4	5′-cgacctgtcacttagctgccgatgcac-3′
Or47a_seq5	5′-gggagcgaaccatgccaacgatggag-3′
Or47a_seq6	5′-cgcccacacaagcttatttcactcttcaaccgtctg-3′
Or56a_seq1	5′-cggttgttctcgctgcctgggcttc-3′
Or56a_seq2	5′-cgatttcgcccttaaccaccggtaaactgg-3′
Or56a_seq3	5′-ggacgcttcgtgttggctgtttcacttctg-3′
Or56a_seq4	5′-ccggctgctccttctttcaaccacacg-3′
Or56a_seq5	5′-ggagtcagaccacacgagctctcgatgg-3′
Or59c_seq1	5′-cggaggagcgcatcgaggatgacacg-3′
Or59c_seq2	5′-ccagtgtggcacgtgcaatgtgccac-3′
Or67d_seq1	5′-gctgctgatttcgctctggcctgccaacttatgc-3′
Or67d_seq2	5′-ccccaaactgctgagaaaccacaggcatgac-3′
Or67d_seq3	5′-ccaccgcccaactgcggatgtcc-3′
Or67d_seq4	5′-ggtcacatgacggtcctggcagttcctag-3′
Or67d_seq5	5′-cggaatgccacgcactttccactggaagaag-3′
Or71a_seq1	5′-gctgagctgcttctgagtcccagtcacagg-3′
Or71a_seq2	5′-ggacatcgccaccgagttggagcag-3′
Or71a_seq3	5′-cggggcactatttgttgttcttttgtgcgacacc-3′
Or71a_seq4	5′-cgatctctcccgatcccatgcgctctctc-3′
Or85a_seq1	5′-ggagtcatcggcagcggggataccg-3′
Orco_seq1	5′-gcacgtgagttgctgaagctgccagatgg-3′
Orco_seq2	5′-cgtgctgcagttctgggaaagggagcag-3′
Orco_seq3	5′-cgcacactatgaaaccgaatggcacacac-3′
Orco_seq4	5′-ggctgcagggctcacgatgtccg-3′
Orco_seq5	5′-gcctaccgaaattcagtgcctatgagaactgagaacg-3′
Or85a_seq2	5′-cgtggtacctggccaggatcttggacac-3′
Or85b_seq1	5′-ggatgggaatcgtgattgcgtttgcctaggc-3′
Or85b_seq2	5′-cggttggataggtatctgcgatcttgttcacg-3′
Or85c_seq1	5′-ccagcgtccttttgctccagctcctg-3′
Or85c_seq2	5′-ggttgtcccgctttctttggggttcaattggc-3′
Or85c_seq3	5′-gggaccagcagcgtacattgatgcatatcctgc-3′
Or85c_seq4	5′-ccagattcttgtcggccggatgttgtaggc-3′
Or85c_seq5	5′-ccacataccacactcactcccacatccacacc-3′

Table S2 Sequencing Primers: Smaller OR promoters could be sequenced in the pBP-GAL80uW-6 destination vector using Attr_for and Attr_rev primers. Primers used to sequence larger promoters are identified by OR name.

Auxiliary Projects

Restoring Function to Neighboring Neurons

As shown in **Figure 5**, a single neuron working alone in an otherwise silent olfactory system was insufficient to restore aversive behavior. But what if multiple neurons were added back? In each sensillum on the periphery, OSNs exist in characteristic pairs, or sometimes groups of 3 and 4. For example, an Or47a-expressing neuron always co-exists with an Or82a-expressing neuron inside the ab5 sensilla. (Ab5 stands for "antennal basiconic 5"; basiconic is one of several senillary classes. Classes are based on outward appearance and shape.)[10,71,72] In 2012, *Su et al* beautifully demonstrated the principle of "lateral inhibition." I.e. neurons that share a sensillum on the periphery but that share no synapses can still modify each other's responsiveness. E.g. when the Or47a OSN is responding to an odorant, it hyperpolarizes the Or82a OSN.[63] Even though these two neurons don't respond to a single common odorant,[8,9,11,13] they may still interact nonsynaptically to influence perception and behavior.

The genotypes given in **Figure 5** were expanded upon to examine the effects of neighboring neurons on olfactory behaviors. As examples, Or22a and Or82a were used since they represent opposite ends of the odorant tuning spectrum—Or22a is very broadly tuned (meaning it responds to a wide variety of odorants) while Or82a is very narrowly tuned. An Or22a OSN pairs with and Or85b OSN in Ab3 sensilla (**Figure A1a**). Both receptors are broadly tuned and both respond strongly to Isoamyl acetate (IAA). The Or82a OSN responds to only one known odorant, Geranyl acetate (GAc.) However, it is paired in its sensillum with Or47a OSNs which are broadly tuned to many odorants, but cannot detect GAc[8,9,11,13] (**Figure A1d**).

First, the function of each OSN was removed individually using *UAS-Kir2.1*. When *Or22a-GAL4 or Or85b-GAL4* are crossed to *UAS-Kir2.1,* flies have significantly diminished responsiveness to IAA (**Figure A1c**). This is somewhat surprising; even though these neurons are capable of detecting IAA and are rendered nonfunctional, there are multiple additional ORs that respond to IAA that are still functional. Apparently, the coordinated effort of some or all IAA-sensing neurons is necessary to produce aversion behavior. Similarly, GAc aversion is lost in *Or82a-GAL4, UAS-Kir2.1* flies. This is understandable, as Or82a is the only OR in the entire receptor repertoire that can respond to GAc. [8,9,11,13] What is interesting however, is that GAc aversion is also lost in *Or47a-GAL4, UAS-Kir2.1* flies (**Figure A1f**). This illustrates that some input from Or47a OSNs is required for appropriate perception and reaction to GAc, even though Or47a OSNs themselves do not detect GAc.

Would neuron pairs functioning together in a nonfunctional background be sufficient to restore aversion? Or22a and Or85b function was added back to an Orco null background using *Or85b-GAL4, Or22a-GAL4, and UAS-Orco*. The same was done for the ab5 pair of Or82a and Or47a using *Or82a-GAL4, Or47a-GAL4, and UAS-Orco*. In either case, the functional pair was insufficient to restore aversion (**Figure A1**, green). Because of this negative result, the experiment was not repeated using a GAL80 strategy (I.e. *Orco-GAL4, UAS-Kir2.1, Or82a-GAL80, Or47a-GAL80*.) However, this does show that even for an exclusive odorant/OR pairing such GAc/Or82a, input from more than one OSN is required to produce a behavior. This is predictable, considering

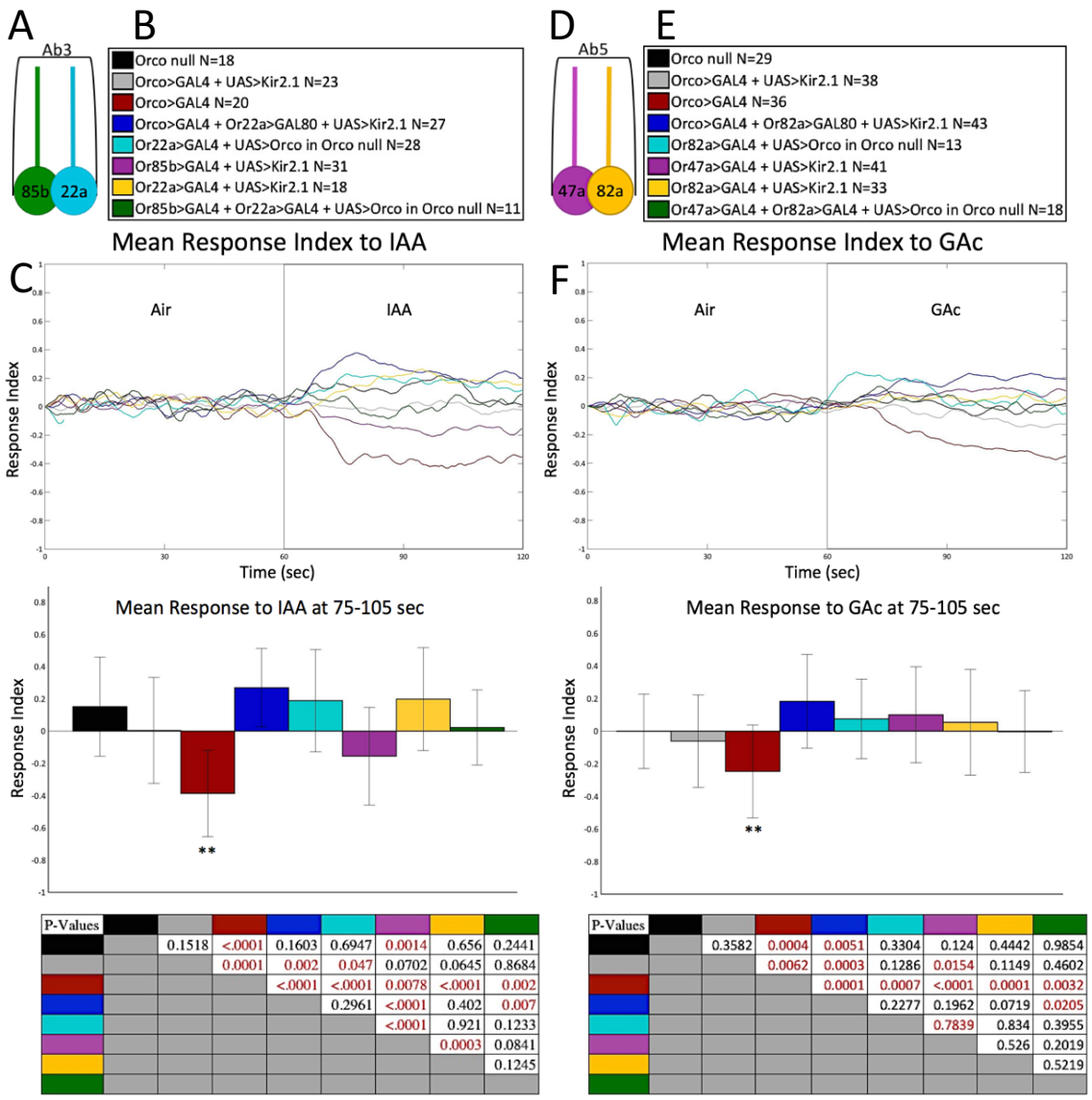

Figure A1: Peripheral Neuronal Pairings in a Behavioral Assay The olfactory arena setup was described in Figure 4. The first five genotypes for each graph (black, grey, red, blue and teal) are the same as those described in Figure 4. Each N represents a trial of 20-30 flies. a) **Or22a and Or85b**. Neurons expressing Or22a are paired in the same sensillum (ab3) as those expressing Or85b. Both neurons are broadly tuned and have a strong electrical response to the odorant Isoamyl acetate (IAA). b) **Genotypes for experiments using IAA**. The color legend for the olfactory arena experiments shown in C. c) **Or22a and Or85b in a behavioral assay**. Odorant is 1:1000 Isoamyl acetate (IAA) in mineral oil. The top panel shows the mean response index of each genotype over the entire course of the trial. The middle panel shows the mean response index of flies over the middle part of the odorant exposure (time = 75-105 seconds). The bottom panel shows the pairwise p value between each of the genotypes over the middle part of the odorant exposure. *Continued, next page*

Fig A1 cont. When either Or85b (lavender) or Or22a (golden) OSN function is removed with a *UAS-Kir2.1* transgene, there is a significant loss of aversion behavior ($p \leq .0078$). This is despite the presence of many other still-functional OSNs that also respond to IAA. If the OSN pair of Or22a and Or85b is restored in an otherwise nonfunctional background (green), these OSNs alone are insufficient to restore normal aversion. d)**Or82a and Or47a.** Neurons **e**xpressing Or82a are paired in the same sensillum (ab5) as those expressing Or47a. Or47a neurons are broadly tuned but have no response to Geranyl acetate (GAc). Or82a neurons are very narrowly tuned; the only known odorant to cause a response is GAc. e) **Genotypes for experiments using GAc**. The color legend for the olfactory arena experiments shown in F. f) **Or82a and Or47a in a behavioral assay**. Odorant is 1:100 Geranyl acetate (GAc) in mineral oil. Panels are arranged as described in C. When either Or47a (lavender) or Or82a (golden) OSN function is removed with a *UAS-Kir2.1* transgene, there is a significant loss of aversion behavior ($p \leq .0001$). Even though Or47a OSNs have no response to GAc themselves, their function is still required for normal aversion. If the OSN pair of Or82a and Or47a is restored in an otherwise nonfunctional background (green), these OSNs alone are insufficient to restore normal aversion. Despite GAc being a "private odorant" for Or82a, a coordinated effort of multiple OSNs in the olfactory system is still required to achieve a normal behavioral response.

downstream neurons such as interneurons and projection neurons rely on combinatorial input from multiple OSN types.[2,46,65-70]

Single Neuron Contributions to an Exposure Phenotype

Plasticity, i.e. alterations in neuron structure, connectivity, or numbers as a result of experience, is rare in the *Drosophila* olfactory system. Neurons faithfully establish and maintain organization. However, a few papers describe an anatomical plasticity phenotype I will refer to as "exposure volume." In these experiments, young flies were exposed to a high concentration of a single odorant over a period of days. OSNs that specifically respond to the odorant all target a glomerulus in the antennal lobe as described in **Figure 1**. Researchers measured the volume of the target glomerulus and found that exposure caused volumetric changes.[73-75] For example, Or22a OSNs respond to ethyl butyrate and synapse onto the DM2 glomerulus in the antennal lobe. When one

day old flies were exposed to 10^{-1} ethyl butyrate for 4 days, the DM2 glomerulus increased in volume.[73]

To what extend does the exposure volume phenotype rely on a coordinated effort from multiple OSN types? Would a single OSN type be able to reproduce the phenotype without input from any other OSNs? To answer these questions, flies were exposed to either an odorant or to a mineral oil control. As a positive control, only *UAS-effector* lines with no driver were used. The effectors of choice were:

- *shibire^{ts1}*, a dominant dynamin mutant which stops synaptic transmission at elevated temperatures.[35-40]
- *EKO*, a potassium channel which creates pores in the neuron, rendering them electrically inactive.[32,76]
- Kir2.1, a potassium channel similar to EKO but generally considered more effective.[32-34]
- Rpr, a caspase enzyme that triggers apoptosis (cell death).[41,42]

Orco-GAL4, UAS-effector lines were used to silence or kill all OSNs. The experimental group was a single OSN subtype restored in an otherwise nonfunctional olfactory system: *Orco-Gal4, UAS-effector, OrX-GAL80*.

All genotypes were also crossed to a line containing *OrX-LexA, LexAop-Tom*. The LexA/LexAop system is derived from bacteria and functions similarly to the GAL4/UAS system. LexA has been genetically modified to be a transcriptional activator when bound to the operator sequence, LexAop. It can be used with the GAL4/UAS system to drive expression of a separate transgene without interfering with the GAL4/UAS genes.[77,78]

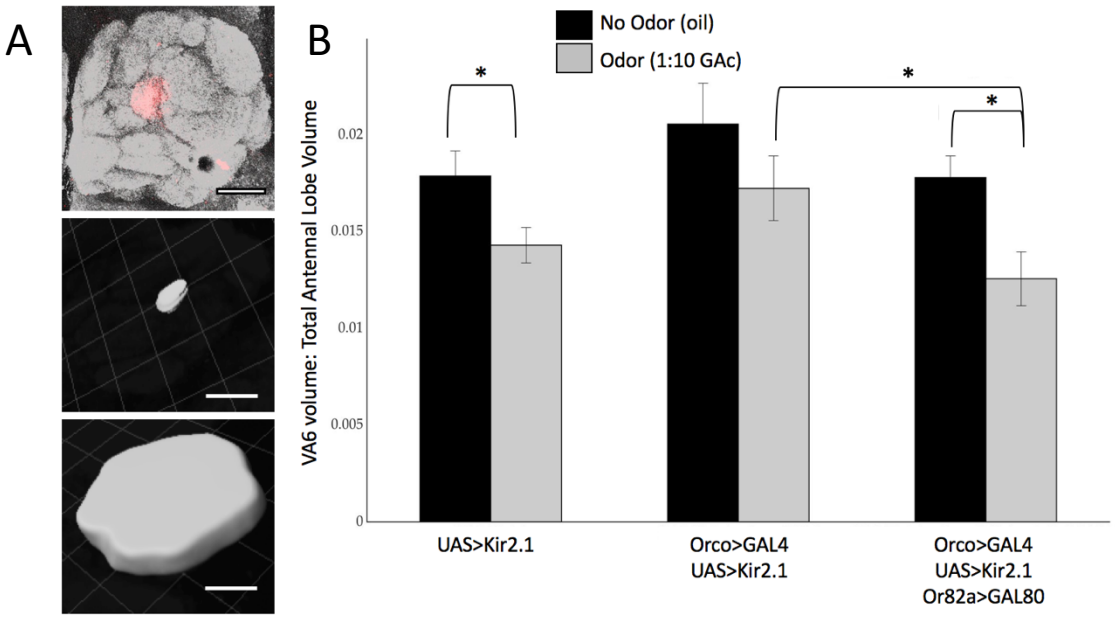

Figure A2: Isolated OSNs and Volumetric Plasticity. a) **Volumetric Measurements of glomeruli and antennal lobes**. White scale bars indicate 20μm. The top image shows an *Or82a-LexA, LexAop2-Tom* line stained with anti-nc82 (grey) and anti-Tom (red). VA6, the target glomerulus for Or82a OSNs, is highlighted in red. The grey antennal lobe or the red glomerulus can be traced slice by slice from a confocal image using IMARIS software. The software then creates a 3D object from these tracings and includes quantitative measurements such as volume. The middle (glomerulus) and bottom (antennal lobe) images show examples of volumes obtained from tracings using IMARIS software. Images are rotated to display the 3D shape. b) **Volumetric changes in response to odorant exposure**. The y-axis shows the ratio of VA6 volume to total antennal lobe volume. *UAS-Kir2.1* flies serve as a control; with no GAL4 driver, no Kir2.1 will be expressed. When control flies are exposed to odorant (1:10 geranyl acetate, GAc, in mineral oil) the relative glomerular volume decreases (N=20 no odor, N=15 with odor, p=.04). When all OSNs are nonfunctional in an *Orco-GAL4, UAS-Kir2.1* line, this volume decrease is not significant (N= 3 no odor, N =9 with odor, p=.32), indicating OSN function is required for this phenotype. If Or82a function is restored in an otherwise nonfunctional olfactory system by adding an *Or82a-GAL80* transgene, this OSN subtype alone is sufficient to restore the phenotype of decreased volume upon odorant exposure (N=15 no odor, N=12 with odor, p=.007). Thus, the phenotype for this specific OR/odorant may not require the coordinated effort of other OSNs.

The LexA lines were made from the same entry vector used to make the OrX-GAL80 library.

After 5 days of exposure, the brains were removed, fixed, immunostained, and imaged by taking confocal stacks. The antennal lobe or glomerulus of interest were then traced, slice by slice, using IMARIS software to render fairly accurate 3D volumes (**Figure A2a**). The ratio of glomerular volume to antennal lobe volume was compared amongst various genotypes and exposure groups.

The most significant result of these experiments is shown in **Figure A2b**. Geranyl Acetate (GAc) specifically activates only Or82a OSNs. Or82a OSNs target the VA6 glomerulus. When controls are exposed to GAc, the VA6 glomerulus decreases significantly in volume (p=.04). If all OSNs are nonfunctional in an *Orco-GAL4, UAS-Kir2.1* genotype, odor exposure does not cause a significant volumetric decrease (p=.32). If Or82a OSN function is restored, the volumetric decrease in response to odorant is restored (p=.007), even without input from any other peripheral OSNs. VA6 glomeruli from exposed flies with functional Or82a OSNs are significantly smaller than VA6 glomeruli in exposed flies with no functional OSNs (p=.04).

Though technically significant, the trends shown in this graph were not convincing enough for publication, since it seems all three genotypes showed some volumetric decrease in response to GAc. Also, there was no clear trend in the parallel experiments using other *UAS-effector* lines (data not shown.) This may be because Shibire^{TS1} and EKO were not strong enough effectors, or, in the case or Rpr, the Ns were too small due to increased fly lethality. As a note, I also tried a similar experiment using Or22a and Isoamyl Acetate exposure while measuring the volume of Or22a's target

glomerulus, DM2. There was no significant change in DM2 volume of control flies when exposed to the odorant (data not shown). This does not contradict the results of a very similar experiment in the literature,[74] as not all glomeruli respond in this way to odorant exposure. However, it is also not useful for answering the question of whether a single neuronal subtype in a nonfunctional background is sufficient to cause the exposure volume phenotype.

A Single Functional OSN Expressing an Ectopic Receptor

Foreign receptors can be expressed using the *Drosophila* olfactory system, and the physiology of the expressing neurons can be measured in response to an array of odorants. However, while researchers have examined the anatomy and physiology of neurons containing an alien OR, the behavioral consequences of an ectopic OR are elusive. Direct behavioral correlations for an OR are difficult to piece out due to the noise of all the other functional OSNs. Could a direct receptor-behavior relationship be achieved by expressing a foreign receptor in a clean/nonfunctional background?

For the principle experiments, the moth pheromone receptor, BmOR1, was used. The flies were genetically engineered to have a completely nonfunctional olfactory system, except for the OSNs expressing BmOR1. The goal was to identify an OSN subtype that could produce a behavior sans input from other OSNs. Such a system could open avenues for engineering flies to have specific behaviors based on the receptors they express. For example, receptors could be designed to detect chemicals not currently recognized by fruit flies. Or behavioral effects could be examined for a receptor that has been engineered to estimate the sequence and structure of an ancestral receptor.

The strategy for a fly expressing BmOr1 in a silent olfactory background is show in **Figure A3.a**. An Orco mutation renders all OSNs nonfunctional. But Or22a receptors must also be absent, so they will not interfere with BmOR1. The deletion Δhalo removes the Or22a gene and has been used in numerous studies in the past to express a different OR in "empty" Or22a OSNs.[8,9,14,27,79] Even without Or22a expression or Orco expression, all olfactory neurons develop normally and target their correct glomeruli.[14,23,57-59] BmOR1 and Orco can then be expressed in the empty neurons using *Or22a-GAL4,UAS-Bmor1, UAS-Orco*. Orco is highly conserved among insect species, and ORs from various species can also utilize *Drosophila* Orco.[17,18,23]

Since both the Orco and the halo mutations must be homozygous, creation of multiple recombinants was necessary in order to fit all the necessary genes onto the two main chromosomes of *Drosophila*. The crossing scheme shown in **Figure A3b** also includes a *UAS-GFP* gene. This reporter gene was used to examine the anatomy of the antennal lobes to ensure the flies with this genotype had normal neuronal targeting (which they did, data not shown.)

BmOR1 receptors have high specificity for the pheromone bombykol.[80-83] In behavioral paradigms, will flies expressing BmOR1 in an otherwise nonfunctional olfactory system respond to bombykol? Orco null flies served as a negative control, since they will be anosmic. OregonR flies, a general "wild-type" line, were used as a positive control. Behavior was measured using simple odor preference tests in both larvae and adults. A chemotaxis assay was used for larvae; animals are placed in a petri dish with an odorant on one end and a control (mineral oil) on the other. Larvae find most pure odorants attractive and will move in the direction of the stimulus.[84,85] For adults,

A

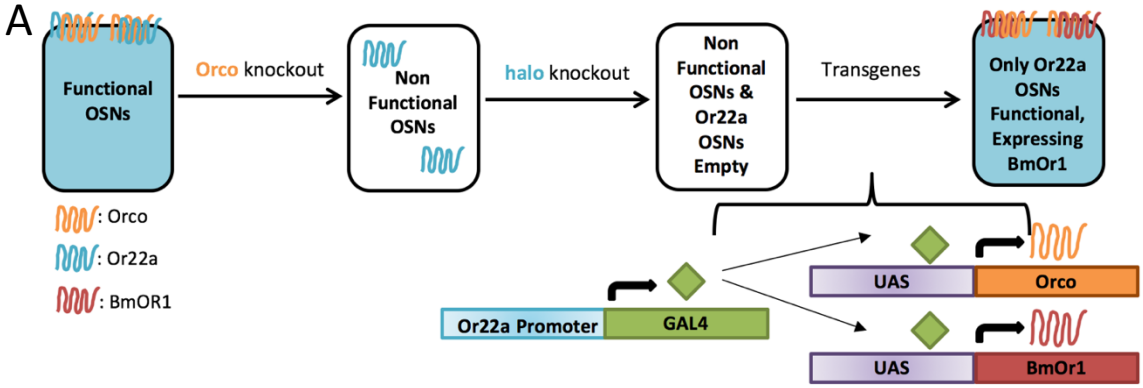
Functional OSNs
Orco knockout
Non Functional OSNs
halo knockout
Non Functional OSNs & Or22a OSNs Empty
Transgenes
Only Or22a OSNs Functional, Expressing BmOr1
: Orco
: Or22a
: BmOR1
Or22a Promoter
GAL4
UAS
Orco
UAS
BmOr1

B

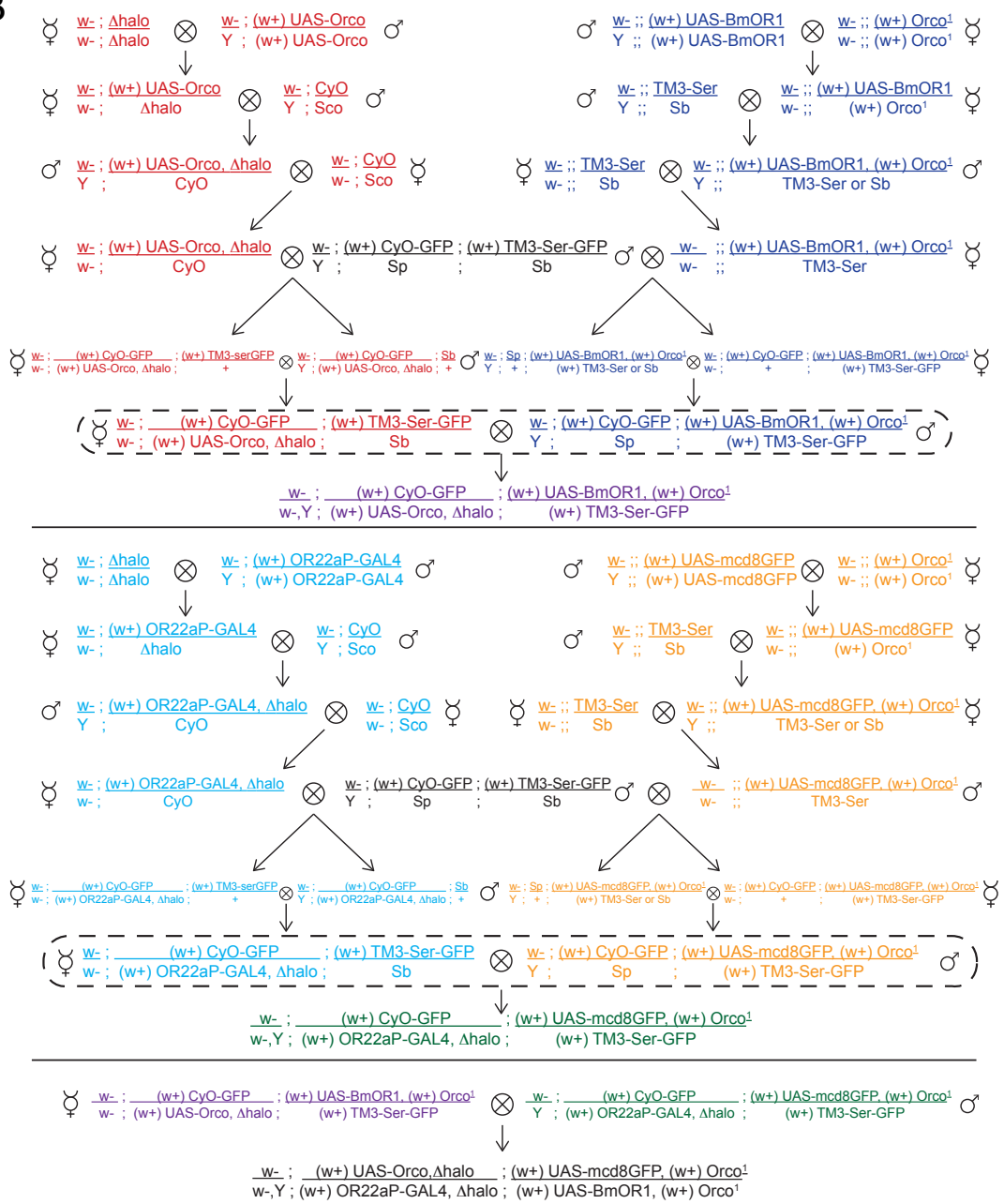
w- ; Δhalo / w- ; Δhalo
w- ; (w+) UAS-Orco / Y ; (w+) UAS-Orco
w- ; (w+) UAS-Orco / w- ; Δhalo
w- ; CyO / Y ; Sco
w- ; (w+) UAS-Orco, Δhalo / Y ; CyO
w- ; CyO / w- ; Sco
w- ; (w+) UAS-Orco, Δhalo / w- ; CyO
w- ; (w+) CyO-GFP ; (w+) TM3-Ser-GFP / Y ; Sp ; Sb
w- ; (w+) CyO-GFP ; (w+) TM3-serGFP / w- ; (w+) UAS-Orco, Δhalo ; +
w- ; (w+) CyO-GFP ; Sb / Y ; (w+) UAS-Orco, Δhalo ; +
w- ; (w+) CyO-GFP ; (w+) TM3-Ser-GFP / w- ; (w+) UAS-Orco, Δhalo ; Sb
w- ; (w+) CyO-GFP ; (w+) UAS-BmOR1, (w+) Orco1 / w-,Y ; (w+) UAS-Orco, Δhalo ; (w+) TM3-Ser-GFP
w- ;; (w+) UAS-BmOR1 / Y ;; (w+) UAS-BmOR1
w- ;; (w+) Orco1 / w- ;; (w+) Orco1
w- ;; TM3-Ser / Y ;; Sb
w- ;; (w+) UAS-BmOR1 / w- ;; (w+) Orco1
w- ;; TM3-Ser / w- ;; Sb
w- ;; (w+) UAS-BmOR1, (w+) Orco1 / Y ;; TM3-Ser or Sb
w- ;; (w+) UAS-BmOR1, (w+) Orco1 / w- ;; TM3-Ser
w- ; Sp ; (w+) UAS-BmOR1, (w+) Orco1 / Y ; + ; (w+) TM3-Ser or Sb
w- ; (w+) CyO-GFP ; (w+) UAS-BmOR1, (w+) Orco1 / w- ; + ; (w+) TM3-Ser-GFP
w- ; Δhalo / w- ; Δhalo
w- ; (w+) OR22aP-GAL4 / Y ; (w+) OR22aP-GAL4
w- ; (w+) OR22aP-GAL4 / w- ; Δhalo
w- ; CyO / Y ; Sco
w- ; (w+) OR22aP-GAL4, Δhalo / Y ; CyO
w- ; CyO / w- ; Sco
w- ; (w+) OR22aP-GAL4, Δhalo / w- ; CyO
w- ; (w+) CyO-GFP ; (w+) TM3-Ser-GFP / Y ; Sp ; Sb
w- ; (w+) CyO-GFP ; (w+) TM3-serGFP / w- ; (w+) OR22aP-GAL4, Δhalo ; +
w- ; (w+) CyO-GFP ; Sb / Y ; (w+) OR22aP-GAL4, Δhalo ; +
w- ; (w+) CyO-GFP ; (w+) TM3-Ser-GFP / w- ; (w+) OR22aP-GAL4, Δhalo ; Sb
w- ; (w+) CyO-GFP ; (w+) UAS-mcd8GFP, (w+) Orco1 / w-,Y ; (w+) OR22aP-GAL4, Δhalo ; (w+) TM3-Ser-GFP
w- ;; (w+) UAS-mcd8GFP / Y ;; (w+) UAS-mcd8GFP
w- ;; (w+) Orco1 / w- ;; (w+) Orco1
w- ;; TM3-Ser / Y ;; Sb
w- ;; (w+) UAS-mcd8GFP / w- ;; (w+) Orco1
w- ;; TM3-Ser / w- ;; Sb
w- ;; (w+) UAS-mcd8GFP, (w+) Orco1 / Y ;; TM3-Ser or Sb
w- ;; (w+) UAS-mcd8GFP, (w+) Orco1 / w- ;; TM3-Ser
w- ; Sp ; (w+) UAS-mcd8GFP, (w+) Orco1 / Y ; + ; (w+) TM3-Ser or Sb
w- ; (w+) CyO-GFP ; (w+) UAS-mcd8GFP, (w+) Orco1 / w- ; + ; (w+) TM3-Ser-GFP
w- ; (w+) CyO-GFP ; (w+) UAS-BmOR1, (w+) Orco1 / w- ; (w+) UAS-Orco, Δhalo ; (w+) TM3-Ser-GFP
w- ; (w+) CyO-GFP ; (w+) UAS-mcd8GFP, (w+) Orco1 / Y ; (w+) OR22aP-GAL4, Δhalo ; (w+) TM3-Ser-GFP
w- ; (w+) UAS-Orco,Δhalo ; (w+) UAS-mcd8GFP, (w+) Orco1 / w-,Y ; (w+) OR22aP-GAL4, Δhalo ; (w+) UAS-BmOR1, (w+) Orco1

Figure A3: Olfactory System with only BmOR1 OSNs a) **Strategy to express a functioning moth receptor in an otherwise nonfunctional olfactory system.** A homozygous Orco null mutant ($Orco^{1}$) renders the olfactory system nonfunctional, with ORs unable to reach the membrane of the neuron or relay signals. A homozygous deletion on chromosome 2L, Δhalo, also removes the Or22a gene, leaving these OSNs devoid of any expressed receptor. Adding transgenes *Or22a-GAL4*, *UAS-Orco,* and *UAS-BmOr1* restores function to this subtype of OSN, which is now expressing only the ectopic moth receptor, BmOr1. b) **Crossing scheme**. In order to obtain the fly described in A, multiple recombinants must be made and validated (via PCR). A *UAS-GFP* gene was also added so neurons could be identified in anatomical studies (not shown). The entire process takes 7 generations.

odorant preference was measured by putting animals in a T-maze. In this assay, flies migrate to one of two arms in a "T"; one arm contains the odorant and the other a control. Adult flies find almost any pure odorant aversive and will avoid the odorant-containing arm. No genotype—Orco null, Oregon R, or BmOR1-only—had any response to bombykol either in the larval or adult assays. The animals segregated evenly with no preference (data not shown.)

Behavioral assays were also tried using (E)-2-Hexenal, as a potential bombykol analog. Although it was unknown if BmOR1 would respond to (E)-2-Hexenal or not, another receptor which detects bombykol also responds to (E)-2-Hexenal.[82] This odorant is useful since adult flies find it aversive and larvae find it attractive, giving a standard of control behavior for comparison against BmOR1-expressing flies. However, once again neither larvae (**Figure A4**) nor adults (data not shown) responded to this odorant when only BmOR1-expressing neurons are functional.

There are many potential reasons there is no behavior in BmOR1-only flies. It may be behavior requires the combinatorial effort of multiple OSNs to manifest from this particular OSN/odorant set. It may be (E)-2-Hexenal is not an appropriate bombykol

analog. In addition, the N was very small in adult assays. BmOR1-only flies are healthy adults once they are born, but they have some difficulty eclosing from the pupal casing, and this diminishes the number of available adults. For larvae, it may be Or22a is not expressed early enough to get strong transgene expression from the Or22a promoter. Whatever the case, it is clear this system was unsuitable for measuring behavioral consequences of a foreign receptor.

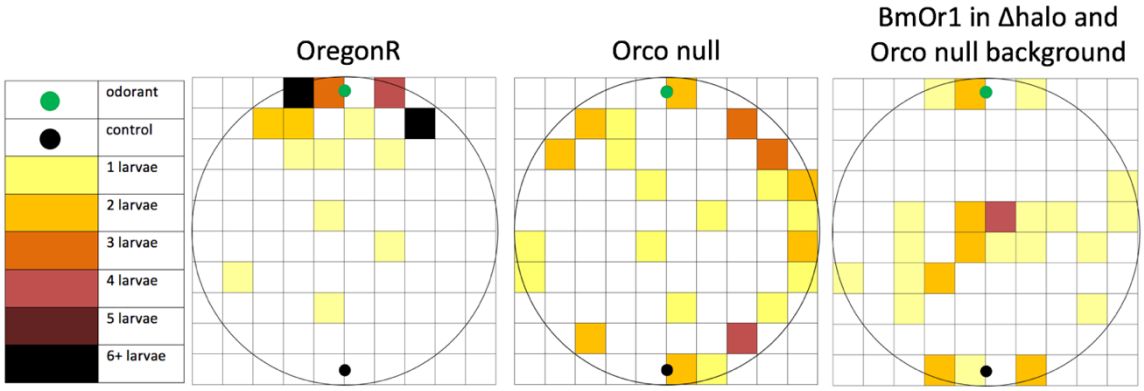

Figure A4: Example of a behavior using the fly described in Figure A3. 30-35 larvae are placed in the middle of a petri dish with agarose and allowed to move freely for 5 minutes. After five minutes, the position of the larvae on the dish is noted. The color map indicates how many larvae were present in a given spatial unit ($10mm^2$). On one end of the petri dish is 2µL pure (E)-2-Hexenal (a potential bombykol analog) on a small round of filter paper atop a pedestal. This is represented by the green circle. On the opposite end of the petri dish is 2µL mineral oil, represented by a black circle. Control larvae (OregonR) are attracted to the odorant and move towards it. Orco null larvae are anosmic and show no preference for either end. Flies with only BmOR1-expressing neurons also show neither attraction nor aversion. BmOR1 OSNs working alone in a nonfunctional olfactory system are insufficient to produce a behavioral response to (E)-2-Hexenal when expressed using the Or22a promoter.

Materials and Methods

Fly Stocks

Flies were reared on standard cornmeal/molasses food and kept at 25C with a 16 hours on/8hours off light cycle. All *OrX-GAL4*, *UAS-mcd8::GFP, and UAS-effector* lines were obtained from Indiana University Bloomington Stock Center and Janelia Farms. Any recombinants made were validated with PCR.

Stock List:

Or7a-GAL4 #23907

Or7a-GAL4 #23908

Or9a-GAL4 #23918

Or10a-GAL4 #9944

Or13a-GAL4 #9946

Or13a-GAL4 #23886

Or19a-Gal4 #24617

Or22a-GAL4 #9951

Or22a-GAL4 #9952

Or22b-GAL4 #23891

Or33c-GAL4 #23893

Or35a-GAL4 #9967

Or42a-GAL4 #9970

Or42b-GAL4 #9971

Or43b-Gal4 #23894

Or46a-GAL4 #23291

Or47a-GAL4 #9981

Or56a-GAL4 #9988

Or59b-GAL4 #23897

Or59c-GAL4 #23899

Or67a-GAL4 #23904

Or67d-GAL4 #9998

Or71a-GAL4 #23121

Or82a-GAL4 #23125

Orco-GAL4 #23292

Orco-GAL4 #26818

Or85a-GAL4 #23133

Or85b-GAL4 #23911

Or85c-GAL4 #23913

Gr21a-GAL4 #24147

Or22a-mcd8::GFP #52620

Gr21a-mcd8::GFP #52619

$Orco^2$ #23130

UAS-Orco #23145

UAS-mcd8::GFP #5130

UAS-mcd8::GFP #5137

UAS-Kir2.1 Janelia stock #3015545

UAS-Kir2.1 Janelia stock #3015298

UAS-Kir2.1::eGFP Janelia stock #BS00312

GAL80 Creation

Primers were designed to capture the entire promoters described by Couto *et al* 2005[10] (see **Supplementary Table 1**) Promoters were amplified from genomic DNA using Q5 High Fidelity PCR (NEB #M0491S) and added to entry vectors using the pENTR/D-TOPO system.[86] Recombination with the pBP-GAL80Uw-6 (Addgene #26236) destination vector was done using the LR Clonase II system.[87] To ensure no mutations, no gaps, and correct orientation, the complete promoters were sequenced in the destination vector using the sequencing primers shown in **Supplementary Table 2**. PhiC31 site-directed transgenesis was performed by Genetivision Inc. All GAL80 transgenes were inserted at the attP2 site.

Immunohistochemistry

Female adult brains were dissected one day after eclosion in cold S2 Schneider's Insect Medium (Sigma Aldrich #S0146) and fixed while nutating for 55 minutes at room temperature in 2mL 2%PFA (Electron Microscopy Sciences #15713) in protein loBind Tubes (Eppendorf #022431102). Brains were washed 4x, 15min per wash while nutating with 2mL PBT buffer (1xPBS, Cellgro #21-040, with 0.5% TritonX-100, Sigma Aldrich #X100). Brains were then blocked with 200μL 5% Goat serum (ThermoFischer. #16210064) in PBT for 90 minutes while nutating, upright. Block was removed and 200 μL primary antibodies in PBT were added for 4 hours at room temperature and then transferred to 4C for 36-48 hours while nutating, upright. Primary antibodies: mouse α-

bruchpilot (Developmental Studies Hybridoma Bank. #nc82-s) at 1:30, rabbit α-GFP at 1:1000 (Thermo Fischer #A11122), or rabbit α-Tom at 1:500 (clontech #632393). Monoclonal antibody nc82 identifies Bruchpilot. Bruchpilot can serve as a general neuropil marker because it is required in synaptic zones [88]. Larval brains were collected from third instar larvae and fixed in 4% PFA. Primary antibodies: mouse α-neuroglian (Developmental Studies Hybridoma Bank. #BP104) at 1:50 and rabbit α-GFP at 1:500. Brains were washed 4x, 15min per wash while nutating with 2mL PBT. 200μL secondary antibodies in PBT were then added for 4 hours at room temperature and then 3 overnights at 4C while nutating upright. Secondary antibodies: AF568 goat α-mouse (Life Technologies #A11031) at 1:400 and AF488 goat α-rabbit (ThermoFischer #A11034) at 1:800. Tubes were protected from light at all times after secondary antibodies had been added. Brains were washed again 4x, 15min per wash while nutating with 2mL PBT. Then washed with 1xPBS and mounted using Vectashield mounting media (Vector Labs #H-1000). Confocal images were taken with Leica800 microscope.

Olfactory Arena

Female flies aged 3-6 days were cold-plate sorted 1-2 days before the assay. The arena was setup and the assay performed as described in Aso *et al* 2016, sans the optogenetic components.[60] Odorants were diluted in mineral oil. After trying starved vs unstarved flies and multiple odorant concentrations (data not shown), it was determined unstarved flies at concentrations of 10^{-3} Isoamyl acetate and 10^{-2} Geranyl acetate gave the most consistent and robust behaviors. Flies in video recordings were tracked using Ctrax software.[61]

Larval Chemotaxis

15% sucrose solution is added to the food to force larvae rise to the top. Third instar larvae are collected from the sucrose solution and rinsed on filter paper before being added to the petri dish. 30-35 larvae are placed in the middle of a 100mmx20mm petri dish with 10mL 1% agarose and allowed to move freely for 5 minutes. After time is up, the position of the larvae on the dish is noted. On one end of the petri dish is 2µL pure odorant on a small round of filter paper atop a pedestal. On the opposite end of the petri dish is 2µL mineral oil.

Odorant Exposure and Volume Rendering

Male and female flies were collected and separated on T0 and placed in a food vial containing a perforated 2mL Eppendorf tube. The tube held 1mL of either odorant diluted in mineral oil, or plain mineral oil. Shibire^{ts1} genotypes were kept at 32C. Other genotypes were kept at 25C. After 5 days of exposure, flies were removed, fixed, and stained as described in the immunohistochemistry protocol above. Confocal stacks were taken and each slice traced using IMARIS software to render a 3D volume for each glomerulus and its corresponding antennal lobe. The two antennal lobe and glomerular volumes per brain were averaged in flies that had clear images for both lobes. In the end, only male measurements were included in the analysis, due to their greater Ns.

Single Sensillum Recordings

SSRs were performed as described in Lin et al 2015 [89]. GFP labeled ab1 sensilla were identified using a Zeiss AxioExaminer D1 compound microscope with eGFP filter cube (FL Filter Set 38 HE GFP shift free). A glass recording electrode filled with ringers solution (7.5g of NaCl+0.35g of KCl+0.279g of $CaCl_2$-$2H_2O$ in 1L of H_2O) was inserted into the base of an ab1 sensillum. CO_2 was delivered through a tube ending with a Pasteur pipette that was inserted for 1 second into a hole in a plastic pipette directed at the antenna. This plastic pipette (Denville Scientific Inc, 10ml pipette) carried a purified continuous air stream (8.3 ml/s) that used a stimulus controller (Syntech) at the time of CO_2 delivery to correct for the increased air flow. Signals were acquired and analyzed using AUTOSPIKE software (USB-IDAC System; Syntech). Spikes were counted in a 500 ms window from 500 ms after CO_2 delivery and multiplied by 2 to calculate spikes/second. Then, the spikes in 1000ms before CO_2 delivery were subtracted to calculate the increase in spike rate in response to CO_2 (Δspikes/second). For each genotype, 6 flies (4-8 days old) were tested, with 1-3 sensilla tested in each fly.

Chapter 2

A Screen to Identify Neuronal Candidates of Color and Translational Motion Pathways in *Drosophila*

Introduction

Vision is the analysis of electromagnetic waves (light) by the brain. Light waves themselves have only three properties: wavelength, frequency, and amplitude. They do not have color, or texture, or contrast, or distance. Yet a brain can take the features of light waves/light particles (photons) and groups of light waves/photons to produce images with all these features and more. Light-sensing neurons work in coordination with other neurons in the brain to perform impressive calculations such distinguishing foreground and background, gauging the speed and direction of a moving object, or estimating the time of day.

Some form of vision has existed for about 700 million years; this sense is hugely valuable for survival and mating. Vision influences many vital behaviors such as finding food and water, courting a mate, navigating the environment, and avoiding predators. How do neurons in the brain convert simple photons into perceived images and ultimately produce an appropriate behavior? To answer this question, the fruit fly *Drosophila melanogaster* was the model of choice. Insect visual anatomy has been established for about 240 million years, and about two-thirds of the insect brain is devoted to vision.[90] Their visual system is capable of complex calculations and behaviors. Like humans, flies see color, contrast, intensity, motion, texture, and even illusions. Using vision, flies can perform incredible acts such as flying through narrow gaps,

foraging in intricate landscapes, remembering landmarks, reaching their tiny bodies over chasms, or dancing to attract a mate. Though fly visual systems are organized and operated similarly to our own, [91] their brains contain only about one millionth the number of neurons. Flies provide genetically malleable, simplified, and less varied systems to study how neurons interpret visual stimuli and produce reactionary behaviors.

Drosophila Visual Anatomy

The primary requirement for vision are opsins. Opsins are light-sensitive proteins; when expressed by neurons in the retina of the eye, they are referred to as rhodopsins. Flies express five main rhodopsins: Rh1 has broad spectral sensitivity, Rh3 and Rh4 are UV-sensitive, Rh5 is blue-sensitive, and Rh6 is green-sensitive.[92-94]

The Optic Lobe of the fly brain contains the visual system and is organized into five main layers of dense neuropil: The Retina, the Lamina, the Medulla, the Lobula, and the Lobula plate (**Figure 1a, 1b**). Neuronal signals are conveyed and modified in each layer until they leave the Optic Lobe via projection neurons to the central brain, which will orchestrate tasks such as memory formation or muscle movement.

The first layer of the fly visual system is the Retina. The compound eye of the fly contains about 750 facets, i.e. visual units, called ommatidia. Each ommatidium contains 6 photoreceptor neurons expressing Rh1 (broad sensitivity). These neurons are named Retina 1-6 (R1-6) and are essential for motion vision. (For more information about the premise for the mechanisms of motion vision, see box insert below, "**A Model for Motion**".) Each ommatium also contains two neurons required for color-vision: one R7

neuron expressing either Rh3 or Rh4 (UV), and one R8 neuron expressing either Rh5 (blue) or Rh6 (green).[93,94]

The second layer of the fly visual system is the Lamina. R1-R6 neurons project into the Lamina and synapse (mainly) onto either Lamina 1 (L1) or L2 neurons.[95,96] L1 typically detects moving light edges while L2 typically detects moving dark edges.[97-104] These are called the "ON" and "OFF" motion pathways, respectively. (For simplicity, the current explanation categorizes neurons as part of the ON or OFF pathways and doesn't delve into the complexities of individual neuron sensitivities, dynamic responses at different conditions/contrasts, or crosstalk between the two pathways.)

Note how the Lamina and all subsequent layers of the Optic Lobe retain a topographic map, i.e. the spatial relationships among neurons are preserved in the anatomical arrangement of each layer. Maintaining spatial information about visual input is essential for forming sensible images. Consider a single R1 neuron in an ommatidium on the Retina, represented in **Figure 1c** by a black dot. It will see the same point in space as R1 neurons in a unit of six adjacent ommatidia. Each R1 from neighboring ommatidia in a unit extracts information from the exact same point in space. These R1's will target neurons in the same Lamina "column," a phenomenon known as "neural superposition."[105,106] This spatial information is then preserved through each layer. Between the Lamina and the Medulla, the position "flips" due to neuronal crossover (presumably to save on neuronal wiring costs, though the purpose is unclear). But the integrity of the topographic map is still preserved (**Figure 1c**).

The Medulla is the third layer in the Optic Lobe. As part of the motion vision pathway, L1 neurons connect to Medulla Intrinsic 1 (Mi1) neurons while L2 neurons

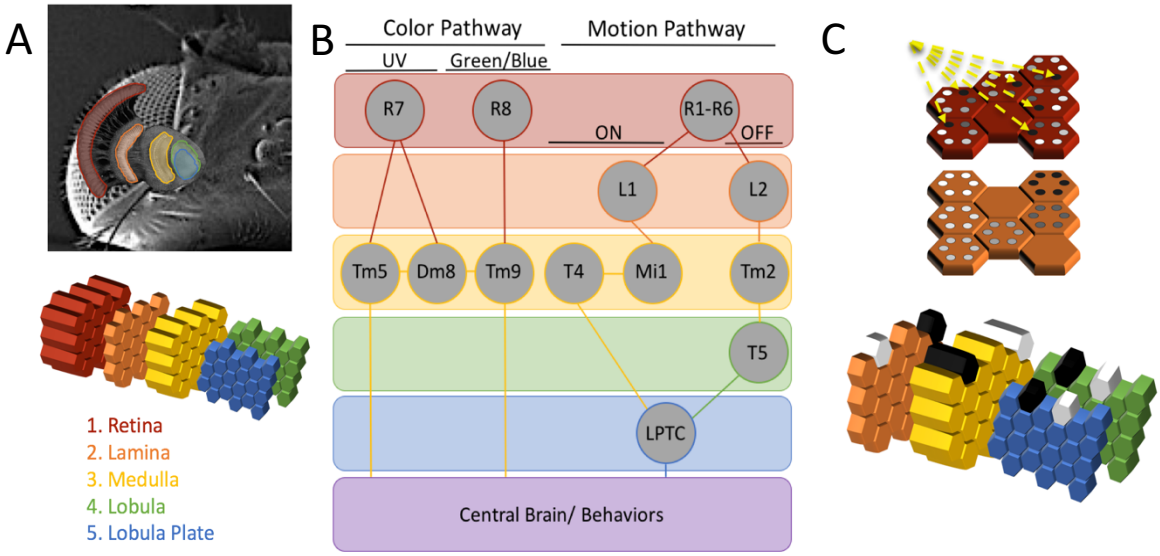

Figure 1: Anatomy of the Visual System. a) **The Optic Lobe**. Confocal image modified from JCB 2010; 189 (5). The Optic Lobe of *Drosophila* contains 5 layers of neuropil: The Retina (red), Lamina (orange), Medulla (yellow), Lobula (green), and Lobula Plate (blue). Each ommatidium in the retina or each column in the descending neuropils is represented by a hexagonal prism. b) **A simplified diagram of color and motion vision.** This schematic (patterned after Zhu *et al* 2013) displays the major known neurons that participate in the color and motion pathways. Dozens of other neuronal types are not shown for simplicity. Retina 7 (R7) neurons express UV-sensitive rhodopsins and target Distal Medulla 8 (Dm8) and Transmedullary 5 (Tm5) neurons. Dm8 also synapses with both Tm5 and Tm9. R8 neurons express green or blue-sensitive rhodopsins and target Tm9 neurons. Tm5 and Tm9 project their axons to target neurons outside the Optic Lobe. R1-R6 neurons express a broadly-sensitive rhodopsin and target Lamina 1 (L1) or L2 neurons in the Lamina. L1 predominantly synapses with Medulla Intrinsic 1 (Mi1) in the Medulla which in turn targets T4. All three of these cell types are mainly sensitive to moving light edges and light increments (ON). L2 predominantly synapses with Tm2 in the medulla which in turn targets T5 neurons in the Lobula. All three of these neuron types are mainly sensitive to moving dark edges and light decrements (OFF). T4 and T5 send ON/OFF and directional information to Lobula Plate Tangential Cell (LPTC) neurons in the Lobula Plate. LPTC neurons send their axons to target neurons outside the Optic Lobe. c) **Spatial information is conserved in the Optic Lobe**. Top: Each ommatidium in the retina contains one of each of the 6 neurons of the motion pathway, R1-6, represented here as dots in greyscale. Each R1 neuron in adjacent ommatidia (black dots) receives light from the same point of space. These neighboring R1s will project their axons to the same column in the Lamina (this phenomena is known as neural superposition). Bottom: Each laminar column represents the light from a single point of view. This spatial representation is conserved in the columns of the remaining neuropil layers of the Optic Lobe, though the pattern inverts between the Lamina and Medulla layers (bottom figure patterned after Borst *et al* 2002.)

connect to Transmedullary 1 (Tm1) neurons. Like their presynaptic partners, Mi1 responds to light increments and Tm1 responds to light decrements.[107] Mi1 in turn synapses with T4 neurons, major neurons of the ON-motion pathway.[101,108-111] Dozens of other medullary neurons exist, but are not mentioned in this discussion for simplicity.

As part of the color-vision pathway, R7 and R8 neurons in the Retina bypass the Lamina and target neurons in the Medulla. Different wavelengths (colors) alone do not elicit different motion responses and the two pathways are generally considered separable.[112,113] (Some neurons seem to be playing an unknown role in communication between the color and motion pathways, [114,115] but they are not discussed here for the sake of simplicity). R8 neurons synapse onto Tm9. R7 neurons synapse onto Tm5 and Distal medulla neuron 8 (Dm8.) Dm8 in turn synapses with both Tm5 and Tm9. [108,115] The color pathway exits the Optic Lobe from the Medulla into central brain complexes while the motion pathway continues its processing in the Lobula Complex.

The Lobula Complex contains two structures: The Lobula and the Lobula Plate. In the Lobula, Tm1 neurons synapse onto T5 neurons, the major players in the OFF pathway.[101,108-111] Together, T4 and T5 provide motion information to Lobula Plate Tangential Cell neurons (LPTCs) with their respective information about moving light and dark edges. T4/T5 are required for motion vision and also seem to be the first neurons in the motion pathway that clearly encode information about the direction of the movement.[101,116-119]

The anatomy of Optic Lobe neurons was described over 100 years ago, and an even more refined anatomy has been available for nearly 30 years. [120] And yet, researchers are only just beginning to understand the intersections of function and

anatomy—how each neuron encodes visual features and how neurons cooperate to make vision possible. Uncovering the mechanisms of vision requires recently-available advancements in technology and tools as well as extensive collaboration among experts from many fields.

The Screen

The summary shown in **Figure 1b** is very simplified and shows only the major known components of the color and motion vision pathways. But there are dozens of other neuronal types in the Optic Lobe. What are they doing? A few of the major neuronal players in vision were identified readily by their strong phenotypes (causing complete motion or color blindness), but what about the plethora of other neurons that work in more subtle ways to process and refine vision? To understand how the brain computes sensory information, it is necessary to know how these other neurons contribute as well.

To identify neural correlates of motion and color vision, a large high-throughput visual screen was conducted. Screens have proved useful in the past for generating new hypotheses and identifying novel neural correlates for behavior. [100,113,124-127] A candidate neurons screen is similar to a forward genetic screen. Many neurons are silenced at once (phase I), analogous to using a large chromosomal deletion line. Then individual neuron types are silenced (phase II) to narrow down the relevant players in a phenotype, similar to a genetic knockout screen.

A Model for Motion: The Hassenstein-Reichardt Elementary Motion Detector[121-123]

A single receptor or neuron sees only one point in space. By itself, it cannot convey any information about an object's motion—its direction or speed. The Hassenstein-Reichardt Elementary Motion Detector model (HR-EMD) provides a simple mechanism to explain how motion vision could work. Several other models exist, but only the most widely-used model is summarized here.

Each HR-EMD circuit consists of the following components: one light-detecting unit with a delay, an adjacent undelayed light-detecting unit, and a multiplier to boost activity.

Imagine an object (represented by the black bar, below) passing over two adjacent light-detectors. As it reaches the first detector, the detector sends an excitatory signal which is delayed for a space of time before continuing on to the multiplier unit. The time of the delay is just long enough for the object to reach the next light-detector, which sends an undelayed signal to the multiplier unit. When both signals converge at once, their signals are multiplied and an excitatory output results. HR-EMD circuits could exist that are sensitive to light increases (ON circuits) or sensitive to light decreases (OFF circuits).

A specific delay time will allow a circuit to be "tuned" to a specific speed. If the object travels faster or slower than the speed tuning of this circuit, the two signals will not converge and be multiplied. Different circuits could be tuned to different speeds to cover a wide range of potential velocities.

A circuit is also tuned for a specific direction. Imagine the object travelling in the reverse direction—it will activate the light-detector with no signal delay first, sending the signal directly to the multiplier. The object then activates the light-detector with the time delay. The signals do not reach the multiplier at the same time, so the signal is not amplified and perpetuated.

Where are the HR-EMD computational units in the brain? This model does not seem to correspond to adjacent receptors or neurons or columns specifically.[100] Rather it is a framework from which useful predictions and calculations can be made. Although the HR-EMD model does not have specific neuronal equivalents, a complex network of interacting neurons adheres to the principles outlined by the HR-EMD model.

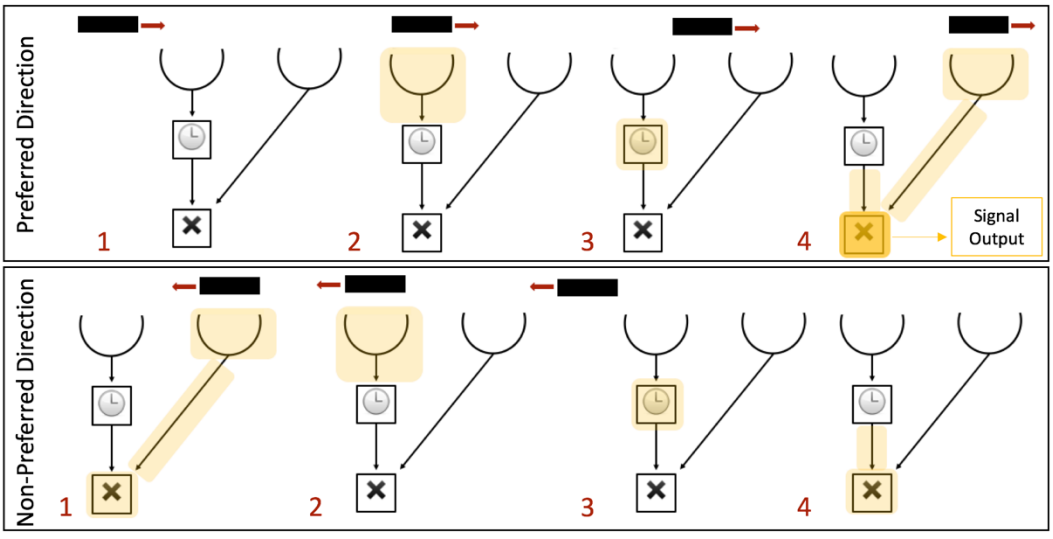

The screen used an *enhancer-GAL4* library; [128] these lines are broadly-used tools, so it is expected that a detailed description of their anatomies and behavioral consequences will prove useful for the vision-research community. GAL4 is a yeast transcription activator that binds to the Upstream Activating Sequence (UAS) and induces expression of downstream genes.[30]

Vision-related behaviors of over 2,000 lines of genotype *GMRX-GAL4, UAS-shibire^{TS}* are described using a novel assay. Shibire^{TS} is a dominant dynamin mutant which stops synaptic transmission at elevated temperatures.[35-40] The *GMRX-GAL4, UAS-shibire^{TS}* genotype allows for selective silencing of neurons during the assay to determine if those neurons are vital for certain visually-directed behaviors. (Credit for phase I: Fly Olympiad Team.)

The anatomical expression pattern of the lines was also obtained by crossing each *GMRX-GAL4* with the reporter gene *UAS-GFP* (credit: Hideo Otsuna, FlyLight, and Aljoscha Nern). Brain-Anatomy maps were constructed by taking data from both the behavioral assay and imaging (credit: Alice Robie, Kristen Branson, and Michael Reiser). With these maps, regions of the brain were identified that are associated with particular phenotypes.

This screen used a hybrid approach: Phase I generated hypotheses and reasonable hypotheses drove the selection of lines during phase II. In phase II of the screen, a split-GAL4 library[54,129] was used to restrict Shibire^{TS} or GFP expression to specific neuronal types of interest before repeating the behavioral and anatomical experiments.

The data shown herein from the dual screen is positioned as a resource for researchers. All anatomical and behavioral data from the widely-used GMR-GAL4

library are available online. Phase II identifies specific contributions made by previously-undescribed interneurons of the visual system. This screen enhances the understanding of neuronal contributions to vision and behavior by identifying poorly-understood neurons that subtly fine-tune visual perception and reactions.

Results

Screening Scheme

The screening apparatus is shown in **Figure 2a.** Six clear plastic corridors are lowered into a box containing 6 hallways. Each hallway contains Green and UV lights on the ends and an LED panel on the side. Each plastic corridor contains 15 freely-walking flies, so each experiment contains an N of about 90. A lid is placed on top of the box with an IR filter window. This leaves the flies in darkness, but an IR camera situated above the box takes videos of the flies' movements. Peltier temperature-control units (not shown) keep the machines at 34C. The elevated temperature increases fly locomotion and is the optimal temperature for silencing $Shibire^{TS}$-expressing neurons.

The animals' movements were tracked in these videos to calculate behavioral phenotypes such as Direction Index (DI). $DI= (Flies_{preferred} - Flies_{nonpreferred})/Total\ Flies$. The "preferred" direction is the direction control flies travel. Each stimulus lasts 10 seconds, and data is averaged from the middle 5 seconds to make the plots shown in **Figure 2b**. DI is calculated for every corridor of 15 flies, and averaged over the 6 corridors per experiment. Furthermore, every stimulus is shown 4 times, twice in each direction, and DI is averaged over all trials. A DI of -1 would indicate all 15 flies are moving against the preferred direction, 0 indicates random walking, and +1 means all 15 flies are moving

in the preferred direction. For control groups, the peak DI values reach about 0.5, indicating 11-12 of the 15 flies are moving in the preferred direction.

As a note, all of the following stimuli were also performed on single flies to ensure that behaviors were not emerging due to collective group interactions. Behaviors can also be "contagious" among *Drosophila* in a social setting. Group life is known to influence behavioral decisions regarding sensory stimuli or environmental stressors in fruit flies. [130-132] In the hallway assay, single flies behaved much the same as groups of flies (**Supplementary Figure 1**.) Group dynamics likely do not have a strong influence on the examined behaviors.

The first stimulus is a series of 6 "buzzes" or vibrations. Each is 0.5 seconds long, 10 seconds apart. When control flies feel the vibration, they pause for a moment, but then increase directionless walking. This gives a baseline locomotion reading. With this reading, genotypes are excluded that have poor behavior because they cannot walk well, and the screen focuses on flies with poor behavior because they cannot see well.

Motion stimuli is displayed using the LEDs on the side of each hallway. Flies respond to moving stripes of light and dark (aka grating patterns) by changing their speed and direction.[133] A fly's classic behavioral response to a moving striped pattern in a hallway is to walk against the direction of the stripes. This visual behavior was first described in 1934 by Hecht and Wald. Walking flies in a glass tube moved against the direction of moving stripes; if the direction of the stripes changed, the flies stopped, backed up a few paces, and then turned around to go the opposite way.[134] Götz replicated this behavior in 1970 by putting flies in a barber pole-like cylinder.[135] Thus, "against" stimuli direction is the preferred direction in all the DI calculations.

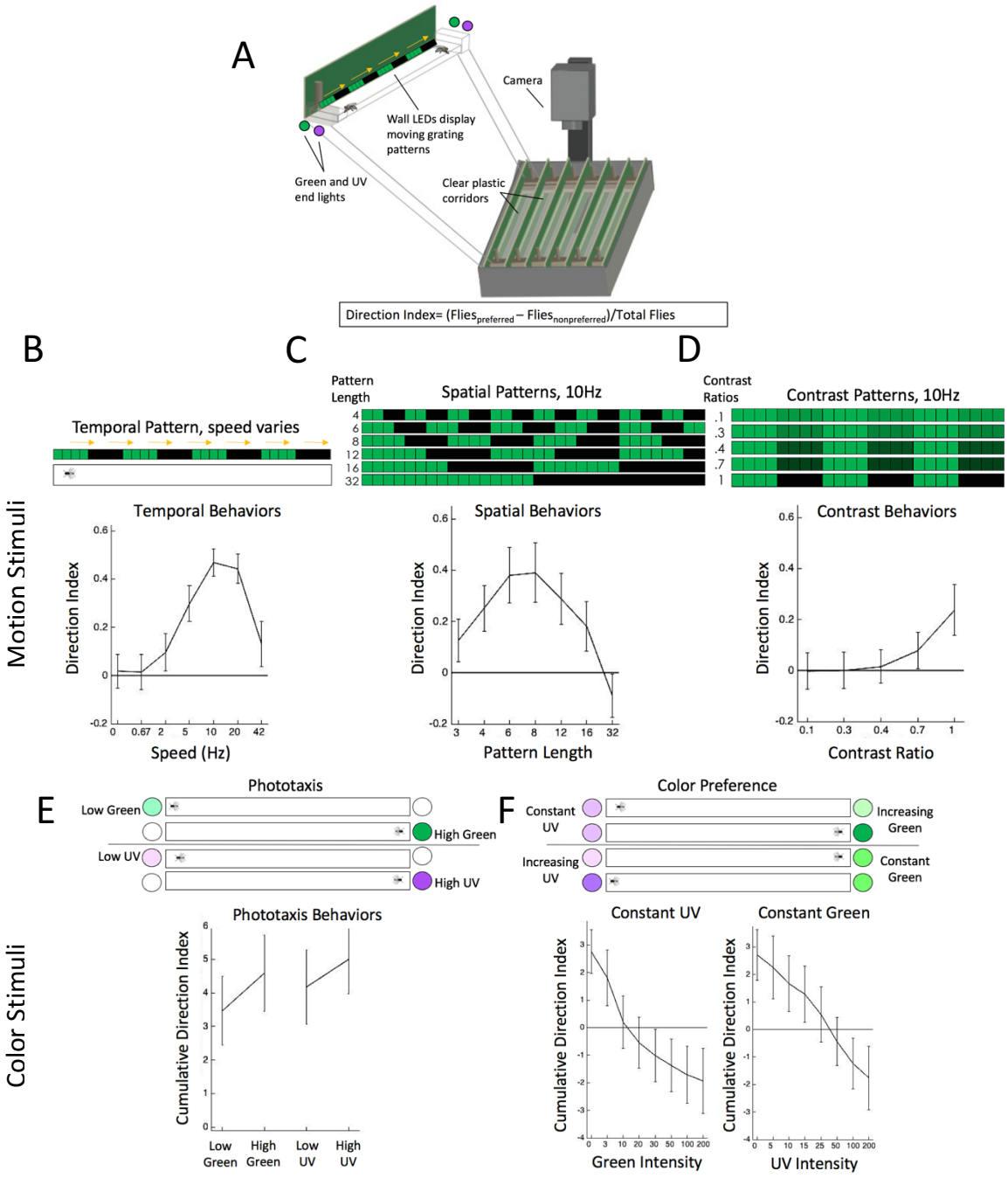

Figure 2: High-Throughput Screen. a) **Apparatus for Screen**. (Picture credit: Emily Nielson.) Fifteen flies are added to a clear plastic corridor and lowered into a hallway. The hallway has green and UV lights on the ends for displaying color patterns, and a row of LEDs against the wall to display moving grating patterns ("on" lights are shown in green and "off" lights are shown in black. The patterns then move along the wall running left-to-right or right-to-left.) Each apparatus contains 6 hallways, allowing for 90 flies to be screened at a time. Other than the lights on the walls or ends, the corridors are kept in the dark, and fly movements are filmed for tracking using an infrared camera. *Figure caption continued on the next page*.

Figure 2, continued. After tracking, a Direction Index for each experiment is calculated and averaged among the 6 corridors and for every trial. Direction Index= ($Flies_{preferred} - Flies_{nonpreferred}$)/Total Flies. A Direction Index of 0.5 means ~11-12 out of the 15 flies are moving in the preferred direction. The preferred direction for motion stimuli is against the direction of the grating, e.g. when the pattern goes right to left, flies run towards the right. b) **Motion Stimuli, Temporal.** The LEDs on the walls of each hallway display a pattern of four lights on, four lights off. This pattern moves at varying speeds of 0, 0.67, 2, 5, 10, 20, and 42 Hz. As speed increases, more flies move in the preferred direction, reaching their peak at about 10Hz. After 10 Hz, increasing the speed results in fewer flies moving in the preferred direction. c) **Motion Stimuli, Spatial**. Flies are shown patterns of varying lengths. Starting at 1 light on/2 lights off (not shown) and ending 16 lights on/ 16 lights off. All spatial patterns move at 10Hz. At about 4 lights on/4 lights off, flies moving in the preferred direction reach their peak. Shorter or longer patterns than this result in fewer flies moving in the preferred direction. d) **Motion Stimuli, Contrast**. Flies are shown patterns of varying contrasts. All patterns are 4 lights higher intensity/4 lights lower intensity and move at 10Hz. Contrast Ratio= (High-Low)/(High+Low). Direction Index is low at low contrasts, but rises exponentially as contrast increases. d) **Color Stimuli, Phototaxis**. Color Stimuli data are shown as cumulative direction index, i.e. the running sum of the direction index over the course of the trial. Flies naturally move towards light, and prefer UV wavelengths and high intensities. When flies are shown low intensity green light, they move towards the light, but as intensity increases, more flies move towards the light. Flies are also show low intensity and high intensity UV light. More flies move for UV light than for green light and more flies move for high intensity UV light than for low intensity UV light. e) **Color Stimuli, Color Preference**. UV light intensity is kept constant at a lower level while green light intensity gradually increases. As long as green intensity is low, flies prefer UV light. But as green intensity increases, more flies walk towards the higher intensity light. The reverse experiment uses a higher-level constant green intensity while increasing UV intensity. At first flies prefer the light of higher intensity, but as UV intensity increases, they prefer the UV light and walk towards it.

Figure 2b shows a control group's response to a grating pattern that changes speed. At 0 Hz, the pattern is static. As expected, flies walk aimlessly, and have no direction preference at 0 Hz, so their DI is around 0. As the grating moves faster, a greater proportion of flies perceive the motion and walk against it accordingly. After a peak of about 10 Hz, the pattern speed is moving too quickly and fewer flies respond. (I.e. even if flies can perceive the motion, their behavior correlates with the motion less at

slow and fast speeds.)

The size of the grating pattern also varied, as shown in **Figure 2c**. When the pattern is very short or very long, fewer flies are able to respond the motion (i.e. even if they can perceive the motion, their behavior correlates with the motion less at short and long pattern lengths). Flies respond with the highest DI at a pattern length of 8 (four lights on and 4 lights off.) All spatial patterns move at 10Hz.

Flies perceive motion best at high contrasts, as evident in **Figure 2d**. When shown very low contrast patterns (4 lights higher intensity/4 lights lower intensity, moving at 10Hz), few if any flies can tell the grating is moving. As the contrast of the pattern increases, more flies can detect the motion and move against the grating, reaching their peak at 1, i.e. 100% contrast. (Contrast Ratio= (High-Low)/(High+Low).) Two contrast protocols were included. In the protocol shown in **Figure 2d**, one stripe (of four lights) remains at a constant high intensity while the other stripe varies in intensity to achieve a certain contrast ratio. This means as contrast reaches 1, the total intensity of light decreases. On the chance that intensity proves important for certain neurons, a second set of contrast patterns was included. The second set of patterns have the same ratios, but the total sum intensity of both stripes together doesn't change (patterns not shown). The behavioral responses look nearly identical, so for simplicity data is only shown for the first set of contrast patterns here.

The apparatus also tests color behaviors. The Y-axis for the color protocols shows cumulative sum DI instead of simply DI, i.e. the running total of flies moving in the preferred direction. Control flies are more attracted to high intensity light than to low intensity light, and are more attracted to UV light than to green light. In the phototaxis

protocol **(Figure 2e)**, one end light is a low intensity green (Intensity=15) and some proportion of flies move towards it. But when green intensity increases (Intensity=200), a greater proportion of flies can perceive the light and respond accordingly. Flies perform similarly when low intensity (20) and high intensity (100) UV lights are used.

Next flies are shown "color preference" sequences (**Figure 2f**). At a constant UV intensity of 5, flies prefer UV to green. But as green intensity increases, more flies begin to prefer green. At the green intensity threshold of about 10, preference switches and flies begin to prefer green over UV. A similar protocol is run with a constant green intensity of 120 while UV intensity was increased. Flies initially prefer green, but when UV intensity reaches about 25-50, flies switch to preferring UV.

A variety of visual behaviors was assayed (i.e. 3 motion vision components and 2 color-vision components), because the screen doesn't just look for neurons that make flies motion-blind. As stated previously, neurons with a strong effect have already been identified. But many other neurons exist that refine and enhance visual features. E.g. a neuron may be "tuned" to a specific speed, or contrast, or spatial pattern. The screen aimed to identify such specialized neurons as well as any with more blatant and generalized effects.

Screen Phase I: GMR-GAL4 lines

Lines from the GMR *enhancer-GAL4* library[128] were crossed to 1) a *UAS-Shibire^{TS}* line and 2) a *UAS-GFP* line (**Figure 3**). Each enhancer line in this library is named "GMR" followed by an alpha numeric ID. The progeny of the Shibire^{TS} crosses were assayed for behavioral phenotypes using the apparatus and protocol described in

Figure 2.

In neurons where the enhancer is expressed, Shibire^{TS} will stop synaptic transmission at the machine's temperature of 34C.[35-40] The behavioral experiment will indicate if neurons targeted by that enhancer are required for color or motion behaviors.

To image which neurons express that enhancer, the brains of progeny from the GFP cross are examined. This high-throughput screen represents the coordinated effort of the Fly Olympiad and Fly Light teams at Janelia Farm (before this author joined the lab).

A summary of Phase I is shown in **Figure 4** and **Table 1**. The screen included 2,236 lines. About 5% had locomotor phenotypes, and were filtered out. But about 65% of the lines had either a color or a motion phenotype, and 50% had both a color and a motion phenotype. As examples, the results for all temporal behaviors and for all phototaxic behaviors of the screened lines are shown in **Figure 4** (Figure credit: Michael Reiser). Each circle (control) or square (enhancer line from the GMR library)

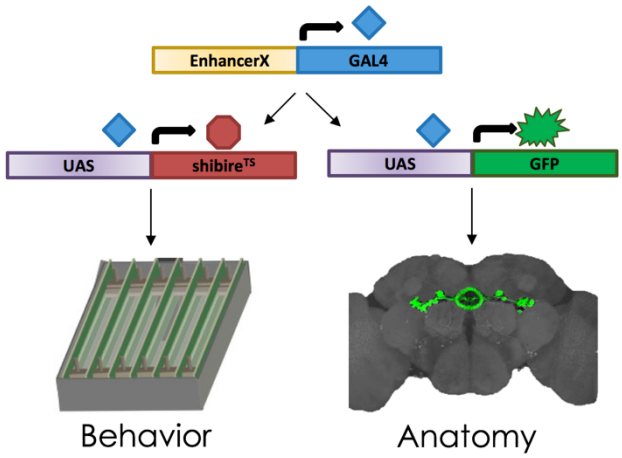

Figure 3: Behavior/Anatomy Screen Schematic. 2, 234 neuronal enhancer lines of genotype *EnhancerX-GAL4* were crossed to both a *UAS-shibire^{TS}* line and a *UAS-GFP* line. EnhancerX will cause target expression of the *UAS-gene* to the specific neurons where the enhancer is expressed. Shibire^{TS} blocks synaptic transmissions at elevated temperatures. To see if neurons targeted by EnhancerX are important in color or motion vision behavior, flies expressing *UAS-shibire^{TS}* are run through the visual corridor assay described in **Figure 2**. Anatomical patterns can be seen when *EnhancerX* is expressed using the GFP reporter gene. Grey shows α-nc82, a general neuropil marker. Green shows α-GFP.

represents the data from one experiment, N=90. The percent of moving flies is shown on the x-axis. The mean percentage for control flies is 66% for temporal behaviors and 65% for phototaxic behaviors. Control lines are empty enhancers crossed to *UAS-shibire^{TS}*. The Y axis for temporal behaviors is the mean velocity of flies moving in the preferred direction during the last three stimulus speeds. For phototaxic behaviors, the Y axis represents the mean displacement of flies over all phototaxic conditions. Displacement distance indicates the velocity of the moving flies over time and is comparable to the mean motion response. Phenotypes within 1 standard deviation of the mean control are considered weak; phenotypes of 2 standard deviations are classified as strong.

Screen Phase I Summary	
Lines Run	**2,236**
Locomotion deficiencies	5%
Motion vision phenotype	35%
Enhanced motion response	15%
Reduced motion response	14%
Color vision phenotype	30%
Both color and motion vision phenotype (overlap)	50%

Table 1: Summary of Screen Phase 1

Note that several control experiments had weak reduction or enhancement phenotypes, showing that there is some variability even amongst controls. However, very few control trials have strong phenotypes. Many of the screened lines show strong phenotypes of enhancement, reduction, or, in the case of phototaxis, reversal. To the right of the summary plots are examples of phenotypes of individual lines, with the controls shown in black and the GMR line shown in red. (These plots are analogous to those shown in Figure 2, except the y axis is velocity in mm/s and displacement in mm to match the summary plots.)

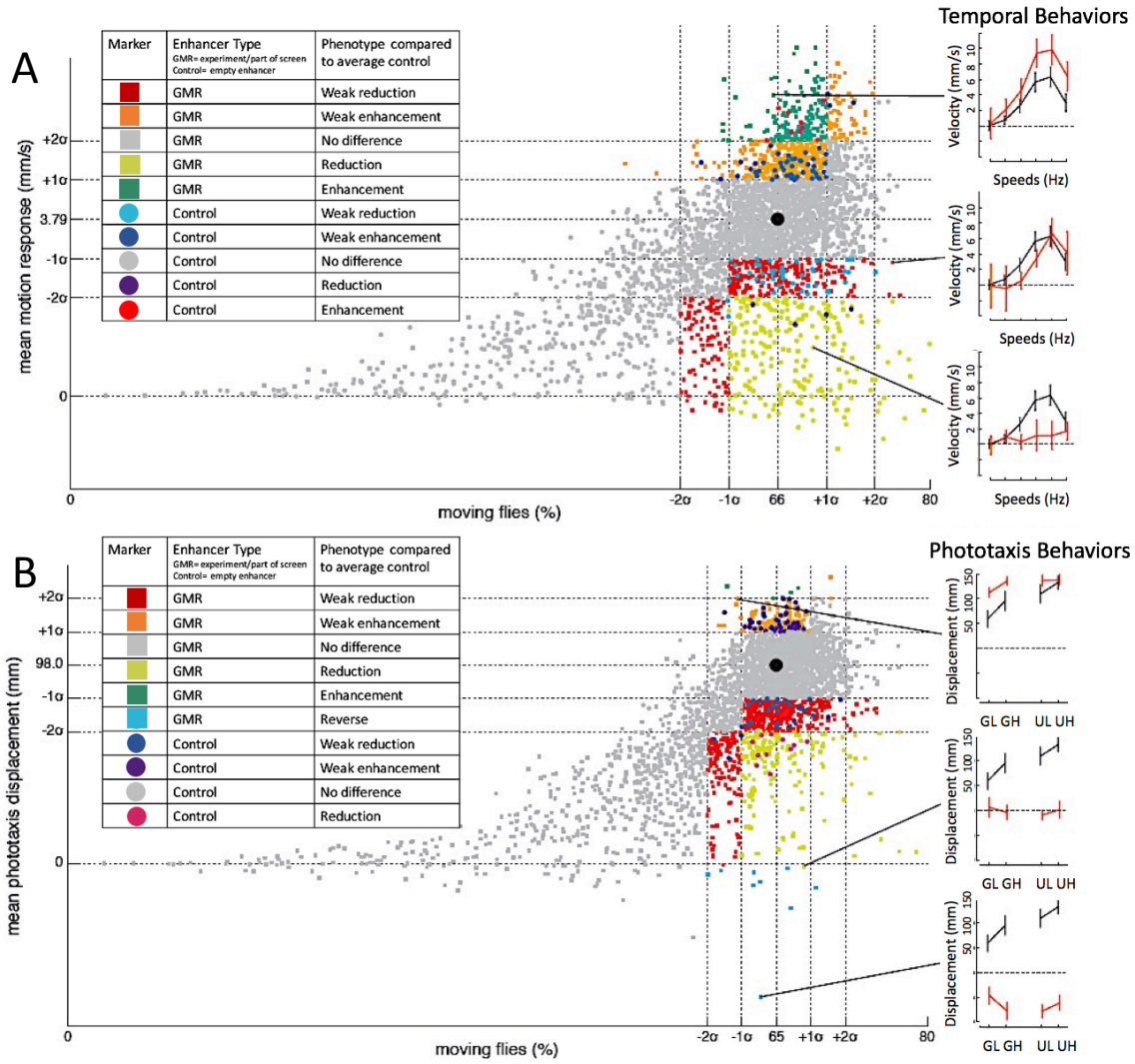

Figure 4: Results of Screen, Phase I. Figure credit: Plots modified slightly from those created by Michael Reiser. a) **Graphical screen summary, temporal behaviors.** The large black dot indicates the average response of all control trials (these have an "empty enhancer"). The x-axis shows the percentage of flies that were moving and the Y axis shows the mean velocity for the top three speeds of the temporal patterns as given in Figure 2. Standard deviations from control fly behaviors for are indicated by the dotted lines. Experiments for each screened enhancer line are indicated by squares while control experiments are indicated by circles. Enhancer lines with no significant difference from the average control are shown in grey. Some control runs showed weak enhancement (dark blue) or weak reduction (light blue). A small number (13 purple or red circles) gave strong reduction or enhancement phenotypes. These experiments show the variation of the controls over the 18 months of the screen and are quite small considering the large number of control experiments that were run overall. Many of the screened enhancer lines gave weak phenotypes (red and orange squares) or strong phenotypes (light green and dark green squares. An example of a strong enhancement, a strong reduction, and an insignificant behavioral phenotype are shown on the right. *Figure caption continued next page*.

Figure 4 continued. Controls are shown in black and the GMR line is shown in red. These plots are analogous to those shown in Figure 2, except the y-variable is changed to match the summary plots. b) **Graphical screen summary, phototaxic behaviors.** The graph is arranged as described for a, but the Y axis gives mean displacement for all conditions. Phototaxic behaviors and patterns were described in Figure 2. Some control runs showed weak reduction (dark blue) or weak enhancement (purple). A small number (11 pink) gave a strong reduction. Some screened lines had weak phenotypes (red and orange squares) while others had strong phenotypes (light green and dark green squares.) Several of the screened lines had a "reverse phototaxis" behavior, where they behaved in the opposite manner to controls. Examples of enhancement, reduction, and reverse phototaxis phenotypes are shown on the right. Controls are shown in black and the GMR line is shown in red. These plots are analogous to those shown in Figure 2, except the y-variable is changed to match the summary plots. GL= green low, GH= green high, UH= UV high, UL=UV low.

All the data from Phase I of the screen is included in a website (design by Emily Nielson and Austin Edwards.) **Figure 5** shows an example of what a single webpage looks like for GMR82D11. The image is a maximum intensity projection derived from over 200 confocal slices, provided by Hideo Otsuna. The image is colored to indicate the layer of expression from anterior slices (violet) to posterior slices (pink).

Next, each webpage shows behavioral summary plots for every individual trial of this line. This example line was run 5 times (Total N ~450), each represented by a different color. The mean of all control trials is shown in black. The behavioral data may vary somewhat from that shown in **Figure 1**. For example, here the y axis for colored plots is displacement rather than cumulative direction index. The webpage also shows startle data with the average velocity in the dark, the highest velocity reached, the dip in walking that immediately follows the vibration, and the increase in walking post-vibration (recovery). This line has no locomotor defects compared to control lines, and it has no color phenotypes. However, these flies appear to be severely motion-blind.

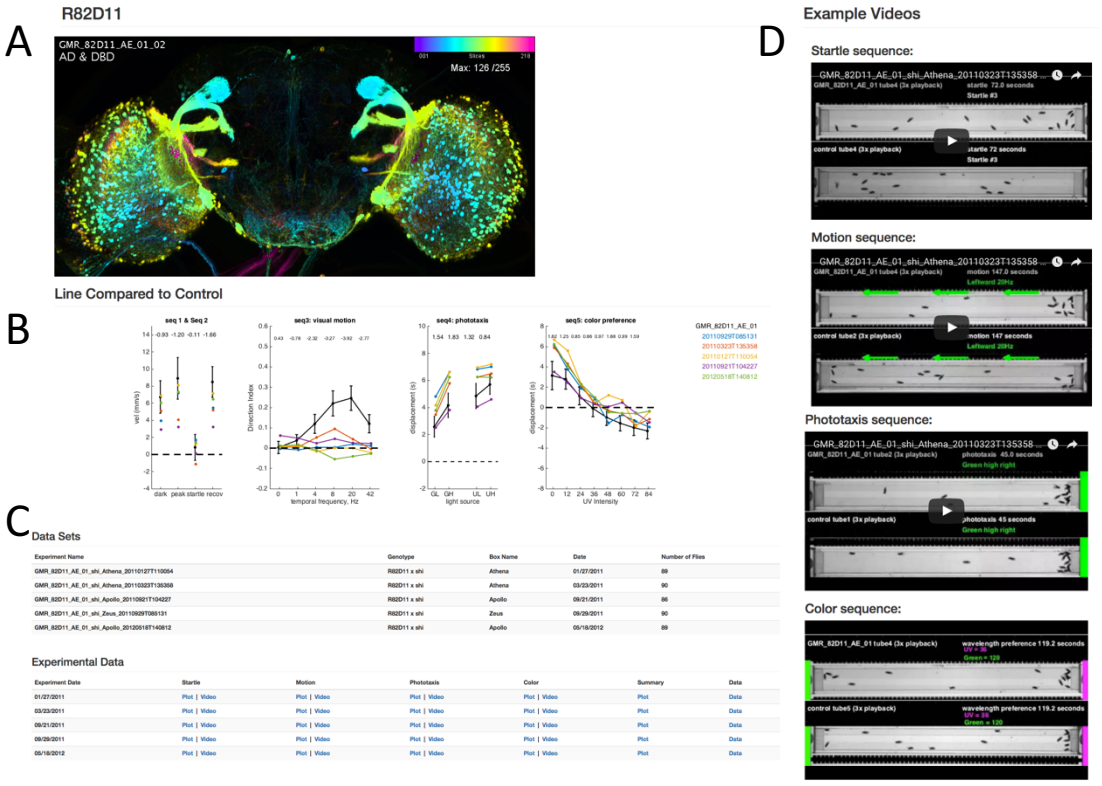

Figure 5: Sample Web Page. Website design by Austin Edwards and Emily Nielson. Each enhancer line (indexed by alpha numeric GMR value) has its own webpage similar to the example shown here for line GMR82D11. a) **Anatomy**. The page includes the anatomy image from crossing the enhancer with a UAS-GFP line. The image is a maximum projection of all layers from a confocal stack—violet is most anterior and pink is most posterior. Images curtesy of Hideo Otsuna. b) **Behavioral data**. The page includes behavioral data: raw locomotion, temporal behavior, phototaxis behavior, and color preference behavior. Each colored line shows a different experiment of 90 flies for the same line on different dates. c) **Detailed plots and videos**. Details about the runs, including the name of which apparatus was used during each experiment are shown below the behavioral data. Videos and plots for individual corridors of each experiment are also available here. d) **Sample videos**. Next a sample video is shown for each of the behaviors. The top corridor of each video shows a representative group from the enhancer line of interest, chosen based on the mean response of this group compared to the mean response for all trials.) The bottom corridor in each video shows a representative control group.

Detailed data are included in these webpages, including the specific machine used for a particular experiment, the total N for each experiment, the date and time of each experiment, individual videos, and individual plots for every corridor of 15 flies in every experiment. (The average of all these plots was used to make the summary plots above.)

Finally, each page shows labeled sample videos of every behavior. The sample videos show one corridor of 15 GMR flies compared to a corridor with 15 control flies. The sample groups were chosen to best represent the mean of all trials.

Using Phase I data, behavioral phenotypes were compared to expression data to see if any regions in the brain are significantly associated with a particular behavior. The process to create these Brain-Anatomy Maps is shown in **Figure 6**; images in this figure were modified from Robie *et al* 2017 and further detail about the calculations used to arrive at these maps can be found there. [136]

The brain can be divided into 38 structures or regions (**Figure 6a**). Each of those regions can further be divided into "supervoxels." A voxel is a volumetric pixel, and a supervoxel is a group of voxels. Examples of three brain regions and their supervoxel divisions are shown in **Figure 6b**. The brain can be divided into about 7,000 total supervoxels.

Behavior of each enhancer line is compared to the behavior of control lines (**Figure 6c, top**). Each GAL4 line is analyzed for significant deviation from control behaviors, with enhancement shown in red and reductions shown in blue. GAL4 lines are arranged in vertical columns along the x-axis while behaviors are arranged by horizontal rows along the Y-axis. For example, if the top row behavior is "average walking speed,"

the zoomed-in frame shows that multiple enhancer lines—identified by their alpha numeric GMR ID—have significantly greater average walking speed compared to controls.

Figure 6c, bottom displays the expression patterns of each line in the screen. Supervoxels make up every row on the y-axis, and the 38 brain regions are separated by horizontal lines. If GFP expression is present for a GAL4 line at a particular supervoxel, the expression level is indicated in greyscale.

Bootstrapping analysis was used to determine areas of the brain that significantly correlate with a particular behavior. **Figure 6d** shows supervoxels aligned with behaviors, and p values indicating the significance level of each association. From this, a map of the brain can be constructed for every behavior. **Figure 6e** shows an example of supervoxels in the brain that are significantly correlated with reduced walking speed in response to temporal motion patterns. I.e. enhancer lines that had motion vision defects in response to temporal stimuli also had overlapping expression patterns in the areas indicated on the map. The Optic Lobes were an obvious and expected result. Unfortunately, specific areas in the Optic Lobe cannot be resolved for this behavior. However, the map also alludes to areas in the central brain that may contribute to motion processing. These areas of interest can be examined more closely by using enhancer lines that cleanly target them.

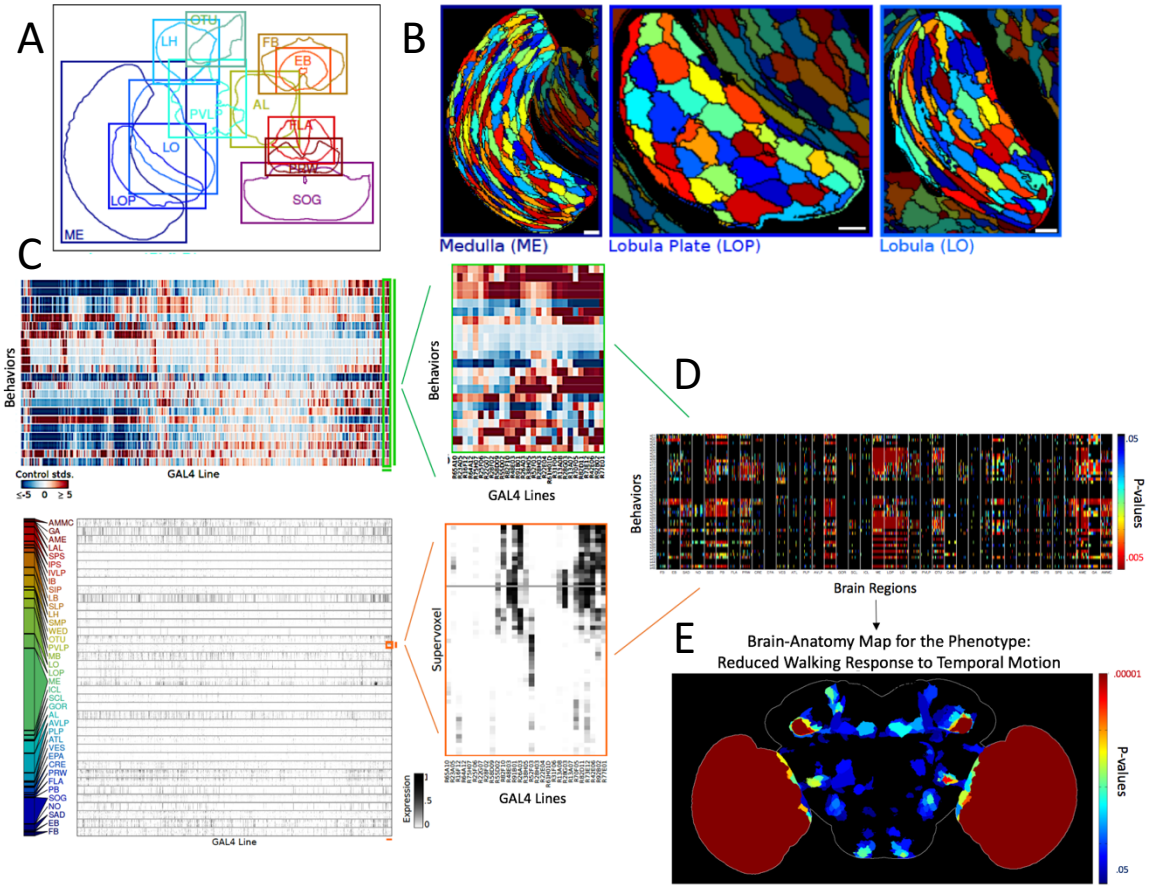

Figure 6: Brain Anatomy Maps. Figure adapted from Robie *et al* (2017) a) **Brain Regions**. The fly brain can be divided into 38 larger regions, among them, the Medulla (ME), Lobula Plate (LOP), and Lobula (LO.) b) **Supervoxel Subdivisions.** Each of these larger brain segments can be further subdivided into "supervoxels"—groups of voxels (volumetric pixels). This allows the brain to be divided further from the 38 larger regions into about 7,000 total supervoxels. Such divisions are useful for describing the expression patterns seen in *GMRX-GAL4, UAS-GFP* lines. c) **Aligning enhancer lines with behavior (top) and expression (bottom)**. On the left, the X-axis of each panel represents each of the thousands of *GMRX-GAL4* lines. The rows for the top panel represent behaviors and the rows for the bottom panel represents each of the 7,000 supervoxels. The top panel indicates if the GAL4 line had significantly more (red) or significantly less (blue) of each behavior compared to the controls. The bottom panel shows the level of GFP expression in every supervoxel for a particular GAL4 line in greyscale. d)**Bootstrapping**. Every behavior (rows) is compared to every supervoxel (column) to find specific areas of the brain that correlate to a particular behavior (p-values calculated through bootstrapping). e) **The Map**. An anatomical map was created for every behavior, showing regions of the brain where expression associated with that behavior. This example includes any lines that showed lower walking responses than control flies while being shown temporal motion patterns as described in Figure 1. The Optic Lobes are significantly correlated with motion vision, as expected However, there are additional interesting targets in the mid brain that could also be important for motion vision.

Screen Phase II: Split-GAL4 lines

The problem with a GMR-GAL4 screen is the wide expression patterns of the enhancer lines. It is difficult to pinpoint single groups of neurons responsible for a behavior, since the enhancers are expressed in many different kinds of neurons. To restrict expression to single neuronal types in the second screening effort, a split-GAL4 library was created.[54,129] In the split GAL4 system, the GAL4 protein is divided into its activation domain (AD) and its DNA binding Domain (DBD). Each domain is driven from its own enhancer. Transcriptional activation is only reconstituted in neurons where the expression of both enhancers intersects (**Figure 7a**). As before, these split lines can be crossed to both *UAS-shibire^{TS}* and examined for behavioral phenotypes, or crossed to *UAS-GFP* and examined for anatomical expression.

As an example, consider the two *GMR-GAL4* lines shown in **Figure 7b**.

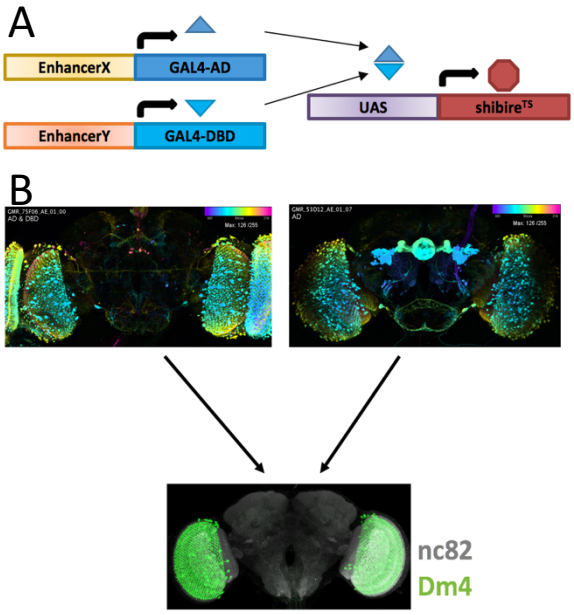

Figure 7: Screen Phase II. a) **Split GAL4 System**. Specific cell types can be targeted using a split-GAL4 system. One enhancer drives expression of the DNA-binding domain of a GAL4 protein (DBD). Another enhancer drives expression of the transcriptional activation domain of a GAL4 protein (AD). Expression of *UAS-transgene* (Shibire^{TS} or GFP) occurs only at the intersection of expression for both enhancers. b) **Split GAL4 example**. Notice how two lines from Phase I of the screen, GMR75F06 and GMR53D12, have overlapping expression for a specific cell type in the Medulla. Both these lines had motion vision deficiencies during the phase I screen, so their common neuronal target is likely involved in motion vision. To isolate that cell type from the other expression noise, split GAL4 halves were created from each of these enhancers. The resulting line only has expression in Dm4 neurons.

Both these lines had strong reduction of behavioral responses to any motion stimuli during Phase I of the screen. Notice the only cell type they have in common is in the Medulla of the Optic Lobe. When a split line is made from these two enhancers, the result is very specific expression in only Dm4 neurons. (Expression is specific, despite the wide labeling of the Medulla, because the Medulla contains many Dm4 neurons.) The GMR-GAL4 images are from Hideo Otsuna and the split images were created by Aljoscha Nern and Fly Light.

Results of Phase II are shown in **Table 2**. Lines were selected in Phase II to target neurons of interest based on Phase I results and the behavior-anatomy maps, and the screen mainly focused on neurons within the Optic Lobe. The screen included 281 total split-GAL4 lines, and about 30% showed a visual phenotype with 4% showing both color and motion vision defects.

Screen Phase II Summary	
Split Lines Run	281
Motion vision phenotype	18%
Color vision phenotype	12%
Both color and motion vision phenotype (overlap)	4%

Table 2: Summary of Screen Phase 2

Some hits from this screen were expected. For example, **Figure 1** showed that Dm8 is an important component of UV perception in the color vision pathway. [108,115] **Figure 8a** shows the anatomy and behavior of a split GAL4 line with specific expression for all Dm8 neurons. Notice how this line has perfect motion vision and no deficiencies for green phototaxis or for green color preference. However, flies with silenced Dm8 neurons have decreased, though not eliminated, responses to UV. Dm8 must modify and fine-tune UV behaviors, but additional neurons in the pathway are contributing to UV perception and behavior. I.e. Dm8 is contributing to the UV pathway but is not critical for it, since some UV perception remains even when Dm8 neurons are nonfunctional. Dm8-

silenced flies perform worse than controls in UV phototaxis. In UV color preference, they do not transition to preferring UV over green until a UV intensity of 50-100, while controls switch to preferring UV around 25.

T4/T5 neurons, vital players in the motion vision pathway, are expected to give motion phenotypes when silenced.[101,116-119] The split GAL4 line, with restricted expression to only T4 and T5 neurons, is shown in **Figure 8b**. Silencing T4/T5 has no effect on color phenotypes. But any motion vision is effectively eliminated. The expected results from silencing Dm8 and T4/T5 confirm the assay can effectively identify neural correlates of color and motion vision.

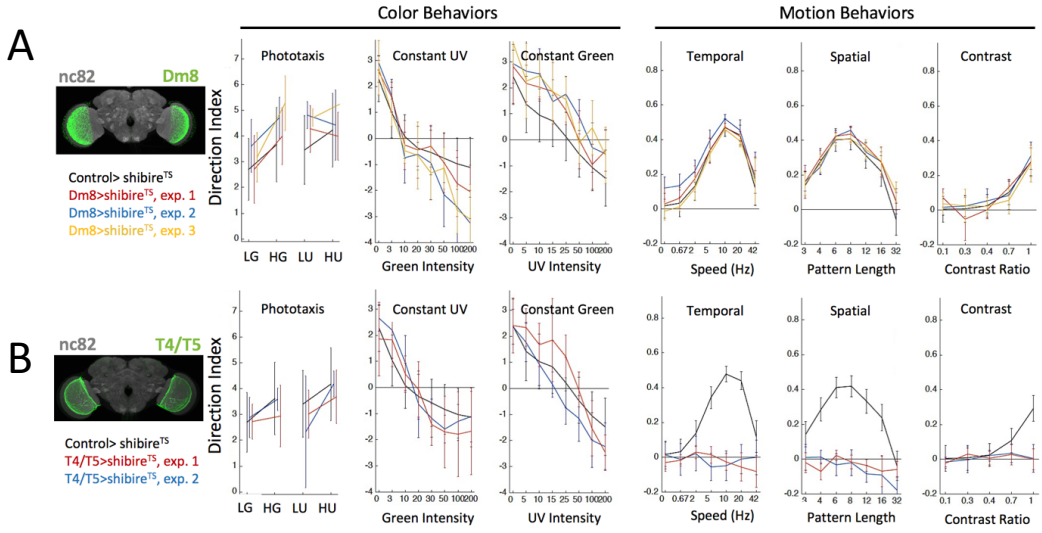

Figure 8: Expected Hits from Screen Phase II. All brain images are curtesy of Aljoscha Nern and are shown posterior-side up. Staining is α-nc82 (grey, a neuropil marker) and α-GFP (green.) The graphs axes are arranged as described in Figure 2. The x-axis for phototaxis has been abbreviated to: LG= Low green, HG= High green, LU= Low UV, HU=High UV. Black lines show control data, a split GAL4 line with empty enhancers. Each colored line represents a single experiment of the split line. N=90 per experiment. a) **Dm8**. Dm8 neurons are well-established contributors to the color-vision pathway. They receive input from R7 neurons; R7 neurons express a rhodopsin which is sensitive to UV light. When Dm8 neurons are silenced with Shibire^{TS}, no motion-related phenotypes are affected. Green phototaxis and green color preference are also unaffected. However, Dm8-silenced flies show deficiencies in UV phototaxis and UV color preference. b) **T4/T5**. T4 and T5 are well-known contributors to the motion vision pathway. When T4/T5 neurons are silenced, no color-related phenotypes are affected. However, any motion perception or reaction is eliminated.

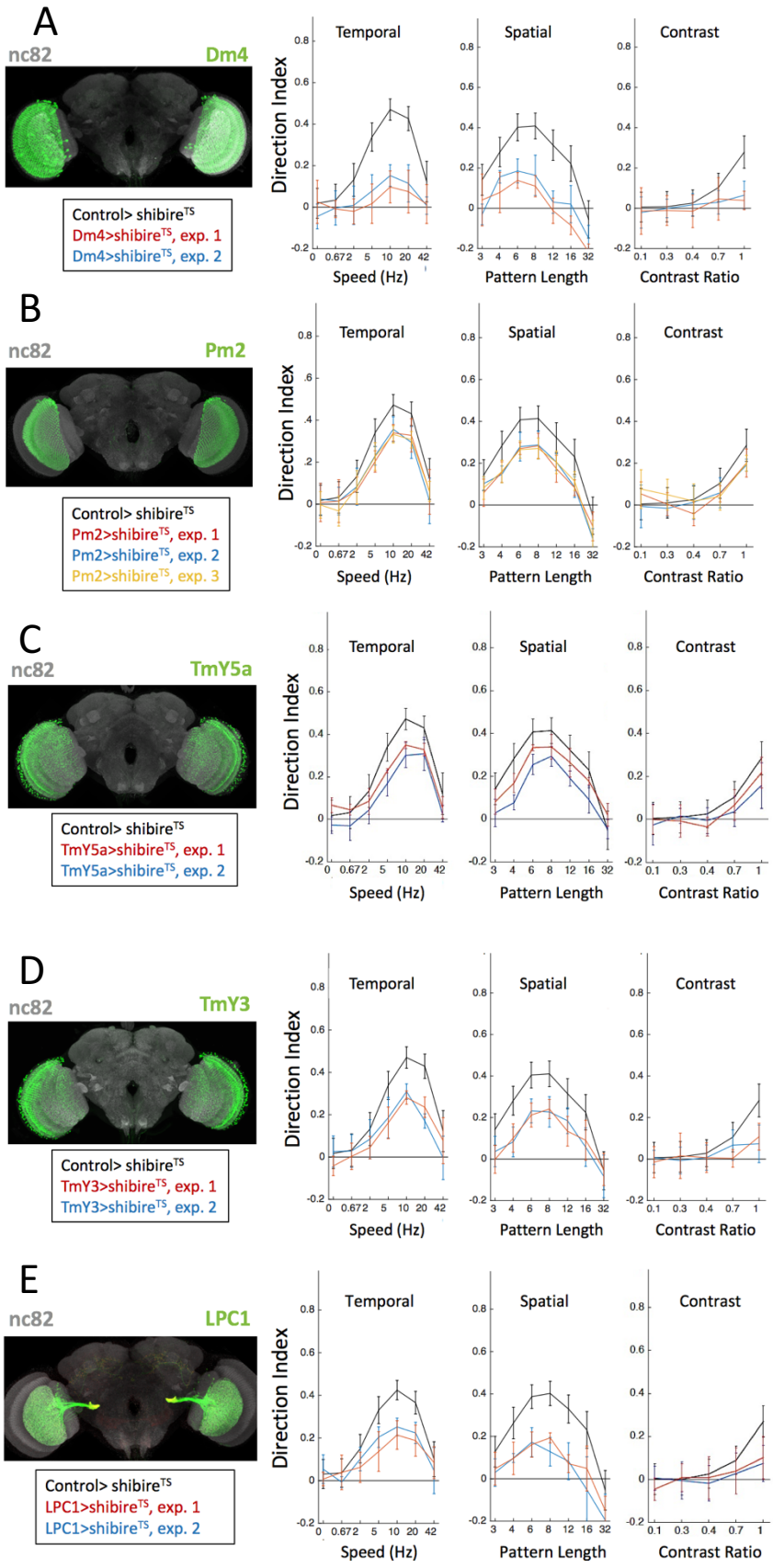

Figure 9: Novel Neural Correlates of Motion Vision Images and graphs are as described in Figure 8. Each of the interneurons shown (a-d) has a described anatomy but unknown function. Silencing these neurons gives reproducible defects in motion vision behaviors. Images provided by and anatomies identified by Aljoscha Nern. a) **Dm4** b) **Pm2**. c) **TmY5a**. d) **TmY3**. e) **LPC1**. Lobula Plate Columnar Neuron 1 (LPC1) has not been described anatomically or functionally. It is an output neuron that projects its axons from the Lobula Plate, an important structure in motion vision. This neuron was named for its target glomerulus in the central brain. Silencing LPC1 neurons causes deficiencies in motion-related phenotypes.

Phase II of the screen identified multiple interneuron types and an output neuron type with previously-unknown contributions to the motion vision pathway (**Figure 9**). Although about 50 lines in the screen showed a motion-vision phenotype, many of these lines had expression in the same neuronal subtype. About a dozen different neuronal subtypes were uncovered in the screen, but discussion and description in this chapter is limited to the 5 lines that showed the strongest effects, shown in **Figure 9.** These undescribed participants in the motion pathway confirm the assay can effectively identify novel neural correlates of motion vision. The properties and hypothesized roles of these five "hits" will be discussed in the next section.

Discussion

Significance of the Screen

This assay effectively and efficiently identified enhancer lines that target neurons involved in color and motion vision. The comprehensive results of Phase I will be available online as a resource. The GMR-GAL4 library is commonly used, and the website provides detailed information about expression and behavior for these lines. In Phase II, the hypothesis-driven screen was able to identify several known and unknown specific neuronal subtypes that contribute to motion and color vision.

Other groups have used walking assays similar to this apparatus, but this screen builds upon and enhances these other studies. Katsov *et al* screened over 400 enhancer lines using a setup where freely-walking flies in glass test tubes were shown visual stimuli underneath the tubes.[124] Silies *et el* performed a screen of 911 lines using a similar setup to Katsov.[127] The screen of 300 enhancer lines by Zhu *et al* involved a setup that

resembles this one: flies in a clear plastic corridor are shown grating patterns on an LED wall.[113] Each of these screens reported one line or neuronal subtype with a striking phenotype and characterized that line further.

With over 2,000 lines screened, this high-throughput method is both more comprehensive and more specific than previous walking screens. Combining the Phase I screen with behavior-anatomy analysis and split-GAL4 screening allowed for identification of many novel neural correlates of motion vision. Previous screens have relied on enhancer lines with wide expression. Often phenotypes seen in those screens could not be resolved to specific neurons because the lines simply had expression in too many neuronal types. The Kastov *et al* screen picked out the driver line *foma-1*, which has expression in 6-8 neurons in the lobula/lobula plate and in a large cluster of neurons in the central brain. [124] It is unclear if one of our Phase I lines matches the *foma-1* expression pattern, though Phase II of the screen did pinpoint specific neurons in the lobula complex that are important for motion vision. The screen of Silies *et al* identified L3 specifically as being important for motion vision, and the screen of Zhu *et al* had a hit from line Ln-GAL4 which is expressed in L2, L3, L4, and L5 neurons. [113,127] Our phase I screen did not identify L3 in particular, though when L3 was targeted specifically in Phase II, flies did show a motion phenotype. From our phase I screen, line GMR78B10 most closely resembles the Ln-Gal4 line with expression in L2, L3, and L4. GMR78B10 gave a subtle motion vision phenotype in our assay.

The split-GAL4 imaging also contributes to the body of anatomical data for visual neurons. Previous methods to examine anatomy (including Golgi impregnation, dye infiltration, MARCM, and flip-out techniques) label neurons stochastically.[137] But the

split-GAL4 lines that were used and created will allow researchers to study these specific neuronal types reproducibly.

Properties of Identified Neurons

Most of the identified interneurons did not make flies completely "motion blind." At least, not with Shibire^{TS} alone. That is because surprisingly few neurons are essential for motion vision; i.e. removing their function makes the animal completely motion blind. Those neurons have obvious striking phenotypes and have already been identified as being involved in the canonical vision pathways shown in **Figure 1**. Other neurons serve to refine or augment the sensitivity and responsiveness of the major neurons to visual features.[100]

It is worth noting that some of the hit lines from the Phase II screen were crossed to a "double silencer" effector, a *UAS-shibire^{TS}, UAS-kir2.1* line. Kir2.1 is an inward rectifier potassium channel that will electrically inactivate expressing neurons by hyperpolarizing the membrane membrane.[32-34] Unlike Shibire^{TS}, Kir2.1 can affect non-synaptic communication among neurons, e.g. through electrical gap junctions. The role of gap junctions in the nervous system of Drosophila is not well understood.[100] Whether Kir2.1 exacerbated phenotypes because Shibire^{TS} expression was not totally effective, or whether these neurons communicate both synaptically and nonsynaptically is unresolved.

The behavioral responses to spatial patterns for lines crossed to *UAS-shibire^{TS}, UAS-kir2.1* are shown in **Supplementary Figure 2**. Certain hits such as Dm4 showed no enhancement of the phenotype with the added Kir2.1. Others showed strong enhancement. LPC1 with Shibire^{TS} alone was motion deficient, but with Shibire^{TS} and

Kir2.1 together, silencing these neurons caused complete motion blindness, and possibly even some directional inversion at longer pattern lengths. TmY5a has only a modest motion phenotype when silenced with Shibire^{TS}. When Kir2.1 is added, the phenotype becomes striking—flies invert their walking direction at longer pattern lengths.

The Fly EM Team at Janelia created a connectome of seven columns in the Optic Lobe using electron microscopy data. This data set helped identify some of the synaptic connections for the neurons identified in the screen.

- Distal medulla neuron 4, Dm4. Dm4 may be at the intersection of motion and color vision. The main input to Dm4 is L3. L3 was not discussed in the introduction as part of the canonical motion pathway, but it also receives input from R1-R6 and may be required for orientation-related behaviors.[99] L3 seems to work combinatorially with L2 and L1, and modifies an animal's contrast sensitivity in a manner which is dependent on the speed of motion stimuli. [100,127] L3 also synapses with Tm5 and Tm9, suggesting a connection between the motion and color pathways.[114,115] The major post-synaptic partner of Dm4 is Mi4. Mi4 is also at the intersection of motion and color vision, receiving input from both R8 and L5. Mi4 also intersects the ON and OFF motion pathways. L5 is not shown in Figure 1 but is postsynaptic to both L1 and L2.[96,108]
- Proximal Medulla 2, Pm2. Pm2 may be at the intersection of communication between the ON and OFF motion pathways. It receives input from both Mi1 and Tm1 neurons. Targets of Pm2 also seem to be mainly Tm1 and Mi1 neurons.

- Transmedullary Y 5a, TmY5a. TmY neurons arborize in the distal and proximal medulla and connect the medulla to both the lobula and the lobula plate.[120] TmY neurons are therefore potentially part of the motion pathway. TmY5a seems to be a versatile neuron that could communicate with ON, OFF, and color pathways. The major presynaptic inputs to TmY5a in the medulla are Tm3 and Tm4. Tm3 is postsynaptic to L1 and responds to light increments, while Tm4 is postsynaptic to L2 and is part of the OFF-motion pathway.[107,108] One study also claimed TmY5a is postsynaptic to R7, implicating this neuron in the color vision pathway as well, though the results were not confirmed by other studies.[114]
- Transmedullary Y 3, TmY3. TmY3 receives input from Mi4, L2, and L5 (all part of the OFF pathway as described for Dm4). However, it also seems to be presynaptic to Tm3, a neuron of the ON motion pathway.
- Lobula Plate Columnar Neuron 1, LPC1. A type of output neuron was identified that arborizes throughout the lobula plate and sends axons to an optic glomerulus in the central brain. This neuron is previously undescribed. Projection neurons like LPC1 have long axons; neurons like this are often missed by the Golgi impregnation techniques that were used to anatomically characterize and report on the rest of the above neurons more than 30 years ago.[137] Most of chapter 3 will be spent exploring this interesting little neuron further.

Relevance of Walking Phenotypes

Most think of the dominant behavior for flies as being, well, flying. But foraging and mating occur during walking, making this behavior highly relevant for survival and reproduction. Several other reports have shown that responsiveness of visual neurons is enhanced during walking as well as during flight.[19,138-142]

Walking against the direction of the stimuli is a well-known phenotype and was seen in the screens that are mentioned above as well as in other experimental setups.[113,124,127,134,135] When direction of the pattern reverses, flies likewise reverse to continue walking in the opposite direction.[134]

Katsov *et al* proposed two explanations for this behavior. Orientation in the direction of the stimulus may inhibit the walking speed of flies moving in that direction, causing them to slow down, and ultimately resulting in a biased diffusion of flies in the opposite direction of the motion. Alternatively, the orientation of flies heading in the opposite direction to the stimulus may be stabilized, while flies moving in the same direction as the stimulus are free to turn. Eventually turning flies fall into the orientation trap when they turn away from the direction of the moving stimulus (See **Supplementary Figure 3**). Video evidence from hallway recordings is more consistent with the Orientation Trap model.

Flies walking in these hallway simulations go in the opposite direction of what is expected from the classic "optomotor response." In an optomotor response, flying and walking flies turn with the directions of the gratings when those gratings are shown in a circular arena rather than in a hallway.[19,98,104,118,119,138,139,143-158] The equilibrium model tries to explain this behavior by proposing that flies turn in the direction of the stimulus to

balance optic flow across both eyes. Optic flow is the movement of an image pattern across the retina caused by motion of self or surroundings. E.g. If you're a fly and the wind is blowing you to the left, your world view spins right, and you'll want to turn right to compensate for the change in your bodily direction. Under the equilibrium model, flies would always be trying to minimize optic flow; the model does not predict that flies would turn against the direction of the stimulus, as they do in these experiments and in others, because that would increase optic flow across the retina. Such behavior should be suppressed as it indicates deviation from a desired course.[124] The classic equilibrium model to explain optomotor behavior is inconsistent with these observations and the observations of related studies. Tammero *et al*. proposed an alternative to the equilibrium model of optic flow by suggesting that flies turn to minimize motion vectors behind them and prioritize motion in front of them.[159] However, this model also does not completely explain the "Against" phenotype in a hallway paradigm.

How does this screen which shows grating stimuli along the wall of a hallway compare to experiments which show grating stimuli on a semi-circular arena? All the motion vision correlates identified in this screen have a classic optomotor response when presented with grating in the semi-circular arena. Their turning phenotypes match those of control flies, while primary components of the motion pathway such as T4/T5 have a strong effect on motion perception when silenced in both the hallway experiment and in the arena experiment (**See Supplementary Figure 4**.) This assay likely identifies neural correlates of *translational motion*, while the arena display shows flies *rotational motion*. Separation of the rotational and translational pathways may occur downstream of the medulla, so some identified neurons (e.g. T4/T5) could be inputs to either pathway and

therefore silencing them would have an effect in either assay. A full discussion about translational vs rotational motion and the separate neural pathways that encode them will be taken up in chapter 3. For now, it is sufficient to state that the data suggests this experimental setup is best suited for identifying neural substrates of translational motion.

Supplemental Figures

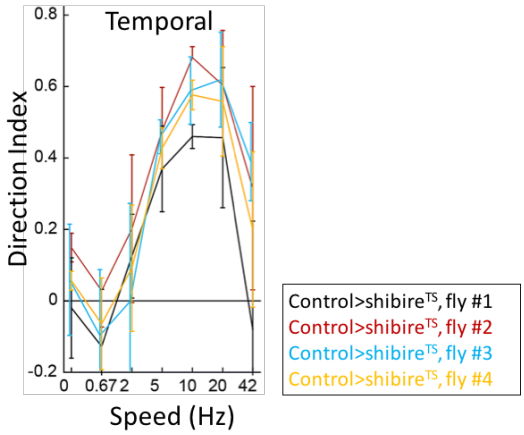

Figure S1: Single Fly Behavior. The direction index during temporal stimuli is shown as an example of behavioral results for individual flies. This graph shows four separated flies. Solitary flies behave similarly to hallway stimuli whether in a group or by themselves. The results are reproducible. The control line for this figure is a split line in the central complex that had no phenotype in the hallway when flies were tested as a group.

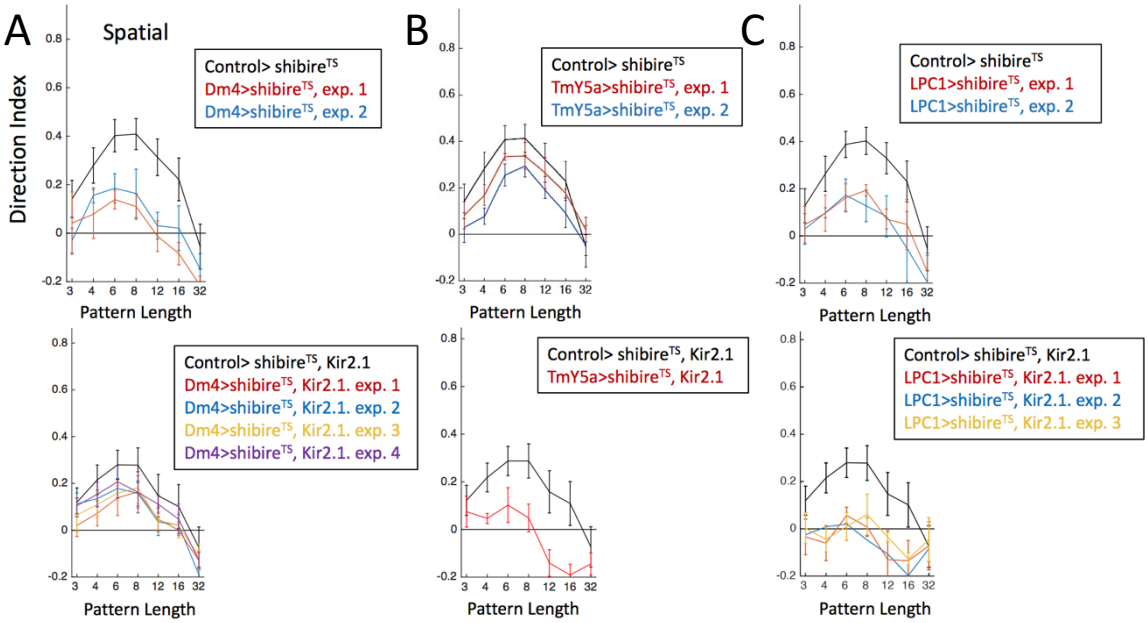

Figure S2: Adding Kir2.1 to Screen Phase II. After hits were identified using shibire^{TS}, lines were then crossed to a *UAS-shibire^{TS}*, *UAS-Kir2.1* line. Three examples are shown here comparing spatial behavior data of Shibire^{TS} genotypes to the Shibire^{TS} + Kir2.1 genotypes. Controls (black lines) with the double effector have lower direction index values than with Shibire^{TS} alone. Shibire^{TS} will silence only synaptic communication, while Kir2.1 silences any activity at all, including nonsynaptic communication. a) **Dm4.** Adding Kir2.1 does not worsen the motion-related phenotypes of Dm4 silencing. b) **TmY5a**. Adding Kir2.1 greatly exacerbates the TmY5a phenotype, even leading to a reversal of the direction index compared to controls at longer pattern lengths. c) **LPC1.** Adding Kir2.1 takes the LPC1-silenced phenotype from somewhat motion blind to completely motion-blind. Perhaps some phenotype reversal is also present at longer pattern lengths.

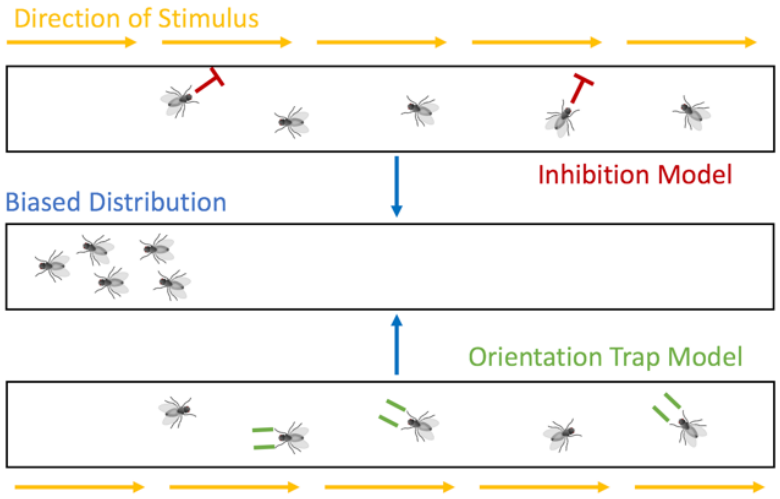

Figure S3: Two models for "Against" Behavior. This Figure is patterned after one made by Katsov *et al* (2008). A grating pattern moving to the right (yellow arrows), causes flies to move left and congregate on the left side of the corridor. Walking speed of flies may be inhibited when they walk in the same direction as the stimulus (inhibition model, red). Alternatively, turning may be inhibited in flies walking against the stimulus (orientation trap model, green). Either would result in the observed biased diffusion. Though, it can be noted that in the video recordings of single flies in the hallway, their walking speed does not decrease when moving in the same direction as the stimulus (Inhibition Model.)

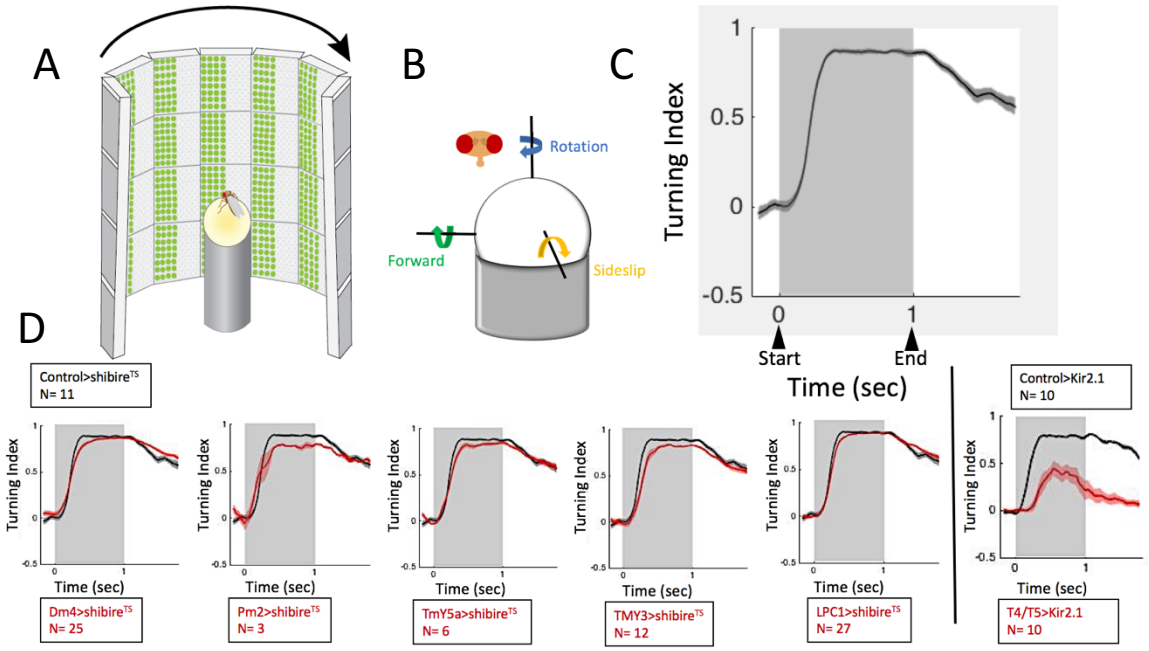

Figure S4: Hits from screen with treadmill assay. Once neuronal types important for motion vision were identified in the screen, they were used in another assay, the fly treadmill. This assay is already well-established to look at motion phenotypes. a) **Treadmill setup**. (Picture credit: Emily Nielson) Flies with glued wings are tethered to a pin and lowered onto an air-suspended ball. A cylindrical panel of LEDs surrounds the fly on three sides. This panel displays a variety of motion-stimuli on LEDs. A simple optomotor grating (lights on/lights off pattern) is show in this image. b) **Walking directions**. Flies can walk freely in any direction: forward/backwards (green), turn right/turn left (blue), and side to side (golden). The movement of the treadmill ball is captured by a camera and tracked. The three-dimensional movements are shown here from the perspective of the fly facing forward. c) **Example of optomotor behavior at 12Hz temporal frequency and 100% contrast**. When shown a moving grating on the display, control flies (N=11) turn in the direction of the stimulus. The Y-axis is turning index, or the amount of turning the fly is doing. +1 is pure turning in the direction of the stimulus while -1 would be pure turning in the opposite direction of the stimulus. When no stimulus is shown, flies have no net turning, and turning index is around 0. When the stimulus is shown for one second (shaded box), flies turn vigorously in the direction of the stimulus. The solid line shows the mean and the shaded area indicates standard deviation. d) **Hits during optomotor behavior on the treadmill**. All data shown at 12Hz speed. Lines identified during the Phase II screen as being important for motion vision do not have strong optomotor deficiencies on the treadmill. *T4/T5-GAL4, UAS-Kir2.1* is shown as an example of a strong optomotor deficiency phenotype. This shows that the screen setup can specifically identify neuron types that are involved in translational motion and may have been missed by previous studies that used the treadmill assay.

Materials and Methods

Fly Rearing

Enhancer lines[128] were crossed to *UAS-shibire^{TS}* virgins and raised on standard molasses food at 22C on a 16 hours on/8 hours off light cycle. Male progeny was cold-plate sorted when 0-2 days old and transferred to fresh food vials. Experiments were run two days after sorting on 2-4 day-old males. Flies were transferred to standard starvation media one hour before experimentation. All experiments were run between 1-3 hours before the off time of the light cycle when flies were at peak daily activity.

Apparatus Details

The apparatus used for screening is shown in **Figure 2a**. Not shown in this figure: a temperature control unit on the outside of the apparatus allowed for temperature inside the machine to stay at 34C. The machines were kept in a humidity and temperature-controlled chamber at 21C and 60% humidity.

LEDs on the wall are 0.3cm tall, 0.1cm wide and have an intensity range from 0-15. End lights are 0.3cm tall, 0.2cm wide and have intensity ranges from 0-200. The hallways inside the unit measure 14.5cm long and 2cm wide each. The clear plastic corridors where flies are loaded and then lowered into the hallways measure 13 cm long (including the two 0.5cm-thick clear plastic end seals), 0.5cm high, and 1.2cm wide. The camera is fixed 60cm above the device. The corridor seals on either end have small magnets attached that allow them to be fixed onto the lid of the machine. When the lid is lowered, the corridors are suspended such that their wall aligns with the LEDs on the wall

of the hallway. Corridors and their seals were washed with water and lab glass detergents at the end of each day to remove any lingering odorants and particles.

Full Sequence of Visual Stimuli, Phase II

(Phase I had a slightly different ordering and parameters for the following protocols.)

1) Startle
    a. 6 vibrations, 0.5sec long, 10sec apart
2) Temporal: Increasing the frequency of 4 LED on/4 LED off. Patterns are shown for 10 seconds. Each change in direction (every 10sec) is accompanied by a 0.5sec vibration.
    a. 0 Hz right
    b. 0 Hz left
    c. .67 Hz right
    d. .67 Hz left
    e. 2 Hz right
    f. 2 Hz left
    g. 5 Hz right
    h. 5 Hz left
    i. 10 Hz right
    j. 10 Hz left
    k. 20 Hz right
    l. 20 Hz left
    m. 42 Hz right

n. 42 Hz left

o. Repeat a-n in reverse order

3) Contrast, constant total intensity: At a constant speed of 10Hz, the contrast of the stripes with a pattern length of 4 LED high intensity/4 LED low intensity is increased. Total intensity is maintained at 15. A 0.5 second vibration is concurrent with the changes in direction, every 10 seconds. Contrast ratios are calculated as follows: (High-Low)/(High+Low).

   a. High: 8, Low: 7, right

   b. High: 8, Low: 7, left

   c. High: 9, Low: 6, right

   d. High: 9, Low: 6, left

   e. High: 11, Low: 4, right

   f. High: 11, Low: 4, left

   g. High: 13, Low: 2, right

   h. High: 13, Low: 2, left

   i. High: 15, Low: 0, right

   j. High: 15, Low: 0, left

   k. Repeat a-j in reverse order

4) Contrast, decreasing total intensity: At a constant speed of 10Hz, increase the contrast of the stripes with a pattern length of 4 LED high intensity/4 LED low intensity. A 0.5 second vibration is concurrent with the changes in direction, every 10 seconds. Contrast ratios are calculated as follows: (High-Low)/(High+Low). This contrast pattern is the one shown in **Figure 2**.

a. High: 15, Low: 12, right
b. High: 15, Low: 12, left
c. High: 15, Low: 9, right
d. High: 15, Low: 9, left
e. High: 15, Low: 6, right
f. High: 15, Low: 6, left
g. High: 15, Low: 3, right
h. High: 15, Low: 3, left
i. High: 15, Low: 0, right
j. High: 15, Low: 0, left
k. Repeat a-j in reverse order

5) Spatial: Increase the size of the bars, maintaining a 10Hz speed for each pattern, i.e. the number of times the edge of a specific stripe in the pattern goes past a particular point on the wall remains unchanged. A startle is concurrent with the changes in direction, every 10 seconds.
    a. 1 on: 2 off (pattern not shown in **Figure 2**), right at 32ms/step
    b. 1 on: 2 off, left at 32ms/step
    c. 2 on: 2 off, right at 24ms/step
    d. 2 on: 2 off, left at 24ms/step
    e. 3 on: 3 off, right at 16ms/step
    f. 3 on: 3 off, left at 16ms/step
    g. 4 on: 4 off, right at 12ms/step
    h. 4 on: 4 off, left at 12ms/step

i. 6 on: 6 off, right at 8ms/step

j. 6 on: 6 off, left at 8ms/step

k. 8 on: 8 off, right at 6ms/step

l. 8 on: 8 off, left at 6ms/step

m. 16 on: 16 off, right at 3ms/step

n. 16 on: 16 off, left at 3ms/step

o. Repeat patterns a-n in reverse order

6) Phototaxis: low UV, high UV, low green, or high green intensities. Each change in intensity and direction is accompanied by a 0.5sec vibration. Changes in direction occur every 15 seconds.

a. UV=20, right

b. UV=20, left

c. UV=100, right

d. UV=100, left

e. Green=15, right

f. Green =15, left

g. Green =200, right

h. Green =200, left

i. Repeat a-h in reverse order

7) Color preference, Constant Green: Green intensity kept constant while intensity of UV increases. Every change in direction is accompanied by a 0.5sec vibration. Changes occur every 10 seconds.

a. Green Right= 120, UV Left= 0

b. Green Left= 120, UV Right= 0

c. Green Right= 120, UV Left= 5

d. Green Left= 120, UV Right=5

e. Green Right= 120, UV Left= 10

f. Green Left= 120, UV Right= 10

g. Green Right= 120, UV Left= 15

h. Green Left= 120, UV Right= 15

i. Green Right= 120, UV Left= 25

j. Green Left= 120, UV Right= 25

k. Green Right= 120, UV Left= 50

l. Green Left= 120, UV Right= 50

m. Green Right= 120, UV Left= 100

n. Green Left= 120, UV Right= 100

o. Green Right= 120, UV Left= 200

p. Green Left= 120, UV Right= 200

q. Repeat patterns a-p in reverse order

8) Color preference, Constant UV: UV kept constant and intensity of green increases. Every change in direction is accompanied by a 0.5sec vibration. Changes occur every 10 seconds.

a. Green Right= 0, UV Left= 5

b. Green Left= 0, UV Right= 5

c. Green Right= 3, UV Left= 5

d. Green Left= 3, UV Right= 5

e. Green Right= 10, UV Left= 5
f. Green Left= 10, UV Right= 5
g. Green Right= 20, UV Left= 5
h. Green Left= 20, UV Right= 5
i. Green Right= 30, UV Left= 5
j. Green Left= 30, UV Right= 5
k. Green Right= 50, UV Left= 5
l. Green Left= 50, UV Right= 5
m. Green Right= 100, UV Left= 5
n. Green Left= 100, UV Right= 5
o. Green Right= 200, UV Left= 5
p. Green Left= 200, UV Right= 5
q. Repeat patterns a-p in reverse order

Dissections and Immunostaining

The full protocol for the dissection, immunostaining, and mounting procedure, along with details about the reagents used can be found at: https://www.janelia.org/project-team/flylight/protocols, IHC Adult Split Screen.

Brain Anatomy Maps

Full details about the calculations involved to create the Brain-Anatomy maps can be found in Robie *et al* 2017. [136]

Fly Treadmill

Fly treadmill and subsequent analysis was as described by *Seelig et al 2010*.[158] The treadmill was 9mm in diameter and airflow kept at 400ml/min. Speed is kept in units of pixels per frame, though for the ball size and airflow, it is estimated 1 pixel/frame can be converted to somewhere in the range of 3mm/sec. All flies were female, 3-6 days old; they were cold-sorted at least 2 days before experiments and their wings glued at least 1 day before experiments. The panels used to create the arena display are described by Reiser and Dickinson (2008).[160] The arena was kept inside an incubator at 60% humidity and 32°C. temperatures near the treadmill were measured at 34°C due to the heat from the LEDs.

Chapter 3: A Novel Neuronal Pathway to Encode Regressive Motion and Regulate Forward Walking Speed in *Drosophila*

Introduction

The major goal of neuroscience is to connect sensory input to behavioral output by ascribing function to neurons and neuronal circuits. The visual system of *Drosophila melanogaster* provides an excellent model to study the conversion of sensation into action. The anatomy of neurons in the visual system has been known for over one hundred years, and flies have a variety of interesting visually-guided behaviors. Flies have been using their visual system for 240 million years to survive.[161] Vision is vital for exploration, courtship, navigation, and predator elusion. Yet it is only in the past decade or so that researchers have begun to make substantial progress and associate neuronal anatomy and connectivity with behavioral relevance.

The neuronal infrastructure that makes motion vision possible is of particular interest. Motion vision represents the brain's ability to make complex calculations from sensory stimuli. No one neuron or photoreceptor can perceive movement on its own or provide any information about speed or direction. Neurons must coordinate to encode motion stimuli and to refine the qualities and properties of the movement against a visually noisy background. Which neurons influence motion vision-related behaviors? What visual features are extracted by each neuron? How does each neuron integrate with others in a circuit to produce a behavior?

Flies respond differently to rotational and translational motion.[124,153-155,159,162] When a fly experiences rotational motion—either because its body or its environment is rotating—the optic flow on the fly's retina is uniform in speed and direction (**Figure 1a**). "Optic flow" is the perceived pattern of direction vectors on the retina which represent a moving image. Flies respond to rotational optic flow by turning with the direction of the stimulus. During translation—i.e. when a fly is traversing its environment—optic flow radiates from a single focal point in line with the direction of motion. For example, **Figure 1b** shows a translational movement called "expansion." During forward translation, the focus of expansion is directly in front, and a focus of contraction will be at the opposite pole, 180 degrees behind the animal. Visual features move across the retina from front-to-back (aka progressive motion), and nearer objects will appear to move faster than further objects.[163-

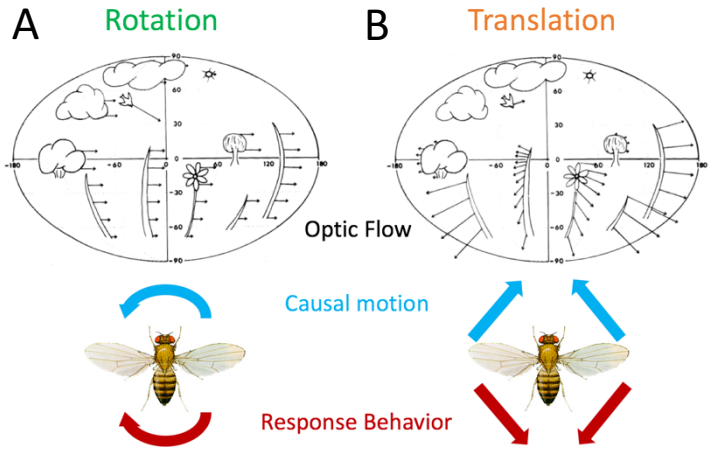

Figure 1: Translation and Rotation Optic Flow. Depictions of optic flow taken from Buchner *et al* (1984). **a) Rotation.** When the observer or scene rotates around a fixed central point, this creates rotational optic flow. Image vectors all move in the same direction and at the same speed. Rotational optic flow causes a traditional optomotor response—flies will move in the direction of the stimulus. **b) Translation.** Translational motion occurs as the observer of the scene moves linearly. During translational motion, optic flow originates from a focus point. Image vectors move in different directions and closer objects appear to be moving faster than further objects. When the vectors move towards the observer, this translational motion is known as expansion (shown here.) When the vectors move away from the observer, this is contraction.

[165] Flies respond to translational optic flow by turning strongly away from the focus of expansion.[127,159,162]

The different responses to translation or rotation suggest the motions calculated by separate neuronal mechanisms. The neural pathways that interpret these two kinds of optic flow show distinct temporal, spatial, and contrast sensitivities.[154,155] Understanding how neurons distinguish rotational and translational motion (and where in the brain the pathways diverge) will help decipher the nuances of motion vision processing.

As part of a screen to identify neural correlates of motion vision (see chapter 2), a previously-undescribed output neuron of the fly visual system was identified and named Lobula Plate Columnar Neuron 1 (LPC1). Projection neurons, like LPC1, are often missed by traditional techniques for anatomical characterization (e.g. Golgi impregnation) because of their long axons.[137] **Figure 2a** shows individual LPC1 neurons, obtained using the FlipOut method.[166] (All images in this chapter are provided curtesy of Aljoscha Nern and FlyLight.) The cell bodies are attached by long thin filaments, removed from the specialized axonal and dendritic ends of the neuron. (This is typical anatomy for *Drosophila* neurons.[120,167]) A Split-GAL4 enhancer line was made by Aljoscha Nern with specific expression in LPC1 neurons. **Figure 2b** shows the anatomy of the entire population of LPC1 neurons (~90) that were targeted using the Split-GAL4 method. LPC1 dendrites branch throughout the Lobula Plate of the Optic Lobe and project their axons to the same optic glomerulus in the central brain. Using RNAseq, it was determined that LPC1 neurons are cholinergic (data not shown).

Initial observations suggested LPC1 is involved in perception of translational motion. During the screen described in chapter 2, LPC1 Split-GAL4 lines were crossed to

UAS-shibire^{TS}. Shibire^{TS} is a temperature-sensitive dominant dynamin mutant which stops synaptic transmission at elevated temperatures.[35-40] At 34C, flies with silenced LPC1

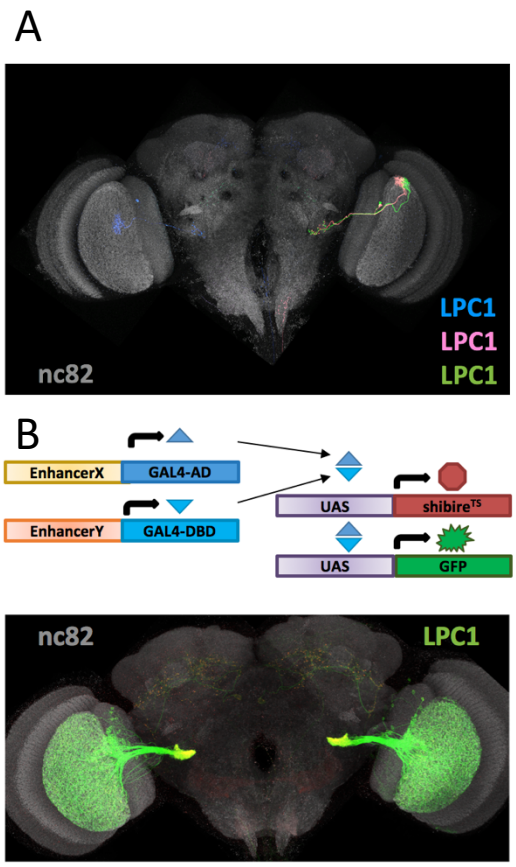

Figure 2: LPC1 Anatomy. Brains are posterior side-up. Grey is the nc82 antibody, an anti-bruchpilot that serves as a general neuropil marker. All images were produced by FlyLight and provided curtesy of Aljoscha Nern. **a) LPC1 FlipOut.** The FlipOut method stochastically labels single neurons. This image shows three LPC1 neurons in blue, pink, and green. LPC1 dendrites arborize in the Lobula Plate and their long axons project to an optic glomerulus in the central brain. The cell bodies are connected by a thin fiber. **b) LPC1 Split-GAL4.** To target LPC1 neurons specifically, Split-GAL4 lines were created. GAL4 is segregated into its Activation Domain (AD) and DNA binding Domain (DBD) and each is driven from its own enhancer. Expression of a *UAS-transgene* such as *GFP* or *shibire*^{TS} only occurs in neurons where expression of the two enhancers intersects. The image shown here is *LPC1-SplitGAL4, UAS-GFP*. (Green is anti-GFP). The population of LPC1 neurons spans the entire Lobula Plate and all LPC1 axons target the same glomerulus.

neurons had deficiencies in motion vision (**Figure 3a.**) Crossing LPC1 to other effectors such as *UAS-Trp* or *UAS-Kir2.1* further exacerbated this phenotype and may have even caused some reversal behavior (**Supplementary Figure 1**.) Trp is a warmth-responsive channel that will activate neurons when expressed at elevated temperatures.[168] Kir2.1 will hyperpolarize and electrically inactivate neurons.[32-34] Kir2.1 eliminates both synaptic and nonsynaptic neuronal signals while Shibire^{TS} only removes synaptic signals. It is unclear whether Kir2.1 aggravates the phenotype because it is a more effective silencer than Shibire^{TS}, or because LPC1 uses both synaptic and lateral electrical communication.

LPC1's involvement in motion vision was further confirmed by replicating the screen results with multiple other Split-GAL4 lines (**Supplementary Figure 2**.) These split lines contain different enhancer "halves" but all showed specific expression for LPC1 neurons.

The screening apparatus described in chapter 2 shows movement along the wall of a hallway, and therefore presents translational optic flow to the flies. The fly treadmill assay is a well-established and widely-used experimental paradigm for rotational optic flow.[98,104,118,119,138,156,157] How will behavior in the hallway compare to behavior on the treadmill?

For the treadmill, flies are tethered to a pin and lowered onto an air-suspended ball. Cameras track the ball's motion as a proxy for the motion of the fly. A cylindrical arena of LED panels surrounds the fly for 270 degrees.[158,160] When shown a rotational moving grating pattern (stripes of on and off lights), LPC1 flies have no motion vision deficiencies; they display the typical optomotor response and turn in the direction of the stimulus (**Figure 3b**). This result suggested that LPC1 specifically detects translational, and not rotational motion.

In this chapter, LPC1 is characterized further to identify its role in the motion vision pathway. LPC1: encodes back-to-front and up translational movements, has the greatest effect at high speeds, regulates forward walking speed, and regulates surge flight behavior. Potential upstream and downstream synaptic partners of this neuron are also identified. Mapping function and connectivity, as demonstrated here with LPC1, allows a greater understanding to be gained regarding how sensory neurons cooperate to encode stimulus information and produce appropriate reactions.

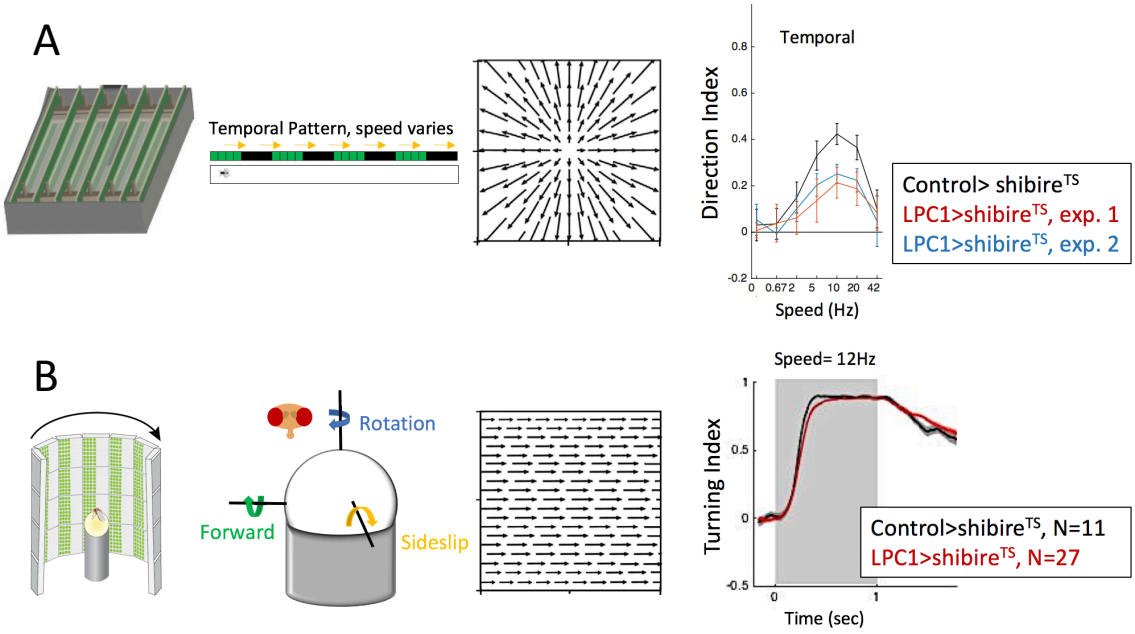

Figure 3: LPC1 Behavior. LPC1 Split-GAL4 lines are crossed to *UAS-shibire^{TS}*. All behavioral experiments are done at 34C to allow Shibire^{TS} to silence LPC1 neurons. Controls are a Split-GAL4 line with empty enhancers. **a) LPC1 in the Hallway.** Flies are freely walking in a corridor with moving grating (stripes of on and off lights) along the wall as described in chapter 2, figure 2. Shown here is behavioral data from a temporal stimulus where the grating patterns move at varying speeds. Each apparatus contains 6 corridors with 15 flies, N= 90 per experiment. Grating in this apparatus will create translational optic flow. Control flies (black) move against the direction of any motion stimuli. Direction Index= ($Flies_{preferred} - Flies_{nonpreferred}$)/Total Flies, and is averaged across all corridors. A direction index of 0.5 indicates ~11-12 of the 15 flies per corridor are walking against the stimulus. When LPC1 is silenced (blue and red), flies are deficient in all motion-related behaviors. **b) LPC1 in the Arena.** Flies with glued wings are tethered to a pin and lowered onto an air-suspended ball surrounded on three sides by a circular arena of LEDs. Flies can walk in any direction on their "treadmill" and cameras capture the changing direction and speed of the ball as a proxy for the fly's movement. Grating shown in the arena will create rotational optic flow. Control flies turn in the direction of the stimuli. The turning index indicates the amount of total fly motion that is attributed to its turning. A turning index of +1 indicates complete turning of the fly in the direction of the stimulus. When LPC1 is silenced, flies resemble controls and are not deficient in visual behaviors. Shown here is a one second (grey box) grating moving at 12Hz. Controls are shown in black and LPC1-silenced flies in red. Solid lines indicate the mean and the shadow represents the standard deviations for every frame. Pictures of arena and box, credit: Emily Nielson. Depictions of optic flow, credit: Horseman *et al* (2011).

Results

LPC1 Regulates Forward Walking Speed

The Hallway apparatus is not directly comparable to the treadmill, so grating patterns were created for the circular arena that would mimic translational optic flow. Grating patterns moved away from (expansion) or towards (contraction) a focal point. The focal point varied from 90, 60, and 30 degrees on the left to 0 degrees in front and then to 30, 60, and 90 degrees on the right. Rotational gratings move unbroken in a clockwise (CW) or counterclockwise (CCW) direction (**Figure 4a**).

When control flies see a focus of expansion, they slow their walking and turn away. Flies also slow down during contraction but orient themselves towards the focus of contraction. The responses at 0 degrees and 90 degrees are shown in **Figure 4b**. All data shown in this figure is for a 9Hz stimulus speed. Negative turning indicates a turn away from the focal point and positive turning indicates a turn towards the focal point. Note that when the expansion is directly in front of the flies, at 0 degrees, they have no preference in turning away right or left, so the average of all flies and trials is around 0. Also note that the 90-degree stimuli responses are averaged. Even though the arena is open on one end behind the fly, stimulus patterns move as if the circle is closed. Therefore, a 90-degree contraction on the right is also a 90-degree expansion on the left. In this figure, turning and forward responses are shown as pixels per frame measurements; un-normalized data gives a good idea of the raw behavioral responses.

Control flies also slow in response to rotational motion. These flies show the classic optomotor response of turning with the stimulus. Negative turning values indicate left turns and positive values indicate right turns (**Figure 4c).**

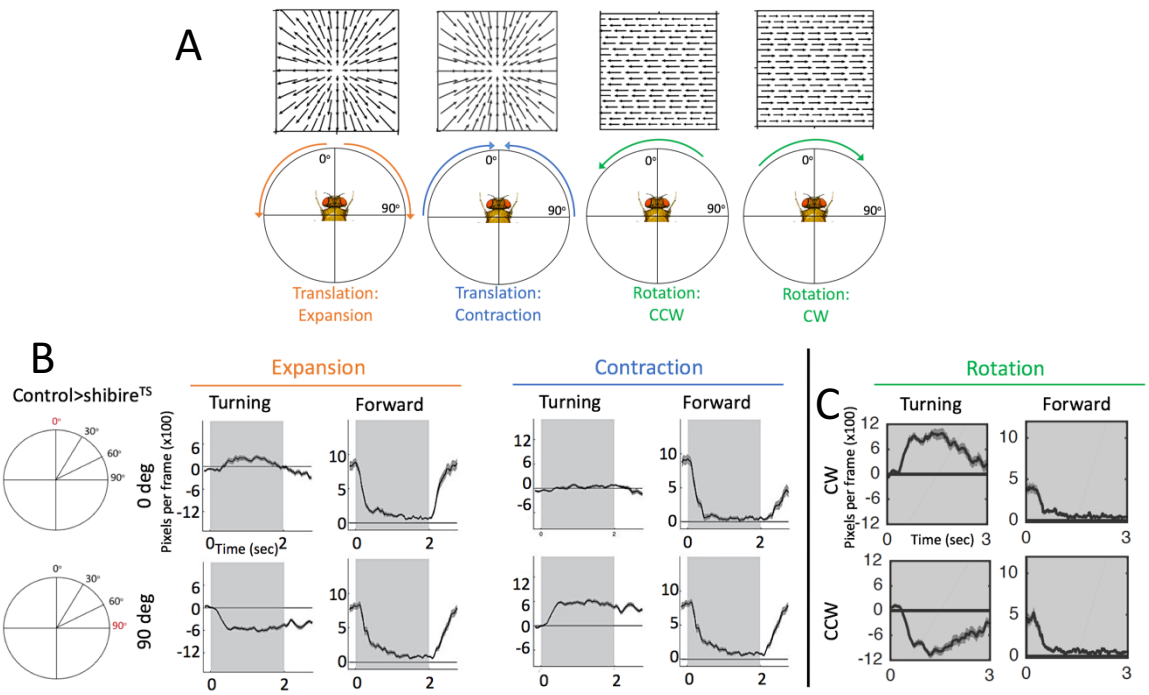

Figure 4: Control responses to translational and rotational stimuli. **a) Stimulus Conditions** Typical arena gratings move in a rotational manner, clockwise and counterclockwise. But Translational optic flow can be recreated in the arena by moving the grating along either side of the fly from an origin point (shown here at 0 degrees, or directly in front of the fly). The grating lines move towards the focal point (contraction) or away from the focal point (expansion). Depictions of optic flow, credit: Horseman *et al* (2011). **b) Translational Behavior**. Control flies (Split-GAL4 with empty enhancers) walking on the treadmill are shown an expansion or contraction grating pattern for two seconds (grey box) at various origin locations. Shown here are the responses at 0 and 90 degrees. The average of all flies is shown as the black line; standard errors for every frame are represented by the shading around the mean. Each fly is given 5 trials of each stimulus and N=26. The Y-axis is raw turning and forward responses of flies. Negative turning numbers indicate turns away from the stimulus origin and positive numbers indicate turns towards the stimulus origin. All stimuli in this figure move at 9Hz. When shown expansion, flies turn away from the focal point and decrease forward motion. When the expansion is at 0 degrees, flies have no preference for turning right or left, so the behavior from multiple flies averages out to around 0. But the responses at 90 degrees demonstrate that flies are turning away. When shown contraction stimuli, flies slow down, but also have no net turning as the try to maintain a straight course towards the focus of contraction. A 90-degree right expansion is the same as a 90-degree left contraction. These graphs average out to be the same, but in opposite directions, because the fly is turning away from the focus of expansion and towards the focus of contraction. **c) Rotational Behavior.** If flies are shown clockwise or counter clockwise stimuli for three seconds (graphs show only stimulus conditions), they turn with the direction of the stimulus and slow down. Negative turning values indicate left turns and positive values indicate right turns. Speed=9Hz, N=18.

What happens to visually-guided behaviors when LPC1 neurons are silenced? **Figure 2** already showed that silencing LPC1 neurons has no effect on rotational behaviors. **Figure 5a** shows turning responses at varying speeds of expansion or contraction, averaged across the entire stimulus duration (2 seconds) and for every fly and trial (5 trials of each stimulus per fly.) Turning index is a calculation of the total amount of motion that can be attributed to turning. A turning index value of +1 would indicate pure turning towards the focal point. A value of -1 would indicate pure turning away from the focal point. At 0 degrees expansion or contraction, flies have no clear turning direction. They simply turn away from expansion or towards contraction in either direction. At every focal point and for every speed, control flies (a Split-GAL4 line with empty enhancers) and LPC1-silenced flies turn away from expansion and turn towards contraction. Their reactions become stronger as speed increases. LPC1-silenced flies show a small turning deficiency at 30 degrees contraction, but otherwise have very normal turning responses.

Control flies slow down when shown contraction or expansion stimuli, and the strength of the response increases as speed increases (**Figure 5b**). Forward walking is normalized to the baseline walking speed (when no stimulus is shown.) LPC1-silenced flies only slow down under certain conditions. Why? Stimuli for which LPC1-silenced flies did *not* slow down also had *more* regressive optic flow. The amount of slowing for LPC1-silenced flies is inversely proportional to the amount of regressive optic flow. At 0 degrees contraction, both eyes see complete back-to-front motion, so percentage of regressive optic flow is 100%. LPC1-silenced flies maintain their walking speed most strongly at 100% regressive optic flow. As back-to front motion decreases, LPC1-

silenced flies behave more like control flies. From these results, it is predicted that LPC1 encodes regressive motion and regulates the slow down in response to strong back-to-front optic flow.

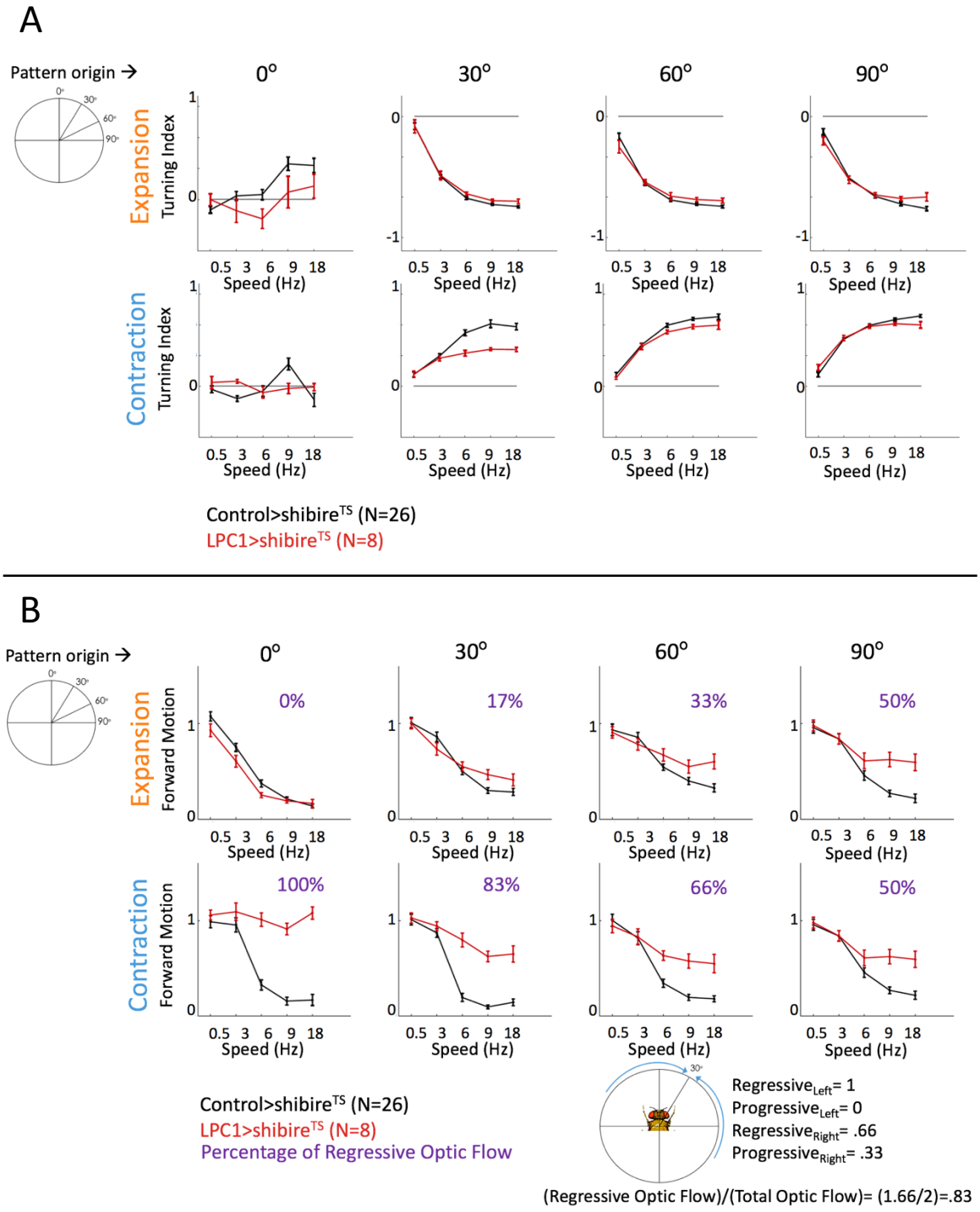

Figure 5 captioned, next page.

Figure 5: LPC1 Modulates Walking Speed during Regressive Motion. Flies are show contraction or expansion gratings at varying points of origin: 90 degrees left, 60 degrees left, 30 degrees left, 0 degrees (in front), 30 degrees right, 60 degrees right, and 90 degrees right. Each grating stimulus was also shown at varying speeds: 0, 2, 6, 9, or 18 Hz. Control flies (black) are a Split-GAL4 line with empty enhancers, N=26. LPC1-silenced flies are shown in red, N=8. Graphs show the average for all flies and all trials; each fly was shown each stimulus 5 times. Right and left stimuli were also averaged. (Since a 90-degree right expansion is the same as a 90-degree left contraction, responses to these two stimuli average out to be the same but in opposite directions.) The experiments were done at 34C to allow for neuronal silencing using Shibire^{TS}. **a) Turning.** Turning responses are measured as turning index. Turning index shows how much total fly movement is attributed to turning. +1 indicates total turning in the direction of the stimulus origin and -1 indicates total turning against the stimulus origin. For all contraction and expansion speeds shown at 0 degrees, flies are turning away from expansion and towards contraction, but the direction they choose, right or left, should be random. Flies turn away from expansion stimuli and towards contraction stimuli at any speed and for any point of origin. Turning responses increase as stimulus speeds increase. Silencing LPC1 had no effect on turning, except flies seem to turn a little less in response to a 30-degree contraction at higher speeds. **b) Forward.** Forward motion is normalized to the average walking speed of the fly without a stimulus. E.g. a value of 0.5 indicates the flies slowed down by half from their normal walking speed. Control flies slow down when they see expansion or contraction. They slow more as stimulus speed increases, which corresponds to their increased turning. When LPC1 is silenced, flies do not slow in response to certain stimuli, even though they turn as much as controls. The amount of slowing for LPC1-silenced flies is inversely proportional to the amount of regressive optic flow (back-to-front motion). As an example, consider a focus of contraction at 30 degrees on the right. The entire left eye will see back-to-front motion. Two-thirds of the right eye will see back-to-front motion and the other third will see progressive (front-to-back motion.) Therefore, at 30 degrees contraction, 83% of the optic flow is regressive. At 30 degrees, flies LPC1-silenced flies have a strong forward motion phenotype.

It is important to notice that turning is nearly unaffected (**Figure 5a**) and does not correlate with walking speeds (**Figure 5b**). It would be logical to assume speed and turning are coupled behaviors, as happens with control flies—the animals need to slow down in order to turn more. However, the un-normalized data shows that LPC1-silenced flies maintain a constant speed while turning as much as control flies.

In summary, Figure 5 data shows: 1) LPC1 plays a role in encoding regressive motion; when a higher percentage of the stimulus involves back-to-front optic flow, the

strength of the phenotype increases. 2) LPC1 has a role in regulating forward walking speed but not turning behaviors in response to translational stimuli. 3) turning and speed responses can be uncoupled—an increase in turning does not necessarily lead to a decrease in forward walking speed.

LPC1 Detects Regressive and Up Translational Motion

To confirm LPC1 neurons encode translational motion, LPC1 activity was directly imaged during stimulus presentation by Matthew Isaacson. The cuticle was removed from flies so live images could be taken directly from the brain as the fly watches stimuli on an LED display (**Figure 6a**). In order to image from LPC1 neurons, GCaMP6s, a calcium-sensitive fluorescent indicator, was expressed.[169] When a neuron depolarizes, there is an influx of calcium. Therefore, a fluorescent signal occurs whenever the GCaMP-expressing neuron is activated by a stimulus. LPC1 was imaged from its axon ends which form the glomerulus (**Figure 6b**).

Optic flow was created that would better resemble rotational or translational motion along any axis. Flies can move any direction for canonical axes. When they turn around an axis, they display rotational motions—yaw, pitch, and roll. When they move along an axis, they display translational motions—lift, slip, and thrust[153] (**Figure 6c**). Grating stimuli were created to mimic each of these possible movements and directions. Then these stimuli were shown to head-fixed flies of genotype *LPC1-SplitGAL4, UAS-GCaMP6s* to image live LPC1 responses. These stimuli were also shown to *LPC1-SplitGAL4, UAS-shibire^{TS}* flies and control flies on the treadmill. All grating stimuli designs and imaging data were provided by Matthew Isaacson.

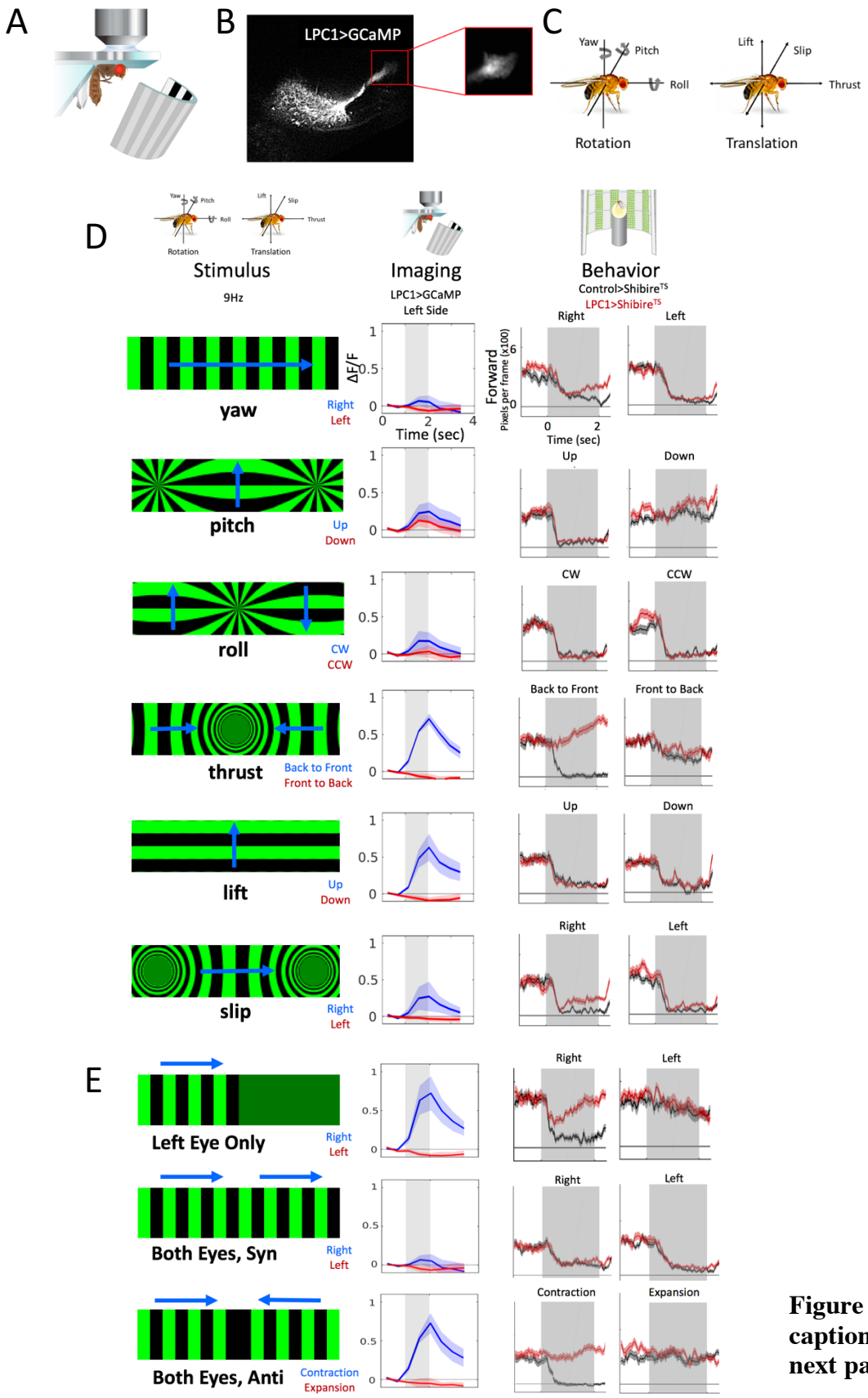

Figure 6 captioned, next page.

Figure 6: LPC1 Imaging and Behavior. a) Imaging setup. Setup depiction taken from Serbe *et al* (2016). Fly heads with exposed brains are positioned under a microscope to capture fluorescent calcium-sensitive signals. Flies are surrounded for 270 degrees by an LED arena which is angled so their head position relative to the display is the same as it would be while walking on the treadmill. **b) LPC1 and GCaMP6s**. LPC1 Split-GAL4 line is crossed to a *UAS-GCaMP6s* line. GCaMP will fluoresce in the presence of calcium, such as the influx of calcium that occurs when an activated neuron depolarizes. Fluorescence is recorded from LPC1's target glomerulus. **c) Translational and Rotational movement**. A fly can move along any axis in 3D. A yaw is rotation right or left around the y axis. Flies rotating clockwise or counterclockwise along the x-axis are performing a roll. A pitch is a rotation up or down around the z-axis. Translational equivalents of these motions are: lift along the y axis, thrust along the x-axis, or slip along the z-axis. **d) Comparison of imaging and behavior.** All stimuli depictions and imaging data provided by Matthew Isaacson**.** Grating stimuli was made to resemble the optic flow during the six rotational or translational movements shown in c. *LPC1-SplitGAL4, UAS-GCaMP6s* flies were imaged from the left side of the brain while being shown each stimulus at 9Hz for one second (shaded box). N=6, 3 trials of each stimulus per fly. The y-axis of the imaging graphs shows the change in fluorescence compared to baseline fluorescence. Data from one stimulus direction are shown in blue and data from the stimulus in the opposite direction are shown in red. Walking flies on the treadmill are shown the same stimulus as the imaged flies for 2 seconds (shaded box) at 9Hz. Each fly was shown each stimulus 5 times. Control flies (Split-GAL4 with empty enhancers crossed to *UAS-shibire^{TS}*, N=19) are shown in black and *LPC1-SplitGAL4, UAS-shibire^{TS}* flies (N=20) are shown in red. The Y-axis shows raw forward motion in pixels per frame (x100). In all graphs, the average of all flies and trials is shown as a solid line and the standard deviation for every frame is depicted with a shadow. LPC1 neurons are not activated by any rotational stimuli (yaw, pitch, or roll) and the forward walking speed of LPC1-silenced flies roughly matches controls. LPC1 responds strongly to the up, front-to-back thrust, and right side slip translational stimuli. When stimuli are shown in the opposite directions, fluorescence dips below baseline, suggesting some inhibition may occur in the non-preferred direction. When LPC1 is silenced, flies do not slow in response to regressive thrust motion, and slow down less than controls for rightward slip motion. Other neurons are likely involved in the regulation of walking speed in response to lift and slip stimuli. e) **Comparing single eye to both eyes**. Data are arranged as described in d. Since imaging data was taken from the left side only, it was unknown if one or both eyes were required for the observed imaging and behavioral responses. When only one eye is shown regressive motion, LPC1 is activated. Likewise, regressive motion on one eye is sufficient to achieve the forward walking phenotype in LPC1-silenced flies. When one eye is shown regressive motion and the other sees progressive motion, LPC1 is not activated and the behavior of LPC1-silenced flies resembles controls. When both eyes are shown regressive motion, LPC1 fluoresces and the behavioral phenotype is restored. It is possible progressive motion from one eye will inhibit LPC1 on the opposite side of the brain. Stimuli in the non-preferred direction cause no activation or behavioral phenotypes.

Figure 6d shows LPC1 imaging responses alongside LPC1-silenced behavioral responses for each stimulus. All stimuli were shown in both directions at 9Hz for 1 second (imaging) or 2 seconds (behavior.) This speed gave maximum responses for both imaging and behavioral experiments when the speed-tuning curve for LPC1 was evaluated (**Supplementary Figure 3**.) Imaging responses were calculated as the change in fluorescence over baseline fluorescence. All imaging was done from the left side of the brain. Notice that for the three kinds of rotational motion (yaw, pitch, and roll), LPC1 neurons show little or no activity and silencing LPC1 has no effect on forward walking. However, LPC1 neurons responded to every translational stimulus (thrust, lift, and slip) but only in one direction (back-to-front, up, and right.) The preferred direction is consistent with regressive or up motion on the left side of the brain, where the imaging is taking place. Once again, there is a strong behavioral phenotype for LPC1-silenced flies during thrust; they do not decrease forward walking in response to back-to-front motion. It could not have been determined that LPC1 detects up and slip from behavioral experiments alone. LPC1-silenced flies decrease forward speed slightly less than controls during rightward slip, probably due to the small amount of regressive motion in the stimulus. Otherwise, LPC1-silenced behavioral responses look very similar to controls. Lift and slip perception must receive input from additional neurons to regulate forward walking speeds.

All the imaging was done from the left eye during full-field stimulus displays; will stimuli on only one eye be sufficient to produce LPC1-related imaging and behavioral responses? (**Figure 6e**) LPC1 is activated when regressive grating is shown to the left eye only, and LPC1-silenced flies do not slow down as much as controls. If the

left-side only grating moves left, the left eye sees progressive motion. LPC1 neurons do not respond and behavior resembles controls. However, fluorescence dips a little, suggesting progressive motion may inhibit LPC1 neurons. If rightward grating is added to the right eye also, the left eye continues to see regressive motion but the right eye is now experiencing progressive motion (as would happen in a typical rotation stimulus). In this condition, LPC1 does not respond and silencing LPC1 has no effect on behavior. This suggests progressive motion on one eye can inhibit LPC1 in the opposite eye. If both eyes see regressive motion (contraction stimulus), LPC1 responds and silencing LPC1 eliminates the slowing response. Once again there is a small dip in fluorescence during the expansion stimulus, when both eyes see progressive motion. This is consistent with the idea that progressive motion may inhibit LPC1.

LPC1 Activation Causes a Surge Phenotype During Flight

It is difficult to imagine an ecologically-relevant situation for walking flies to see regressive motion. Flies rarely walk backwards, so the only times they would see regressive motion while walking is if they landed on a surface that was moving in the opposite direction. However, it is easy to imagine regressive motion scenarios in flight. A sudden gust of headwind or a drop during flight would create translational back-to-front optic flow.

How will LPC1 activation affect flight? Freely-flying flies are attached to a pin and lowered into an LED arena created by Chuntao Dan. An Infrared light shines on the fly to create a shadow from its wings. A wing beat analyzer collects information about the amplitude and frequency of the wing beats (**Figure 7a**).[143] When flies beat their wings

harder and faster, wing beat amplitude (sum of the left and right wing amplitudes, ∑WBA) and wing beat frequency (WBF) increase. The result of increasing WBA and WBF in free flight possibly indicates a forward surge (**Figure 7b**).

LPC1 neurons are activated with a 590nm laser using Chrimson. Chrimson is a light-sensitive channelrhodopsin that will depolarize neurons in response to red light.[170] Flies of genotype *empty-GAL4, UAS-chrimson* (control) and *LPC1-SplitGAL4, UAS-chrimson* were examined in a dark flight arena. No stimulus was shown on the LED display. When flies are in the dark, they maintain a low constant wing beat amplitude and frequency. When the laser is turned on, control flies decrease their WBF and WBA, a slowing response. However, when LPC1 is activated, flies increase their wing beat amplitude and frequency, a surge phenotype (**Figure 7c**).

The surge phenotype when LPC1 is activated is intuitive, though it is opposite of the expected reaction, given the walking data. When LPC1 is activated, it signals to a flying animal that it is experiencing regressive or down optic flow. A fly would experience such optic flow if it is falling or being pushed backwards by wind, so the animal would surge forward to compensate. However, in the walking assays, flies slowed less when LPC1 was silenced. Therefore, it may be expected that flies will slow more if LPC1 is activated. The opposite is true, but that may be because the visual system is modulated differently during flight and walking. Indeed, initial experiments with Chrimson activation on the treadmill show that LPC1 activation forces walking flies to slow down as predicted (data not shown).

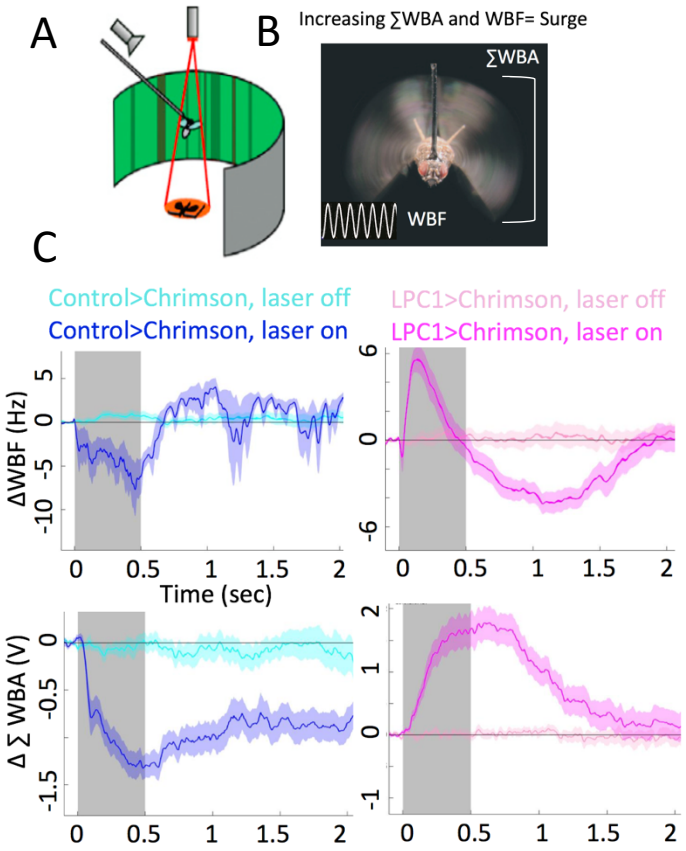

Figure 7: LPC1 Activation. a) **Flight apparatus**. Image credit: Kim *et al* (2017). A fly is tethered to a pin and allowed to fly freely in a circular arena upon which visual stimuli can be displayed. An infrared light shines over the fly, creating a shadow of its wings. A wing beat analyzer measures frequency and amplitude of the wing beats. An amber laser was added to activate chrimson. **b) WBF and ∑WBA**. Photo credit: Michael Dickinson. Freely flying flies alter the frequency (WBF) and amplitude (WBA) of their wings beats. An increase in the frequency or an increase in the sum of right and left wing amplitudes (∑WBA) indicates the fly is exerting more effort in forward motion and is called a surge phenotype. WBF is measured in Hz. WBA is measure in V, an arbitrary unit that is the sum of the left and right wing beat detectors. c) **LPC1 Activation**. For this experiment, flies were simply kept in the dark. The average of all flies and trials is shown by a solid line and the standard deviation for each frame is represented by the shadow. Data analysis and rig design credit: Chuntao Dan. Both control flies (GAL4 with an empty enhancer crossed to *UAS-chrimson*) and *LPC1-SplitGAL4, UAS-chrimson* flies maintain fairly constant low level WBF and WBA (teal and pink, respectively) in the dark. When the laser is on for 0.5 seconds (grey box), control flies decrease WBF and WBA (blue.) However, when the laser activates LPC1, flies increase WBF and WBA in a surge phenotype (magenta).

Synaptic Partners of LPC1

Since LPC1 is an uncharacterized neuron type, it is unknown how it fits within motion vision circuitry. The functional connectivity technique was used to identify potential synaptic partners of LPC1.[171,172] Fly brains are removed and imaged in saline solution while they are still electrically active. One set of neurons expresses chrimson and is activated by a 590nm laser.[170] Another set of neurons expresses GCaMP6f, a calcium-sensitive fluorescent indicator.[169] When chrimson-expressing neurons are depolarized by the laser, they will propagate an electrical signal to their synaptic partners. Those neurons will depolarize, allowing for an influx of calcium that will cause GCaMP to produce a fluorescent signal (**Figure 8a**). All functional connectivity experiments were carried out by Jasmine Le from the Functional Connectome project at Janelia.

Functional connectivity was examined for flies with genotype *LPC1-SplitGAL4, UAS-chrimson, UAS-LexARNAi, nsyb-LexA, LexAop-GCaMP6f.* The LexA/LexAop system is derived from bacteria and functions similarly to the GAL4/UAS system. LexA has been genetically modified to be a transcriptional activator when bound to the operator sequence, LexAop.[77,78] Nsyb is a pan neuronal enhancer, so nearly all neurons will be expressing GCaMP, except for LPC1. To prevent GCaMP fluorescence coming from LPC1 itself after it is activated using chrimson, *UAS-LexARNAi* was added. RNAi will block the expression of LexA in LPC1 neurons.

When LPC1 neurons are activated with the 590m laser, the resulting fluorescent pattern is shown in **Figure 8b**. This pattern closely resembles the anatomy of the un-characterized neuron shown in **Figure 8c**. **Figure 8c** shows a split line that was created as Aljoscha Nern was trying new combinations of split halves, and this line happened to

match the pattern of the downstream synaptic partner quite well. This neuron will be called LPC1-Target. To see if this unknown neuron is the synaptic partner of LPC1, the functional connectivity experiment was repeated using a more specific genotype. *LPC1-LexA, LexAop-Chrimson, LPC1Target-GAL4, UAS-GCaMP6f*. When LPC1 is activated by the laser, the LPC1-Target neuron gives off a GCaMP signal. This is a single large neuron with an axon spanning the mid brain to the opposite side. By crossing the midline of the brain, this neuron may be part of the mechanism that modifies LPC1 activity on the opposite side of the brain (**Figure 6)**. Though LPC1-Target is excitatory (RNAseq data not shown), so it would need to work through intermediaries. The dendrites grip the LPC1 glomerulus and the cell body connects near the dendritic end.

Would silencing the LPC1-Target with Shibire^{TS} have any effect in the hallway assay? When LPC1-Target neurons are silenced with Shibire^{TS}, flies are deficient in motion-related behaviors, just as they are when LPC1 is silenced (**Figure 8c**). As a note, LPC1-Target was also silenced when flies were on the treadmill assay with the conditions shown in **Figure 6**, and silencing had no effect on the phenotype (data not shown). This is not necessarily surprising, since translational motion is detected and behavior is appropriated by a matrix of neurons. LPC1-Target does not need to have the same phenotype as LPC1 under all conditions to still be part of the same pathway. Presumably many other neurons are contributing to and modifying the neural networks.

Since the LPC1-Target neuron had a phenotype resembling LPC1 in the hallway apparatus, could other neurons identified during the screen could also be connected to LPC1? The hits have similar motion-deficiency phenotypes. TmY3 was a hit from the screen that had motion vision deficiencies and also seems to be functionally connected to

LPC1. When flies of genotype *TmY3-SplitGAL4, UAS-Chrimson, LPC1-LexA, LexAop-GCaMP6f* are stimulated with a laser, GCaMP-expressing LPC1 neurons show a fluorescent signal (**Figure 8d**). Therefore, TmY3 is potentially connected upstream of LPC1.

Two neurons may be functionally connected, but not physically connected. Other neurons may be responsible for relaying information between the them. Electron microscopy tracing helps resolve this issue. From a database containing thin electron microscopy slices of an full adult *Drosophila* brain, individual neurons can be traced by a team of dedicated Janelians. In tracing, a single neuron is followed through thin slices of microscopy data. Tracing allows for the annotation of the physical synapses and to get detailed information about neuronal anatomy. LPC1 neurons and LPC1-Target have characteristics will be identified as the project continues (see **Supplementary Figure 4**).

Discussion

LPC1 and Visual Circuitry

The Optic Lobe output neuron LPC1 was characterized and is the first example of an output neuron with a dedicated behavioral function. LPC1 is part of the motion vision pathway and regulates visually-motivated behaviors. LPC1 encodes Up and Back-to-Front translational optic flow and is directionally-selective. This neuron also influences forward-walking behavior, but not turning behavior. Preliminary evidence also suggests LPC1 regulates different behaviors in flight vs walking. LPC1 is a cholinergic neuron and

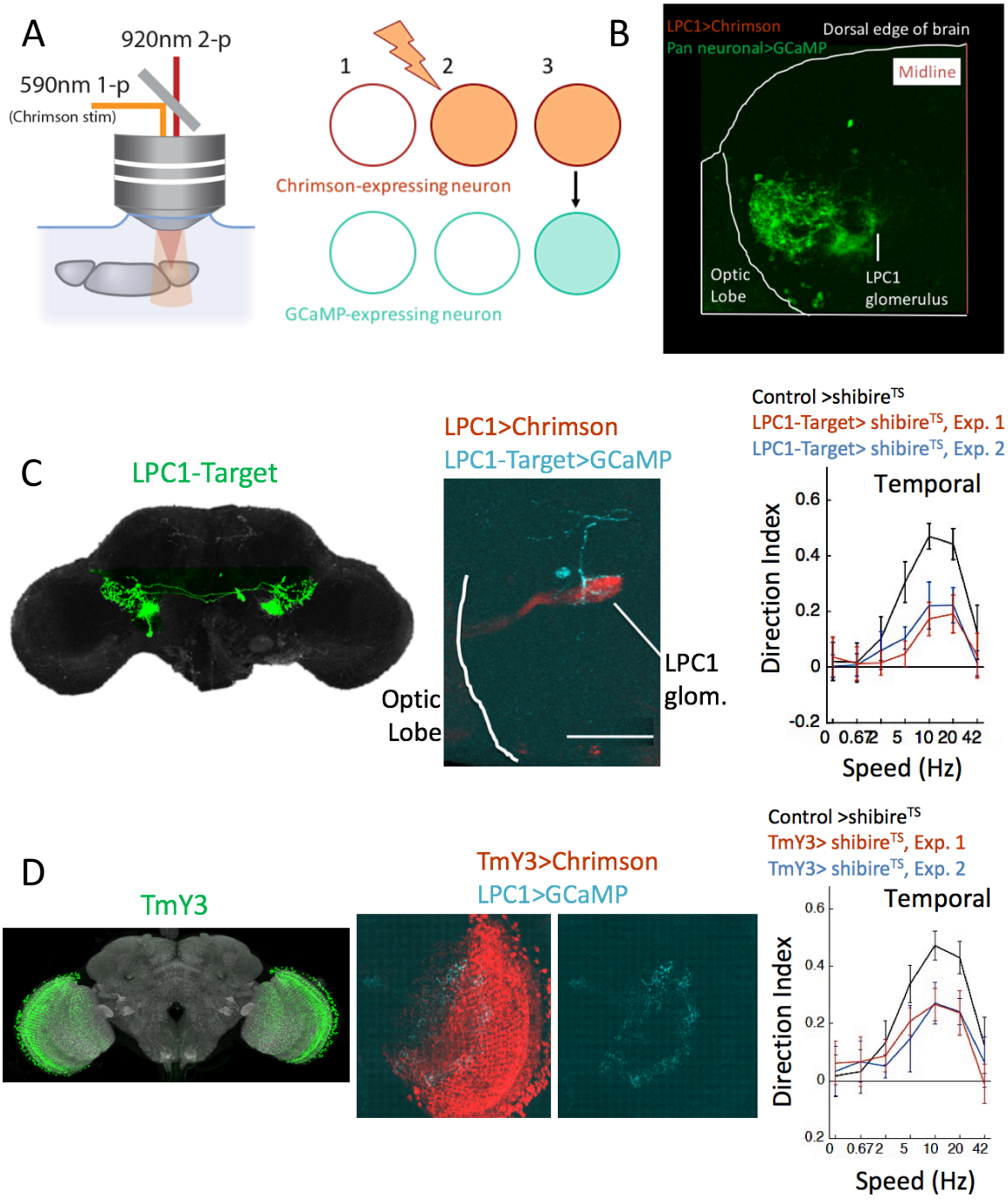

Figure 8: Functional Connectivity of LPC1. These experiments were performed by Jasmine Le using a system designed by Allan Wong. **a) Experimental setup**. Fly brain are removed from the head and transferred to fresh saline solution under a 2-photon microscope to keep them electrically active. Chrimson-expressing neurons are activated by 590nm light and a second laser is used to capture GCaMP fluorescence. Image taken from Strother *et al*. (2017). *Caption continues on the next page*.

Figure 8 continued. b) Genetic Strategy. One enhancer line drives chrimson in a neuron type of interest. A second enhancer line drives GCaMP expression. When chrimson is activated with the laser, it will send an electrical signal to its synaptic partners. When these partners depolarize, an influx of calcium causes the GCaMP to fluoresce. **c) Downstream Synaptic Partner**. The brain shown here has the genotype: *LPC1-SplitGAL4, UAS-Chrimson, UAS-LexARNAi, nsyb-LexA, LexAop-GCaMP6f.* LPC1 neurons express chrimson and all other neurons in the brain express GCaMP. LexA neurons do not express GCaMP because they are also expressing a LexA RNAi which will prevent LexA expression. When LPC1 neurons are activated by the laser, GCaMP fluoresces in the pattern shown in green. **d) Targeting the Downstream Synaptic Partner**. From the experiment in c, the unnamed neuron depicted here could be the downstream partner of LPC1. It is named LPC1-Target. (Anti-GFP shown in green, rest of the brain outlined in black. Image modified from one provided by Aljoscha Nern.) The functional connectivity experiment was repeated using a split line specific for LPC1-Target. When LPC1>chrimson is activated, LPC1-Target>GCaMP fluoresces. This large neuron's dendrites are gripping the LPC1 glomerulus. (Scale bar= 100μm.) This split line was also crossed to *UAS-shibire^{TS}* and used the hallway assay to examine its behavior. The temporal phenotype is shown here as an example. When LPC1-Target is silenced (red and blue, N=90 per experiment), the motion phenotypes resemble LPC1-silenced phenotypes. Flies have motion vision deficiencies compared to control flies (black.) **d) Upstream Synaptic Partner.** Silencing TmY3 neurons causes a hallway phenotype that looks very similar to the LPC1-silenced phenotype. When TmY3 expresses chrimson and is activated with a laser, LPC1 neurons with GCaMP fluoresce, suggesting the two are functionally connected. TmY3 image provided by Aljoscha Nern. Grey is anti-nc82, green is anti-GFP, posterior side

is connected functionally in a circuit with TmY3 (upstream) and LPC1-Target (downstream) and is likely connected physically to many others. LPC1 characterization led to a nearly complete reconstruction of minimal pathway that gives the connections, from perception to behavior, for the neural pathway that receives regressive and up optic flow as stimulus input and produces slowed walking or thrust flying as output.

Speed and Turning

Uncoupled forward speed and turning are consistent with observations from other researchers. Silies *et al* demonstrated that increasing the speed of regressive and

progressive stimuli affected forward walking speed but not turning.[127] Their stimulus was shown only at 0 degrees, and it is unclear if the average turning remained at baseline because flies have no preference in their turning direction, or because they are not turning at all. By showing the translational stimuli at multiple locations, the data herein confirm that flies move towards contraction and turn away from expansion, even for stimuli with a 0-degree origin.

Input from L2 neurons (see chapter 2 figure 1) is required for translational behaviors. More specifically, regulation of forward walking speed requires L2 and L3 while turning requires input from L1, L2, and L3.[124,127] This observation of separate neural pathways supports the idea that walking speed and turning are not completely coupled responses. TmY3 is a candidate presynaptic partner of LPC1 and L2 is one of many inputs to TmY3.

Rotational and Translational Motion

The data reinforce previous observations regarding the characteristic differences between the translational and rotational visual pathways:

1) Translational and rotational stimuli responses have different contrast tuning curves. The contrast of grating patterns was varied for both rotational and translational stimuli and the walking responses were measured on the treadmill. Consistent with previous reports,[154,155] the contrast tuning curves for rotational and translational stimuli differed in both magnitude and shape (**Supplementary Figure 5a**.) This was true for turning behaviors but not true for forward walking behaviors. Rotational and translational responses had

similar contrast tuning curves for speed behavioral output (**Supplementary Figure 5b).** However, unlike previous reports, back-to-front responses (contraction) were not consistently lower than front-to-back (expansion) responses. Results here also contradicted previous observations that rotational responses were greater in magnitude than translational responses.[154,155] This may be attributable to the simple fact that these experiments were done with walking, not flying, animals. The two behavioral paradigms measure very different actions and the visual system is modified differently depending on the behavioral state of the animal. Silencing LPC1 did not have a large effect on contrast tuning curves during walking. Though, as expected, less forward walking occurs during regressive motion at all contrast levels for LPC1-silenced flies (**Supplementary Figure 6**).

2) The magnitude of rotational and translation responses is different. This study shows the response magnitudes are different during rotation vs translation, though the walking response magnitudes here differed from previously-reported magnitudes recorded during flight. In previous reports, responses to translational stimuli were greater than for rotational stimuli.[154,155,159] The opposite seems to be true here: responses to rotational motion were greater than responses to translational stimuli in each experiment. The data also contradict previous reports that responses to regressive motion were lower in magnitude than responses to progressive motion.[154] The measured responses here were roughly equal in magnitude. (see **Figure 4** and **Supplementary Figure 4**). Once again, these differences may be attributable to the fact that

the experiments here were done on walking flies, and previous publications have shown responses during flight. Despite these differences, results generally agree that there is a difference in response magnitude to rotational vs translational stimuli.

3) Flies respond to individual parts of translational motion in the same way as they would to full-field translational motion. When the translational stimuli shown here was broken into its components, the result was similar neuronal and behavioral responses as for the full-field stimuli (see **Figure 4**).

Expansion Avoidance

The expansion avoidance phenotype is well-documented. Flies slow down when presented with expansion stimuli and turn away.[127,159,162] This behavior was observed with walking flies on the treadmill, but not with walking flies in the hallway apparatus. Flies in the hallway turn against the direction of the grating, and therefore effectively walk towards a focus of expansion.

In any behavioral paradigm, expansion avoidance is somewhat paradoxical. It makes sense for collision avoidance, but not for normal navigation. Expansion avoidance suggests flies would prefer the optic flow created by backwards flight. (Expansion avoidance is also not predicted under the equilibrium model of optic flow, but that inconsistency is discussed in chapter 2.) How would flies ever navigate forward if they avoid expansion?[152]

Flies can overcome expansion avoidance in several ways. If the expansion is at very low speeds (0.125-0.5Hz), flies do not avoid it.[152] This cannot explain why flies in

the hallway orient towards expansion, since the speeds were much faster and the two experimental setups are not generally equivalent. Flies will also orient towards a focus of expansion while experiencing a headwind. When headwind is applied to antennae, such as is generated by forward flight, the response to optic flow is altered and allows the fly to steer into progressive motion. This is only true if the focus of expansion is not too large, as that will trigger collision-avoidance behaviors and the fly will turn away.[173] But flies in the hallway apparatus are not experiencing much headwind. Flies may also steer into expansion if they are fixating on an object.

There is another visual response to discuss—object fixation. In brief, during common visual behaviors, flies turn: with rotation, against hallway stripes and expansion, and towards contraction or objects. Expansion avoidance can be overcome by object fixation; if a fly is moving towards an object, it can move forward, creating progressive optic flow.[162] Perhaps the end cap of the hallway provides a sufficient object for flies to fixate upon. However, this would not explain why many other studies have noticed the same behavior as our hallway. Flies walk against the direction of moving stripes in a hallway, even if that hallway is made of clear glass or has no object on its end.[113,124,127,134,135] The ecological relevance of and the exceptions to expansion avoidance behavior requires further illumination.

Supplementary Figures

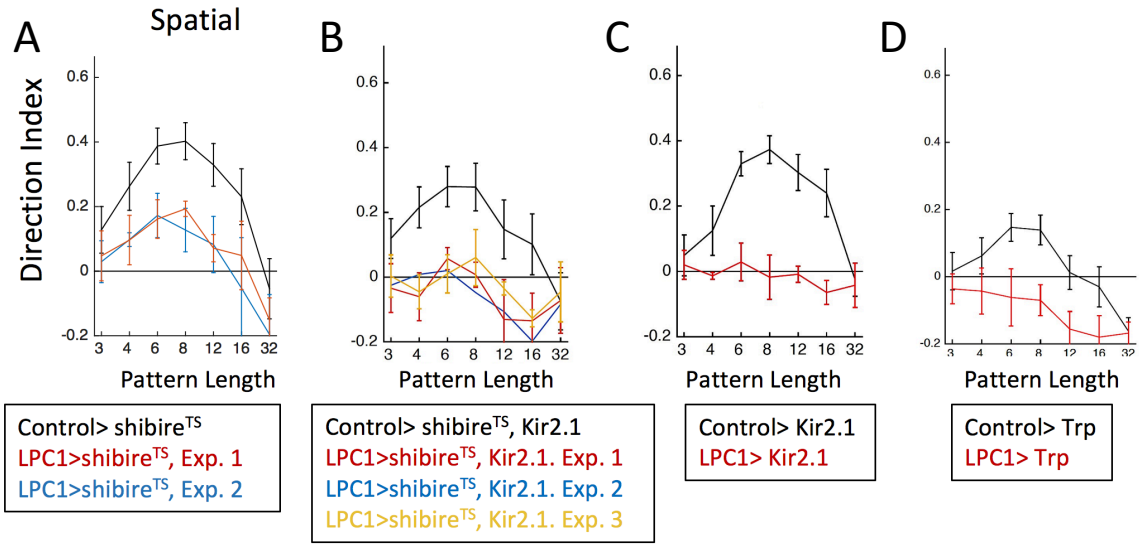

Figure S1: LPC1 with Different Effectors. The LPC1 Split-GAL4 lines were assayed with multiple effectors in the hallway apparatus. As an example, here behavioral responses to spatial patterns are shown, i.e. a grating moving at 10Hz that varies in length. Controls (black) are a Split-GAL4 line with empty enhancers. Every experiment has an N of about 90. a) **Shibire^{TS}**. When crossed to Shibire^{TS}, LPC1-silenced flies have deficiencies in motion vision. b) **Shibire^{TS}+ Kir2.1.** Adding Kir2.1 to Shibire^{TS} in LPC1 neurons eliminates motion vision, and perhaps there is even some reversal phenotype at longer pattern lengths. **c) Kir2.1.** Kir2.1 without Shibire^{TS} can reproduce the phenotype of the double effector. Kir2.1 expression in LPC1 eliminates motion vision. **d)Trp.** LPC1 was also activated using the temperature-sensitive activator Trp. Flies expressing Trp have much lower responses overall, but activated LPC1 flies still have lower responses than the controls, and perhaps even some reversal phenotype. Both activating and silencing LPC1 disrupts motion vision.

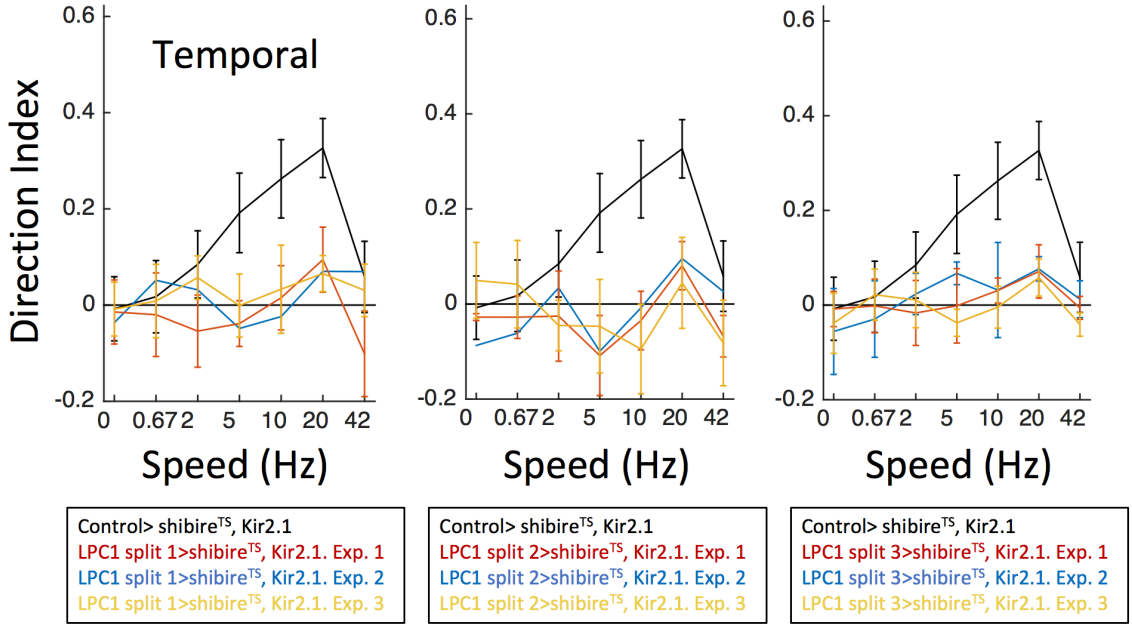

Figure S2: LPC1 Split Lines. Multiple Split-GAL4 lines were created that target LPC1 neurons. Shown here are three separate lines crossed to a double effector: *UAS-shibire^{TS}; UAS-Kir2.1*. Behavioral responses to temporal patterns in the hallway apparatus are used as an example. Stripes of four lights on/4 lights off move at increasing speeds along the wall of the hallway. Control flies (Split-GAL4 with empty enhancers, black) crossed to the double effector have slightly lower responses to motion than flies crossed to *UAS-shibire^{TS}* alone, but still reach peak behavior around 10-12Hz. When crossed to the double effector, LPC1 Split-GAL4 flies are motion blind, as indicated by their direction index values around 0. Not only is the phenotype reproducible for each experiment of a particular line (red, yellow, and blue, N=90 per experiment), it is also reproducible among the different split lines that have specific expression in LPC1 neurons.

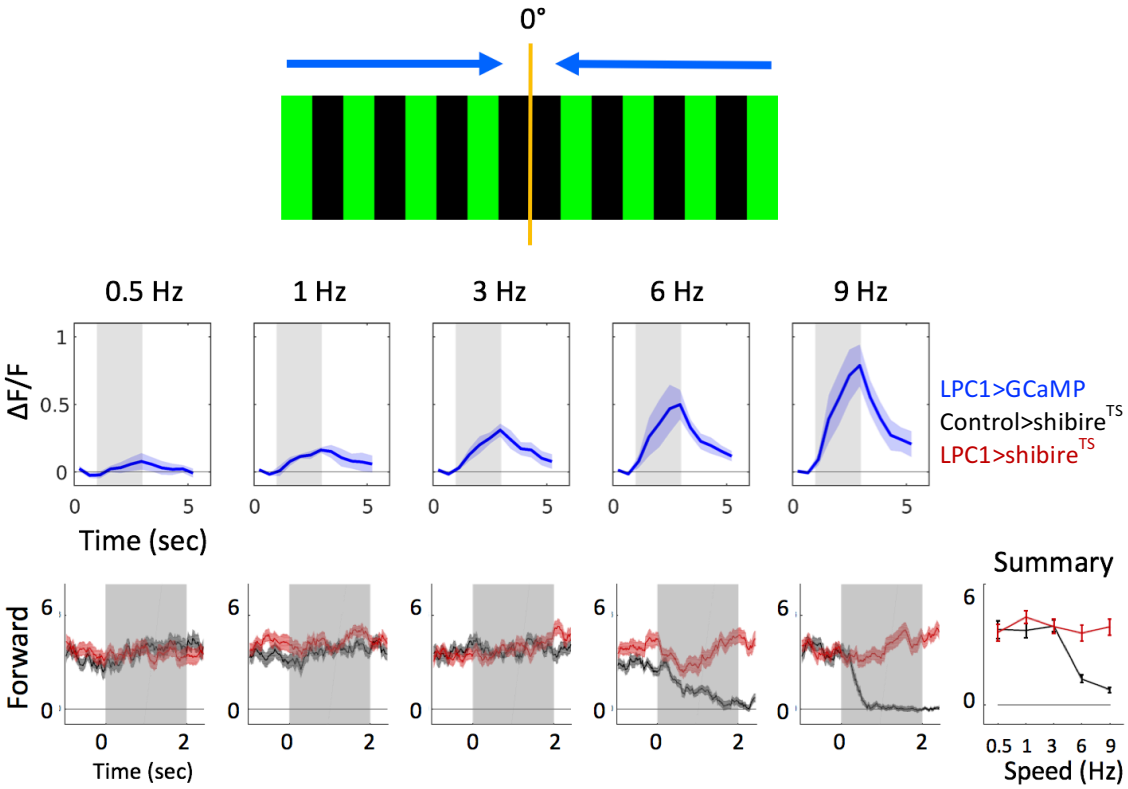

Figure S3: Speed Tuning of LPC1. Flies were shown a contraction stimulus with a focal point at 0 degrees. *LPC1-SplitGAL4, UAS-GCaMP* flies were imaged from the left side of the brain while being shown the stimulus at each speed for one second (shaded box). N=6, 3 trials of each stimulus per fly. The y axis of the imaging graphs shows the change in fluorescence compared to baseline fluorescence. Walking flies on the treadmill are shown the same stimulus as the imaged flies for 2 seconds (shaded box) at each speed. Each walking fly was shown each stimulus 5 times. Control flies (Split-GAL4 with empty enhancers crossed to *UAS-shibire^{TS}*, N=19) are shown in black and LPC1-silenced flies (*LPC1-SplitGAl4*, *UAS-shibire^{TS}* N=20) are shown in red. The Y-axis shows raw forward motion in pixels per frame (x100). The average of all flies and trials are given as solid lines and the standard deviation for every frame is depicted with a shadow. LPC1 neurons do not respond to contraction stimuli until about 6Hz and reach peak activation at 9Hz. Behavioral phenotypes manifest at about 6Hz and reach their peak at 9Hz. The summary plot shows the average forward walking for all flies during the entire time of the trial at each speed. All stimuli depictions and GCaMP data provided by Matthew Isaacson.

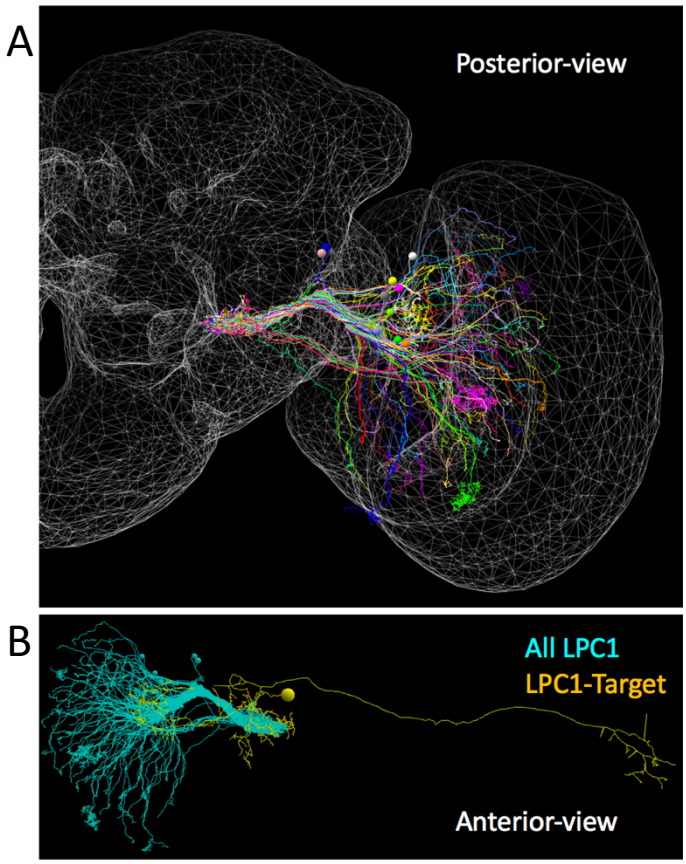

Figure S4: TEM Tracing of LPC1. Using stacks of electron microscopy images, neurons can be traced to identify their synaptic targets and overall anatomy. Cell bodies are shown as spheres. **a) LPC1.** This is a multicolored population of 90 LPC1 neurons that were traced using TEM data. The brain volume is estimated by the white mesh and shows one side of the brain, posterior side up. Notice how LPC1 neurons cover the entire Lobula Plate. **b) LPC1-Target.** LPC1-Target TEM tracing (gold) looks very similar to the expression pattern of the Split-GAL4 line. This neuron grips the same glomerulus targeted by LPC1 neurons (teal).

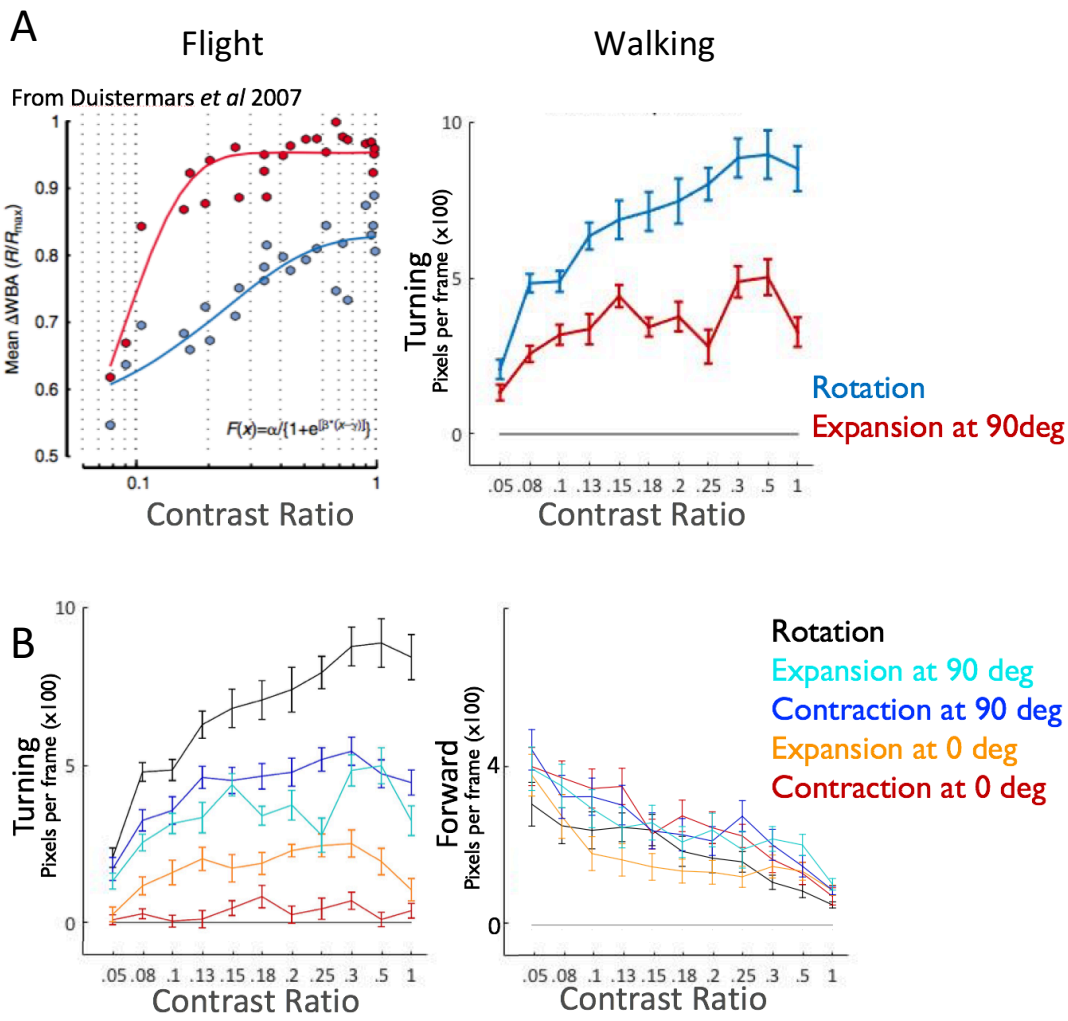

Figure S5: Contrast Tuning of Walking Flies. Contrast ratio=(High-Low)/(High+Low) a) **Contrast Tuning of Expansion vs Rotation**. The left panel in this figure is replicated from Duistermars *et al* (2007). They found that flying flies respond differently to rotation and expansion grating stimuli of varying contrasts. Overall, the response for expansion is greater than for rotation and the tuning curves are of different shapes. This experiment was replicated on the treadmill with control flies (N=18). In walking flies, total turning response is less for expansion grating than for rotation grating. The curves also have slightly different shapes, with expansion tuning being flatter than the logarithmic shape of rotation tuning. b) **Contrast Tuning of Walking flies.** The Duistermars experiment was expanded upon using the treadmill by adding contraction stimuli and by showing stimuli at 0 degrees. Forward walking responses were also analyzed. When turning was measured, the magnitude and curvature of rotational tuning at different contrasts is greater than for all translational stimuli. Note that the reaction to back-to-front stimuli (contraction) was not less than the reaction to front-to-back stimuli (expansion) at 90 degrees as was reported by Duistermars *et al (*2012) in flying animals. The contrast tuning curves for forward walking responses look very similar for all rotational and translational stimuli.

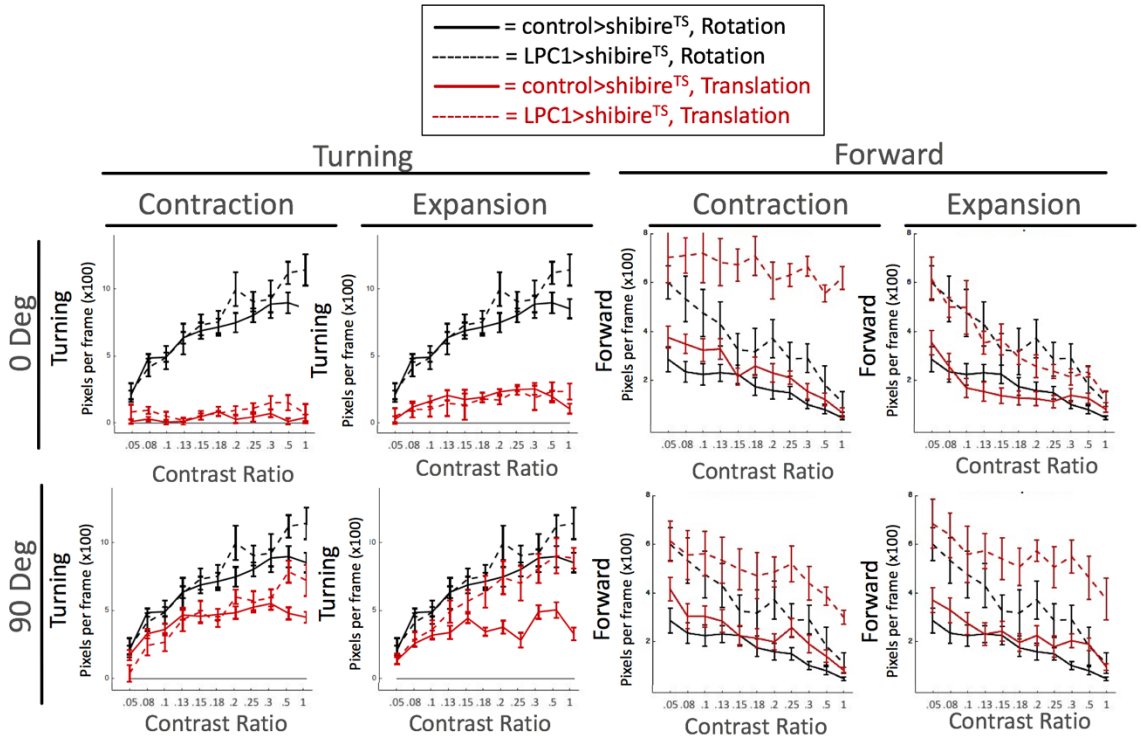

Figure S6: Contrast Tuning of LPC1. Flies on the treadmill were shown grating of varying contrasts. Contrast ratio=(High-Low)/(High+Low). The grating could be rotational (black) or translational (red). Translational grating was shown at 0 degrees and at 90 degrees. Translational stimuli could move back-to-front (contraction) or front-to-back (expansion). Overall turning responses to translational stimuli were less than to rotational stimuli at every contrast. As expected from previous experiments, silencing LPC1 (dotted lines, N=4) did not have a strong effect on forward walking responses to rotational motion at any contrast compared to controls (solid lines, N=18). Though, silencing LPC1 during a 90-degree expansion stimulus may increase overall turning responsiveness. Silencing LPC1 did prevent flies from slowing down in response to translational motion. The prevention is proportional to the amount of regressive in the stimulus, as shown in Figure 5b. The LPC1-silencing phenotype does not seem to be contrast-specific, but rather a general trend across all contrast conditions.

Materials and Methods

Fly Rearing

Flies were raised on standard molasses food with a 16 hours on/8 hours off light cycle. Flies for the hallway experiments were raised at 22C; all other flies were raised at 25C. Enhancer split lines were crossed to the following effector virgin lines: *UAS-shibire^{TS}*, *UAS-mcd8::GFP, UAS-Kir2.1, UAS-TrpA, UAS-Chrimson, UAS-GCAMP6f, UAS-LexARNAi, UAS-GCAMP6s*. Enhancer LexA lines were crossed to the following effector virgin lines: *LexAop2-Chrimson, LexAop2-GCAMP6f*.

Immunostaining and Imaging

All brains shown in this chapter were dissected and stained by the FlyLight team. Images provided curtesy of Aljoscha Nern. Full details about their protocol and reagents can be found at: https://www.janelia.org/project-team/flylight/protocols, IHC Adult Split Screen.

Hallway Apparatus

The measurements and stimulus details of the hallway apparatus are described in Chapter 2, Figure 2 and in Chapter 2 Materials and Methods. Each corridor contained 15 males, 6 corridors per experiment for a total N per experiment of 90. Male progeny was cold-plate sorted when 0-2 days old and transferred to fresh food vials. Experiments were run two days after sorting on 2-4 day-old males. Flies were transferred to standard starvation media one hour before experimentation. All experiments were run between 1-3 hours before the off time of the light cycle when flies were at peak daily activity. Temperature inside the apparatus was 34C and humidity was 60%.

Fly Treadmill

Fly treadmill and subsequent analysis was as described by Seelig *et al* 2010.[158] The treadmill was 9mm in diameter and airflow was kept at 400ml/min. Speed is shown in units of pixels per frame, though for the ball size and airflow, it is estimated 1 pixel/frame can be converted to somewhere in the range of 3mm/sec. All flies were female, 3-6 days old; they were cold-plate sorted at least 2 days before experiments and their wings glued at least 1 day before experiments. The panels used to create the arena display are described by Reiser and Dickinson (2008).[160] The arena was kept inside an incubator at 60% humidity and 32C. Temperatures near the treadmill were measured at 34C due to the heat from the LEDs.

Flying Arena

Females flies 1-3 days old were tethered to a pin using UV-activated glue and freely flying. A wing beat analyzer captured the data from moving wings illuminated by IR lights. Details on the procedure can be found in Maimon *et al* 2008.[174] A 590nm laser was added to activate chrimson in these flies during flight.

EM Tracing

Tracing was performed by the Fly TEM project team at Janelia. All neurons are traced and then proofread by a second person. The displays shown in this document were created using CATMAID software.[175]

Calcium Imaging

All calcium imaging and data analysis was performed by Matthew Isaacson. Flies were head fixed in front of a display and underneath a microscope to capture fluorescent signals as described by Reiff *et al* (2010)[102] and by Strother *et al* (2014).[176] Experiments were performed on female flies aged 2-5. The volume of the central glomerulus of LPC1 was imaged using a two-photon microscope (Prairie Ultima). GCaMP6s was used as the calcium indicator as described by Chen et al (2013).[169]

Functional Connectivity

All functional connectivity experiments and data analysis were performed by Jasmine Le. The experiments were carried out as described in Shirangi *et al (*2016) and Strother *et al* (2017).[171,172] Brains were from one day old flies, male or female.

Thesis Discussion

Main Conclusions

Chapter one described reagents that could be used for examining individual neurons in the olfactory system. These tools were effective and specific and provide advantages over currently-used methods. They improve upon past genetic strategies by providing a system that is more efficient (requiring less generation time to achieve complex genotypes) and more flexible (they can be used with a variety of transgenes). The tools were used experimentally to show that in the olfactory system, a single neuron or neuron pair is insufficient for flies to perceive and react normally to certain odorants.

The results of the screens in chapter two provide a valuable resource for scientists. The GAL4 lines from Phase I are widely used; it is expected that detailed data regarding their expression patterns and their effects on behavior will be helpful to the vision research community. Split-GAL4 lines were also created in Phase II, which will allow researchers to specifically and reproducibly target individual neuronal subtypes in the visual system. Phase I of the screen identified general regions that affect visual behaviors and Phase II of the screen used hypotheses generated by Phase I to target specific neuronal types that were potentially contributing to vision. This dual-screen approach was advantageous over previous screens by allowing for the identification of multiple specific neuronal subtypes that contribute to vision. The screen identified known players in the motion and color pathways, verifying the utility of this screening apparatus. It also identified previously-undescribed neuronal subtypes that contribute to motion vision. One of these neuronal subtypes was unknown both anatomically and functionally. This output neuron was named Lobula Plate Columnar Neuron 1, or LPC1.

Mapping function to LPC1 gave several insights into how motion vision works. In chapter 3, it is shown that this neuron: 1) Encodes translational but not rotational motion, 2) Is directionally selective and responds only to back-to-front or up motion, 3) Is broadly tuned for speeds and contrasts, but has the highest response at speeds over 9Hz, 4) controls forward speed of the animal, which can be uncoupled from turning, and 5) has a nearly complete pathway reconstructed from perception to behavior.

Significance

For over 50 years, scientists have been ascribing functional relevance to neurons. But we still know very little. Dozens of behavioral paradigms, hundreds of neuronal subtypes, and thousands and neurons connected in a circuit to make the brain are known, but the relationships among these behaviors, anatomies, and circuits have not been thoroughly correlated. Though the fly brain is much tinier than our own, there is still much to be discovered.

Only in the last decade or so have the genetic reagents, computational techniques, engineering tools, and extensive collaborations become sophisticated enough to allow significant progress in making contributions of individual neurons accessible to researchers. The work in this thesis utilizes many new techniques and relies upon widespread collaborations to ask questions and make appropriate measurements to uncover new insights into the contributions of single neurons to sensory behaviors.

The work contained herein contributes to the understanding of how sensory input is interpreted and processed by the brain to produce behavioral output. Mapping the function and sensitivity of individual neurons allows for a stronger grasp of how neuronal

anatomy and circuitry operate to make senses from stimuli. *Drosophila melanogaster* sensory systems were the model of choice. Flies were chosen because they are genetically flexible, behaviorally complex enough to be interesting, and neurologically simple enough to be comprehensible.

Though results in this thesis are specific to fruit flies, the conclusions and contributions are relevant to mammals as well. Mammals and insect share many of the same features of neural processing. Mice also use combinatorial coding to detect odorants and have neuropil layers that are analogous to the fly's antenna and antennal lobe (nose and olfactory bulb.) Mammals, like insects, also employ the principle of hierarchal neuropil structures to compute visual features. Both kinds of animals see color, can be fooled by optical illusions, have neurons tuned to specific speeds and contrasts, distinguish different intensities, organize neurons into ON and OFF pathways, use diverging translational and rotational optic flow pathways, modulate neuron activity differently during specific physical activities, filter out self-motion, gauge distance, use visual markers for navigation etc. Both types of animals are genetically accessible and have been used experimentally to assign functional relevance to specific neuron types. [177] However, a mammalian equivalent of LPC1 has not been discovered yet. Mice have neural systems and behaviors which are more variable than in flies. This would make any attempt at this time to perform parallel experiments to those in this thesis nearly prohibitive, though not impossible. The small stereotyped insect brain with its strong reliable optomotor behaviors was a more appropriate model for answering the questions in this thesis.

Neurons do not work in isolation, but are complex circuits capable of making astounding calculations in fractions of a second and producing elaborate behaviors. This dissertation aimed to take the components of sensory circuits and interpret individual contributions of specific neuron types. The GAL80 tools, the screen resource, and the LPC1 characterization each contribute to an understanding of how a neuron's sensitivity and connectivity works within a sensory system to provide perception and produce performance.

Future Directions

- With the GAL80 reagents, it would be impactful to the field to do a screen of all the OR-GAL80s and a panel of odorants. Individual functional ORN types functioning in a silent background may give interesting results when paired with different odorants than those odorants that were tried here. One could ask, which neurons are sufficient alone to produce a behavior? Which ORs are necessary but not sufficient for a behavioral response? Can removing or restoring a particular OR alter an established behavior (e.g. make an aversive reaction into an attractive one)?
- The GAL80 reagents could also be useful in restoring functionality to small groups of neighboring neurons. One could restore neurons one at a time to uncover the minimal number of functioning neurons required for a behavioral response to each odorant in a panel of odorants.

- The screen from chapter 2 can and will continue. With particular emphasis on Phase II. New split lines are being made all the time, and hundreds more exist for the optic lobe that have not yet been tried.
- At some point, it would also be interesting to add lasers to the hallway apparatus so the effects of activating neurons could be screened instead of only silencing neurons.
- The LPC1 flight experiments need to be expanded. LPC1 can be activated or silenced during flight, and the various stimuli in figures 5 and 6 can be shown in the arena. In conditions of seeing regressive motions, flight is more ecologically relevant than walking.
- Synaptic partners of LPC1 are currently being discovered through the tracing project. It would be interesting to see if silencing these neurons affects LPC1 responsive dynamics (e.g. could silencing TmY3 affect LPC1's speed tuning curve) during calcium imaging.

References

1. Ache, B. W. & Young, J. M. Olfaction: Diverse Species, Conserved Principles. *Neuron* **48,** 417–430 (2005).
2. Ng, M. *et al*. Transmission of olfactory information between three populations of neurons in the antennal lobe of the fly. *Neuron* **36,** 463–474 (2002).
3. Vosshall, L. B., Amrein, H., Morozov, P. S., Rzhetsky, A. & Axel, R. A Spatial Map of Olfactory Receptor Expression in the Drosophila Antenna. *Cell* **96,** 725–736 (1999).
4. Robertson, H. M., Warr, C. G. & Carlson, J. R. Molecular evolution of the insect chemoreceptor gene superfamily in Drosophila melanogaster. *Proceedings of the National Academy of Sciences* **100 Suppl 2,** 14537–14542 (2003).
5. Vosshall, L. B., Wong, A. M. & Axel, R. An olfactory sensory map in the fly brain. *Cell* **102,** 147–159 (2000).
6. Clyne, P. J. *et al*. A novel family of divergent seven-transmembrane proteins: candidate odorant receptors in Drosophila. *Neuron* **22,** 327–338 (1999).
7. Goldman, A. L., van der Goes van Naters, W., Lessing, D., Warr, C. G. & Carlson, J. R. Coexpression of Two Functional Odor Receptors in One Neuron. *Neuron* **45,** 661–666 (2005).
8. Hallem, E. A. & Carlson, J. R. Coding of Odors by a Receptor Repertoire. *Cell* **125,** 143–160 (2006).
9. Hallem, E. A., Ho, M. G. & Carlson, J. R. The Molecular Basis of Odor Coding in the Drosophila Antenna. *Cell* **117,** 965–979 (2004).
10. Couto, A., Alenius, M. & Dickson, B. J. Molecular, Anatomical, and Functional

Organization of the Drosophila Olfactory System. *Current Biology* **15,** 1535–1547 (2005).

11. Fishilevich, E. & Vosshall, L. B. Genetic and Functional Subdivision of the Drosophila Antennal Lobe. *Current Biology* **15,** 1548–1553 (2005).
12. de Bruyne, M., Clyne, P. J. & Carlson, J. R. Odor coding in a model olfactory organ: the Drosophila maxillary palp. *J. Neurosci.* **19,** 4520–4532 (1999).
13. de Bruyne, M., Foster, K. & Carlson, J. R. Odor Coding in the Drosophila Antenna. *Neuron* **30,** 537–552 (2001).
14. Dobritsa, A. A., van der Goes van Naters, W., Warr, C. G., Steinbrecht, R. A. & Carlson, J. R. Integrating the molecular and cellular basis of odor coding in the Drosophila antenna. *Neuron* **37,** 827–841 (2003).
15. Elmore, T., Ignell, R., Carlson, J. R. & Smith, D. P. Targeted Mutation of a Drosophila Odor Receptor Defines Receptor Requirement in a Novel Class of Sensillum | Journal of Neuroscience. *J. Neurosci.* **23,** 9906–9912 (2003).
16. Kreher, S. A., Mathew, D., Kim, J. & Carlson, J. R. Translation of sensory input into behavioral output via an olfactory system. *Neuron* **59,** 110–124 (2008).
17. Krieger, J., Klink, O., Mohl, C., Raming, K. & Breer, H. A candidate olfactory receptor subtype highly conserved across different insect orders. *J Comp Physiol A* **189,** 519–526 (2003).
18. Vosshall, L. B. & Hansson, B. S. A Unified Nomenclature System for the Insect Olfactory Coreceptor. *Chemical Senses* **36,** 497–498 (2011).
19. Jung, S. N., borst, A. & Haag, J. Flight activity alters velocity tuning of fly motion-sensitive neurons. *J. Neurosci.* **31,** 9231–9237 (2011).

20. Nakagawa, T. & Vosshall, L. B. Controversy and consensus: noncanonical signaling mechanisms in the insect olfactory system. *Current Opinion in Neurobiology* **19,** 284–292 (2009).

21. Nichols, A. S. & Luetje, C. W. Transmembrane segment 3 of Drosophila melanogaster odorant receptor subunit 85b contributes to ligand-receptor interactions. *J. Biol. Chem.* **285,** 11854–11862 (2010).

22. Jones, P. L., Pask, G. M. & Rinker, D. C. Functional agonism of insect odorant receptor ion channels. in (2011). doi:10.1073/pnas.1102425108/-/DCSupplemental/pnas.201102425SI.pdf

23. Larsson, M. C. *et al*. Or83b Encodes a Broadly Expressed Odorant Receptor Essential for Drosophila Olfaction. *Neuron* **43,** 703–714 (2004).

24. Benton, R., Sachse, S., Michnick, S. W. & Vosshall, L. B. Atypical Membrane Topology and Heteromeric Function of Drosophila Odorant Receptors In Vivo. *Plos Biol* **4,** e20–18 (2006).

25. Silbering, A. F. *et al*. Complementary Function and Integrated Wiring of the Evolutionarily Distinct Drosophila Olfactory Subsystems. *Journal of Neuroscience* **31,** 13357–13375 (2011).

26. Benton, R., Vannice, K. S., Gomez-Diaz, C. & Vosshall, L. B. Variant Ionotropic Glutamate Receptors as Chemosensory Receptors in Drosophila. *Cell* **136,** 149–162 (2009).

27. Kwon, J. Y., Dahanukar, A., Weiss, L. A. & Carlson, J. R. The molecular basis of CO2 reception in Drosophila. *Proceedings of the National Academy of Sciences* **104,** 3574–3578 (2007).

28. Jones, W. D., Cayirlioglu, P., Kadow, I. G. & Vosshall, L. B. Two chemosensory receptors together mediate carbon dioxide detection in Drosophila. *Nature* **445,** 86–90 (2007).

29. Stocker, R. F., Lienhard, M. C., Borst, A. & Fischbach, K. F. Neuronal architecture of the antennal lobe in Drosophila melanogaster. *Cell Tissue Res.* **262,** 9–34 (1990).

30. Giniger, E., Varnum, S. M. & Ptashne, M. Specific DNA binding of GAL4, a positive regulatory protein of yeast. *Cell* **40,** 767–774 (1985).

31. Chen, A. Y., Xia, S., Wilburn, P. & Tully, T. Olfactory deficits in an alpha-synuclein fly model of Parkinson's disease. *PLoS ONE* **9,** e97758 (2014).

32. Hodge, J. J. L. Ion channels to inactivate neurons in Drosophila. *Front. Mol. Neurosci.* **2,** 1–10 (2009).

33. Baines, R. A., Uhler, J. P., Thompson, A., Sweeney, S. T. & Bate, M. Altered Electrical Properties in DrosophilaNeurons Developing without Synaptic Transmission. *Journal of Neuroscience* **21,** 1523–1531 (2001).

34. Johns, D. C., Marx, R., Mains, R. E., O'Rourke, B. & Marbán, E. Inducible genetic suppression of neuronal excitability. *Journal of Neuroscience* **19,** 1691–1697 (1999).

35. van der Bliek, A. M. & Meyerowitz, E. M. Dynamin-like protein encoded by the Drosophila shibire gene associated with vesicular traffic. *Nature* **351,** 411–414 (1991).

36. kitamoto, T. Conditional disruption of synaptic transmission induces male-male courtship behavior in Drosophila. *Proceedings of the National Academy of*

Sciences **99,** 13232–13237 (2002).

37. Kitamoto, T. Conditional modification of behavior in Drosophila by targeted expression of a temperature-sensitive shibire allele in defined neurons. *J. Neurobiol*. **47,** 81–92 (2001).

38. Chen, M. S. *et al*. Multiple forms of dynamin are encoded by shibire, a Drosophila gene involved in endocytosis. *Nature* **351,** 583–586 (1991).

39. Sweeney, S. T., Broadie, K., Keane, J., Niemann, H. & O'Kane, C. J. Targeted expression of tetanus toxin light chain in Drosophila specifically eliminates synaptic transmission and causes behavioral defects. *Neuron* **14,** 341–351 (1995).

40. Baines, R. A., Robinson, S. G., Fujioka, M., Jaynes, J. B. & Bate, M. Postsynaptic expression of tetanus toxin light chain blocks synaptogenesis in Drosophila. *Current Biology* **9,** 1267–1270 (1999).

41. Song, Z. & Steller, H. Death by design: mechanism and control of apoptosis. *Trends Cell Biol*. **9,** M49–52 (1999).

42. Abrams, J. M. An emerging blueprint for apoptosis in Drosophila. *Trends Cell Biol*. **9,** 435–440 (1999).

43. Boyden, E. S. A history of optogenetics: the development of tools for controlling brain circuits with light. *F1000 Biol Rep* **3,** 11 (2011).

44. Pulver, S. R., Pashkovski, S. L., Hornstein, N. J., Garrity, P. A. & Griffith, L. C. Temporal dynamics of neuronal activation by Channelrhodopsin-2 and TRPA1 determine behavioral output in Drosophila larvae. *Journal of Neurophysiology* **101,** 3075–3088 (2009).

45. Ma, J. & Ptashne, M. The carboxy-terminal 30 amino acids of GAL4 are

recognized by GAL80. *Cell* **50,** 137–142 (1987).

46. Olsen, S. R., Bhandawat, V. & Wilson, R. I. Excitatory Interactions between Olfactory Processing Channels in the Drosophila Antennal Lobe. *Neuron* **54,** 89–103 (2007).

47. DasGupta, S. & Waddell, S. Learned Odor Discrimination in Drosophila without Combinatorial Odor Maps in the Antennal Lobe. *Current Biology* **18,** 1668–1674 (2008).

48. Hoare, D. J., McCrohan, C. R. & Cobb, M. Precise and Fuzzy Coding by Olfactory Sensory Neurons. *Journal of Neuroscience* **28,** 9710–9722 (2008).

49. Hoare, D. J. *et al*. Modeling Peripheral Olfactory Coding in Drosophila Larvae. *PLoS ONE* **6,** e22996–11 (2011).

50. Fishilevich, E. *et al*. Chemotaxis behavior mediated by single larval olfactory neurons in Drosophila. *Current Biology* **15,** 2086–2096 (2005).

51. Smart, R. *et al*. Drosophila odorant receptors are novel seven transmembrane domain proteins that can signal independently of heterotrimeric G proteins. *Insect Biochemistry and Molecular Biology* **38,** 770–780 (2008).

52. Neuhaus, E. M. *et al*. Odorant receptor heterodimerization in the olfactory system of Drosophila melanogaster. *Nat Neurosci* **8,** 15–17 (2005).

53. Benton, R. Evolution and Revolution in Odor Detection. *Science* **326,** 382–383 (2009).

54. Pfeiffer, B. D. *et al*. Refinement of Tools for Targeted Gene Expression in Drosophila. *Genetics* **186,** 735–755 (2010).

55. Gao, X. J., Clandinin, T. R. & Luo, L. Extremely sparse olfactory inputs are

sufficient to mediate innate aversion in Drosophila. *PLoS ONE* **10,** e0125986 (2015).

56. Pfeiffer, B. D. *et al*. Tools for neuroanatomy and neurogenetics in Drosophila. *Proceedings of the National Academy of Sciences* **105,** 9715–9720 (2008).

57. Berdnik, D., Chihara, T., Couto, A. & Luo, L. Wiring Stability of the Adult Drosophila Olfactory Circuit after Lesion. *Journal of Neuroscience* **26,** 3367–3376 (2006).

58. Wong, A. M., Wang, J. W. & Axel, R. Spatial Representation of the Glomerular Map in the Drosophila Protocerebrum. *Cell* **109,** 229–241 (2002).

59. Elmore, T. & Smith, D. P. Putative Drosophila odor receptor OR43b localizes to dendrites of olfactory neurons. *Insect Biochemistry and Molecular Biology* **31,** 791–798 (2001).

60. Aso, Y. & Rubin, G. M. Dopaminergic neurons write and update memories with cell-type-specific rules. *Elife* **5,** 156 (2016).

61. Branson, K., Robie, A. A., Bender, J., Pietro Perona & Dickinson, M. H. High-throughput ethomics in large groups of Drosophila. *Nat Meth* **6,** 451–457 (2009).

62. Bhandawat, V., Maimon, G., Dickinson, M. H. & Wilson, R. I. Olfactory modulation of flight in Drosophila is sensitive, selective and rapid. *Journal of Experimental Biology* **213,** 3625–3635 (2010).

63. Su, C.-Y., Menuz, K., Reisert, J. & Carlson, J. R. Non-synaptic inhibition between grouped neurons in an olfactory circuit. *Nature* **492,** 66–71 (2012).

64. Kazama, H. & Wilson, R. I. Origins of correlated activity in an olfactory circuit. *Nat Neurosci* **12,** 1136–1144 (2009).

65. Chou, Y.-H. *et al*. Diversity and wiring variability of olfactory local interneurons in the Drosophila antennal lobe. *Nat Neurosci* 1–13 (2010). doi:10.1038/nn.2489

66. Wilson, R. I. Understanding the functional consequences of synaptic specialization: insight from the Drosophila antennal lobe. *Current Opinion in Neurobiology* **21,** 254–260 (2011).

67. Yaksi, E. & Wilson, R. I. Electrical Coupling between Olfactory Glomeruli. *Neuron* **67,** 1034–1047 (2010).

68. Hong, E. J. & Wilson, R. I. Simultaneous Encoding of Odors by Channels with Diverse Sensitivity to Inhibition. *Neuron* **85,** 573–589 (2015).

69. Kazama, H., Yaksi, E. & Wilson, R. I. Cell Death Triggers Olfactory Circuit Plasticity via Glial Signaling in Drosophila. *Journal of Neuroscience* **31,** 7619–7630 (2011).

70. Acebes, A., Martín-Peña, A., Chevalier, V. & Ferrús, A. Synapse loss in olfactory local interneurons modifies perception. *J. Neurosci*. **31,** 2734–2745 (2011).

71. Riesgo-Escovar, J. R., Piekos, W. B. & Carlson, J. R. The Drosophila antenna: ultrastructural and physiological studies in wild-type and lozenge mutants. *J Comp Physiol A* **180,** 151–160 (1997).

72. Tunstall, N. E. & Warr, C. G. Chemical communication in insects: the peripheral odour coding system of Drosophila melanogaster. *Adv. Exp. Med. Biol*. **739,** 59–77 (2012).

73. Sachse, S. *et al*. Activity-Dependent Plasticity in an Olfactory Circuit. *Neuron* **56,** 838–850 (2007).

74. Devaud, J. M., Acebes, A. & Ferrus, A. Odor exposure causes central adaptation and morphological changes in selected olfactory glomeruli in Drosophila. *J. Neurosci*. **21,** 6274–6282 (2001).

75. Devaud, J.-M., Acebes, A., Ramaswami, M. & Ferrús, A. Structural and functional changes in the olfactory pathway of adult Drosophila take place at a critical age. *J. Neurobiol*. **56,** 13–23 (2003).

76. White, B. H. *et al*. Targeted Attenuation of Electrical Activity in Drosophila Using a Genetically Modified K+ Channel. *Neuron* **31,** 699–711 (2001).

77. del Valle Rodríguez, A., Didiano, D. & Desplan, C. Power tools for gene expression and clonal analysis in Drosophila. *Nat Meth* **9,** 47–55 (2012).

78. Lai, S.-L. & Lee, T. Genetic mosaic with dual binary transcriptional systems in Drosophila. *Nat Neurosci* **9,** 703–709 (2006).

79. Marshall, B., Warr, C. G. & de Bruyne, M. Detection of Volatile Indicators of Illicit Substances by the Olfactory Receptors of Drosophila melanogaster. *Chemical Senses* **35,** 613–625 (2010).

80. Sakurai, T. *et al*. Identification and functional characterization of a sex pheromone receptor in the silkmoth Bombyx mori. *Proceedings of the National Academy of Sciences* **101,** 16653–16658 (2004).

81. Syed, Z., Kopp, A., Kimbrell, D. A. & Leal, W. S. Bombykol receptors in the silkworm moth and the fruit fly. *Proceedings of the National Academy of Sciences* 1–4 (2010). doi:10.1073/pnas.1003881107/-/DCSupplemental

82. Syed, Z., Ishida, Y., Taylor, K., Kimbrell, D. A. & Leal, W. S. Pheromone reception in fruit flies expressing a moth's odorant receptor. *Proceedings of the*

National Academy of Sciences **103,** 16538–16543 (2006).

83. Krieger, J., Große-Wilde, E., Gohl, T. & Breer, H. Candidate pheromone receptors of the silkmoth Bombyx mori. *European Journal of Neuroscience* **21,** 2167–2176 (2005).

84. Fishilevich, E. *et al*. Chemotaxis Behavior Mediated by Single Larval Olfactory Neurons in Drosophila. *Current Biology* **15,** 2086–2096 (2005).

85. Louis, M., Piccinotti, S. & Vosshall, L. B. High-resolution Measurement of Odor-Driven Behavior in Drosophila Larvae. *JoVE* 1–4 (2008). doi:10.3791/638

86. Invitrogen. pENTR™ Directional TOPO® Cloning Kits. 1–52 (2012).

87. Invitrogen. pBAD/Thio His TOPO manual. 1–74 (2012).

88. Wagh, D. A. *et al*. Bruchpilot, a protein with homology to ELKS/CAST, is required for structural integrity and function of synaptic active zones in Drosophila. *Neuron* **49,** 833–844 (2006).

89. Lin, C.-C. & Potter, C. J. Re-Classification of Drosophila melanogaster Trichoid and Intermediate Sensilla Using Fluorescence-Guided Single Sensillum Recording. *PLoS ONE* **10,** e0139675 (2015).

90. Frye, M. A. & Dickinson, M. H. Fly flight: a model for the neural control of complex behavior. *Neuron* **32,** 385–388 (2001).

91. Sanes, J. R. & Zipursky, S. L. Design principles of insect and vertebrate visual systems. *Neuron* **66,** 15–36 (2010).

92. Harris, W. A., Stark, W. S. & Walker, J. A. Genetic dissection of the photoreceptor system in the compound eye of Drosophila melanogaster. *J. Physiol. (Lond.)* **256,** 415–439 (1976).

93. Feiler, R. *et al*. Ectopic expression of ultraviolet-rhodopsins in the blue photoreceptor cells of Drosophila: visual physiology and photochemistry of transgenic animals. *Journal of Neuroscience* **12,** 3862–3868 (1992).

94. Salcedo, E. *et al*. Blue- and Green-Absorbing Visual Pigments ofDrosophila: Ectopic Expression and Physiological Characterization of the R8 Photoreceptor Cell-Specific Rh5 and Rh6 Rhodopsins. *Journal of Neuroscience* **19,** 10716–10726 (1999).

95. Meinertzhagen, I. A. & O'Neil, S. D. Synaptic organization of columnar elements in the lamina of the wild type in Drosophila melanogaster. *J. Comp. Neurol.* **305,** 232–263 (1991).

96. Rivera-Alba, M. *et al*. Wiring Economy and Volume Exclusion Determine Neuronal Placement in the Drosophila Brain. *Current Biology* **21,** 2000–2005 (2011).

97. Joesch, M., Schnell, B., Raghu, S. V., Reiff, D. F. & borst, A. ON and OFF pathways in Drosophila motion vision. *Nature* **468,** 300–304 (2010).

98. Clark, D. A., Bursztyn, L., Horowitz, M. A., Schnitzer, M. J. & Clandinin, T. R. Defining the computational structure of the motion detector in Drosophila. *Neuron* **70,** 1165–1177 (2011).

99. Rister, J. *et al*. Dissection of the peripheral motion channel in the visual system of Drosophila melanogaster. *Neuron* **56,** 155–170 (2007).

100. Tuthill, J. C., Nern, A., Holtz, S. L., Rubin, G. M. & Reiser, M. B. Contributions of the 12 Neuron Classes in the Fly Lamina to Motion Vision. *Neuron* **79,** 128–140 (2013).

101. Meier, M. *et al*. Neural circuit components of the Drosophila OFF motion vision pathway. *Curr*. *Biol*. **24,** 385–392 (2014).

102. Reiff, D. F., Plett, J., Mank, M., Griesbeck, O. & borst, A. Visualizing retinotopic half-wave rectified input to the motion detection circuitry of Drosophila. *Nat Neurosci* **13,** 973–978 (2010).

103. Joesch, M., Weber, F., Eichner, H. & borst, A. Functional specialization of parallel motion detection circuits in the fly. *J*. *Neurosci*. **33,** 902–905 (2013).

104. Bahl, A., Serbe, E., Meier, M., Ammer, G. & borst, A. Neural Mechanisms for Drosophila Contrast Vision. *Neuron* **88,** 1240–1252 (2015).

105. Morante, J. & Desplan, C. Building a projection map for photoreceptor neurons in the Drosophila optic lobes. *Semin*. *Cell Dev*. *Biol*. **15,** 137–143 (2004).

106. Clandinin, T. R. & Zipursky, S. L. Afferent growth cone interactions control synaptic specificity in the Drosophila visual system. *Neuron* **28,** 427–436 (2000).

107. Behnia, R., Clark, D. A., Carter, A. G., Clandinin, T. R. & Desplan, C. Processing properties of ON and OFF pathways for Drosophila motion detection. *Nature* **512,** 427–430 (2014).

108. Takemura, S.-Y. *et al*. A visual motion detection circuit suggested by Drosophila connectomics. *Nature* **500,** 175–181 (2013).

109. Shinomiya, K. *et al*. Candidate neural substrates for off-edge motion detection in Drosophila. *Curr*. *Biol*. **24,** 1062–1070 (2014).

110. Bausenwein, B., Dittrich, A. P. M. & Fischbach, K. F. The optic lobe of Drosophila melanogaster. *Cell Tissue Res*. **267,** 17–28 (1992).

111. Bausenwein, B. & Fischbach, K. F. Activity labeling patterns in the medulla of

Drosophila melanogaster caused by motion stimuli. *Cell Tissue Res*. **270,** 25–35 (1992).

112. Yamaguchi, S., Wolf, R., Desplan, C. & Heisenberg, M. Motion vision is independent of color in Drosophila. *Proc. Natl. Acad. Sci. U.S.A.* **105,** 4910–4915 (2008).

113. Zhu, Y., Nern, A., Zipursky, S. L. & Frye, M. A. Peripheral visual circuits functionally segregate motion and phototaxis behaviors in the fly. *Curr. Biol.* **19,** 613–619 (2009).

114. Morante, J. & Desplan, C. The color-vision circuit in the medulla of Drosophila. *Current Biology* **18,** 553–565 (2008).

115. Gao, S. *et al*. The Neural Substrate of Spectral Preference in Drosophila. *Neuron* **60,** 328–342 (2008).

116. Maisak, M. S. *et al*. A directional tuning map of Drosophila elementary motion detectors. *Nature* **500,** 212–216 (2013).

117. Schnell, B., Raghu, S. V., Nern, A. & borst, A. Columnar cells necessary for motion responses of wide-field visual interneurons in Drosophila. *J. Comp. Physiol. A Neuroethol. Sens. Neural. Behav. Physiol.* **198,** 389–395 (2012).

118. Leonhardt, A. *et al*. Asymmetry of Drosophila ON and OFF motion detectors enhances real-world velocity estimation. *Nat Neurosci* (2016). doi:10.1038/nn.4262

119. Serbe, E., Meier, M., Leonhardt, A. & borst, A. Comprehensive Characterization of the Major Presynaptic Elements to the Drosophila OFF Motion Detector. *Neuron* **89,** 829–841 (2016).

120. Fischbach, P. K. F. & Dittrich, A. P. M. The optic lobe of Drosophila melanogaster. I. A Golgi analysis of wild-type structure. *Cell Tissue Res*. **258,** 441–475 (1989).

121. Frye, M. Elementary motion detectors. *Curr*. *Biol*. **25,** R215–7 (2015).

122. Borst, A. Correlation versus gradient type motion detectors: the pros and cons. *Philosophical Transactions of the Royal Society B: Biological Sciences* **362,** 369–374 (2007).

123. Eichner, H., Joesch, M., Schnell, B., Reiff, D. F. & borst, A. Internal structure of the fly elementary motion detector. *Neuron* **70,** 1155–1164 (2011).

124. Katsov, A. Y. & Clandinin, T. R. Motion processing streams in Drosophila are behaviorally specialized. *Neuron* **59,** 322–335 (2008).

125. Aso, Y. *et al*. Mushroom body output neurons encode valence and guide memory-based action selection in Drosophila. *Elife* **3,** e04580 (2014).

126. Ohyama, T. *et al*. A multilevel multimodal circuit enhances action selection in Drosophila. *Nature* **520,** 633–639 (2015).

127. Silies, M. *et al*. Modular use of peripheral input channels tunes motion-detecting circuitry. *Neuron* **79,** 111–127 (2013).

128. Jenett, A. *et al*. A GAL4-driver line resource for Drosophila neurobiology. *Cell Rep* **2,** 991–1001 (2012).

129. Luan, H., Peabody, N. C., Vinson, C. R. & White, B. H. Refined spatial manipulation of neuronal function by combinatorial restriction of transgene expression. *Neuron* **52,** 425–436 (2006).

130. Ramdya, P. *et al*. Mechanosensory Interactions Drive Collective Behaviour in

Drosophila. *Nature* **519,** 233–236 (2015).

131. Ramdya, P., Schneider, J. & Levine, J. D. The neurogenetics of group behavior in Drosophila melanogaster. *J. Exp. Biol.* **220,** 35–41 (2017).

132. Lihoreau, M., Clarke, I. M., Buhl, J., Sumpter, D. J. T. & Simpson, S. J. Collective selection of food patches in Drosophila. *Journal of Experimental Biology* **219,** 668–675 (2016).

133. Götz, K. G. & Wenking, H. Visual control of locomotion in the walking fruitflyDrosophila. *J Comp Physiol A* **85,** 235–266 (1973).

134. Hecht, S. & Wald, G. THE VISUAL ACUITY AND INTENSITY DISCRIMINATION OF DROSOPHILA. *J. Gen. Physiol.* **17,** 517–547 (1934).

135. Götz, K. G. Fractionation of Drosophila populations according to optomotor traits. *Journal of Experimental Biology* **52,** 419–436 (1970).

136. Robie, A. A. *et al.* Mapping the Neural Substrates of Behavior. *Cell* **170,** 393–406.e28 (2017).

137. Otsuna, H. & Ito, K. Systematic analysis of the visual projection neurons of Drosophila melanogaster. I. Lobula-specific pathways. *J. Comp. Neurol.* **497,** 928–958 (2006).

138. Chiappe, M. E., Seelig, J. D., Reiser, M. B. & Jayaraman, V. Walking modulates speed sensitivity in Drosophila motion vision. *Curr. Biol.* **20,** 1470–1475 (2010).

139. Maimon, G., Straw, A. D. & Dickinson, M. H. Active flight increases the gain of visual motion processing in Drosophila. *Nat Neurosci* **13,** 393–399 (2010).

140. Longden, K. D. & Krapp, H. G. State-dependent performance of optic-flow processing interneurons. *Journal of Neurophysiology* **102,** 3606–3618 (2009).

141. van Breugel, F., Suver, M. P. & Dickinson, M. H. Octopaminergic modulation of the visual flight speed regulator of Drosophila. *J. Exp. Biol.* **217,** 1737–1744 (2014).

142. Tuthill, J. C., Nern, A., Rubin, G. M. & Reiser, M. B. Wide-field feedback neurons dynamically tune early visual processing. *Neuron* **82,** 887–895 (2014).

143. Kim, A. J., Fenk, L. M., Lyu, C. & Maimon, G. Quantitative Predictions Orchestrate Visual Signaling in Drosophila. *Cell* **168,** 280–294.e12 (2017).

144. Kim, A. J., Fitzgerald, J. K. & Maimon, G. Cellular evidence for efference copy in Drosophila visuomotor processing. *Nat Neurosci* (2015). doi:10.1038/nn.4083

145. Aptekar, J. W., Shoemaker, P. A. & Frye, M. A. Figure tracking by flies is supported by parallel visual streams. *Curr. Biol.* **22,** 482–487 (2012).

146. Theobald, J. C., Shoemaker, P. A., Ringach, D. L. & Frye, M. A. Theta motion processing in fruit flies. *Front Behav Neurosci* **4,** (2010).

147. Theobald, J. C., Duistermars, B. J., Ringach, D. L. & Frye, M. A. Flies see second-order motion. *Current Biology* **18,** R464–5 (2008).

148. Frye, M. A. & Dickinson, M. H. Motor output reflects the linear superposition of visual and olfactory inputs in Drosophila. *Journal of Experimental Biology* **207,** 123–131 (2004).

149. Wasserman, S. M. *et al*. Olfactory neuromodulation of motion vision circuitry in Drosophila. *Curr. Biol.* **25,** 467–472 (2015).

150. Fox, J. L., Aptekar, J. W., Zolotova, N. M., Shoemaker, P. A. & Frye, M. A. Figure-ground discrimination behavior in Drosophila. I. Spatial organization of wing-steering responses. *J. Exp. Biol.* **217,** 558–569 (2014).

151. Fox, J. L. & Frye, M. A. Figure-ground discrimination behavior in Drosophila. II. Visual influences on head movement behavior. *J. Exp. Biol.* **217,** 570–579 (2014).

152. Reiser, M. B. & Dickinson, M. H. Visual motion speed determines a behavioral switch from forward flight to expansion avoidance in Drosophila. *J. Exp. Biol.* **216,** 719–732 (2013).

153. Theobald, J. C., Ringach, D. L. & Frye, M. A. Dynamics of optomotor responses in Drosophila to perturbations in optic flow. *J. Exp. Biol.* **213,** 1366–1375 (2010).

154. Duistermars, B. J., Care, R. A. & Frye, M. A. Binocular interactions underlying the classic optomotor responses of flying flies. *Front Behav Neurosci* **6,** 6 (2012).

155. Duistermars, B. J., Chow, D. M., Condro, M. & Frye, M. A. The spatial, temporal and contrast properties of expansion and rotation flight optomotor responses in Drosophila. *Journal of Experimental Biology* **210,** 3218–3227 (2007).

156. Bahl, A., Ammer, G., Schilling, T. & borst, A. Object tracking in motion-blind flies. *Nat Neurosci* **16,** 730–738 (2013).

157. Fujiwara, T., Cruz, T. L., Bohnslav, J. P. & Chiappe, M. E. A faithful internal representation of walking movements in the Drosophila visual system. *Nat Neurosci* **20,** 72–81 (2017).

158. Seelig, J. D. *et al*. Two-photon calcium imaging from head-fixed Drosophila during optomotor walking behavior. *Nat Meth* **7,** 535–540 (2010).

159. Tammero, L. F., Frye, M. A. & Dickinson, M. H. Spatial organization of visuomotor reflexes in Drosophila. *Journal of Experimental Biology* **207,** 113–122 (2004).

160. Reiser, M. B. & Dickinson, M. H. A modular display system for insect behavioral neuroscience. *Journal of Neuroscience Methods* **167,** 127–139 (2008).

161. Buschbeck, E. K. & Strausfeld, N. J. Visual motion-detection circuits in flies: small-field retinotopic elements responding to motion are evolutionarily conserved across taxa. *Journal of Neuroscience* **16,** 4563–4578 (1996).

162. Reiser, M. B. & Dickinson, M. H. Drosophila fly straight by fixating objects in the face of expanding optic flow. *Journal of Experimental Biology* **213,** 1771–1781 (2010).

163. Tammero, L. F. & Dickinson, M. H. The influence of visual landscape on the free flight behavior of the fruit fly Drosophila melanogaster. *Journal of Experimental Biology* **205,** 327–343 (2002).

164. Buchner, E. in *Photoreception and Vision in Invertebrates* 561–621 (Springer US, 1984). doi:10.1007/978-1-4613-2743-1_16

165. Horseman, B. G., Macauley, M. W. S. & Barnes, W. J. P. Neuronal processing of translational optic flow in the visual system of the shore crab Carcinus maenas. *Journal of Experimental Biology* **214,** 1586–1598 (2011).

166. Nern, A., Pfeiffer, B. D. & Rubin, G. M. Optimized tools for multicolor stochastic labeling reveal diverse stereotyped cell arrangements in the fly visual system. *Proc. Natl. Acad. Sci. U.S.A.* **112,** E2967–76 (2015).

167. Ito, K. *et al*. A Systematic Nomenclature for the Insect Brain. *Neuron* **81,** 755–

765 (2014).

168. Hamada, F. N. *et al*. An internal thermal sensor controlling temperature preference in Drosophila. *Nature* **454,** 217–220 (2008).

169. Chen, T.-W. *et al*. Ultrasensitive fluorescent proteins for imaging neuronal activity. *Nature* **499,** 295–300 (2013).

170. Klapoetke, N. C. *et al*. Independent optical excitation of distinct neural populations. *Nat Meth* **11,** 338–346 (2014).

171. Shirangi, T. R., Wong, A. M., Truman, J. W. & Stern, D. L. Doublesex Regulates the Connectivity of a Neural Circuit Controlling Drosophila Male Courtship Song. *Dev. Cell* **37,** 533–544 (2016).

172. Strother, J. A. *et al*. The Emergence of Directional Selectivity in the Visual Motion Pathway of Drosophila. *Neuron* **94,** 168–182.e10 (2017).

173. Budick, S. A., Reiser, M. B. & Dickinson, M. H. The role of visual and mechanosensory cues in structuring forward flight in Drosophila melanogaster. *Journal of Experimental Biology* **210,** 4092–4103 (2007).

174. Maimon, G., Straw, A. D. & Dickinson, M. H. A simple vision-based algorithm for decision making in flying Drosophila. *Current Biology* **18,** 464–470 (2008).

175. Saalfeld, S., Cardona, A., Hartenstein, V. & Tomancak, P. CATMAID: collaborative annotation toolkit for massive amounts of image data. *Bioinformatics* **25,** 1984–1986 (2009).

176. Strother, J. A., Nern, A. & Reiser, M. B. Direct observation of ON and OFF pathways in the Drosophila visual system. *Curr. Biol.* **24,** 976–983 (2014).

177. borst, A. & Helmstaedter, M. Common circuit design in fly and mammalian

motion vision. *Nat Neurosci* **18,** 1067–1076 (2015).